

Bølgeprognosemodel for havvindmølleparker

PSO-projektrapport

Eltraprojektnr. 3187

Eltra

**Endelig Rapport
31. marts 2003**

Bølgeprognosemodel for havvindmølleparker

31. marts 2003

Techwise
Kraftværksvej 53
7000 Fredericia

DHI – Institut for Vand og Miljø
Agern Allé 11
2970 Hørsholm

Tlf: 7923 3333
Fax: 7556 4477
E-mail: mail@techwise.dk
Web: www.techwise.dk

Tlf: 4516 9200
Fax: 4516 9292
E-mail: dhi@dhi.dk
Web: www.dhi.dk

Klient	Klientens repræsentant
Eltra	Fritz Luxhøj

Projekt	Projekt nr.			
Bølgeprognosemodel for havvindmølleparker	DHI51390 / Techwise13061			
Forfattere	Dato			
Morten Ruggberg (DHI) Jan Pedersen (Techwise) Ole Sørensen (DHI) Claus Denker Christensen (DHI) Vladan Babovic (DHI)		31. marts 2003		
	Endelig Rapport	MNR		31-3-2003
Revision	Beskrivelse	Udført	Kontrolleret	Godkendt
Nøgleord	Klassifikation			
havvindmøllepark bølgeprognose bølgemålinger offshore wind farm wave forecast wave measurements	<input checked="" type="checkbox"/> Åben <input type="checkbox"/> Intern <input type="checkbox"/> Tilhører klienten			

Distribution	Antal kopier
Eltra	2
Elsam	1
Techwise	2
DHI:	5
Fritz Luxhøj	
Peggy Fris	
JPE	
MNR, ORS, CDC, VJ, PHD	



INDHOLDSFORTEGNELSE

KORT SAMMENFATNING.....	I
EXECUTIVE SUMMARY	II
1 INDLEDNING OG BAGGRUND	1-1
2 PROJEKTETS ORGANISERING, FINANSIERING OG TIDSPLAN.....	2-1
2.1 Generelt	2-1
2.2 Projektorganisation.....	2-1
2.3 Projektfinansiering.....	2-1
2.4 Projekttidsplan.....	2-2
3 PROJEKTETS RESULTATER	3-1
3.1 Generelt	3-1
3.2 Bølgeprognoser for Horns Rev Havvindmøllepark.....	3-1
3.3 Bølgeprognosesystemet for andre havvindmølle parker	3-4
3.4 Formidling af projektets resultater	3-5
3.5 Økonomiske fordele ved anvendelse af bølgeprognosesystemet	3-5
4 DETALJERET BESKRIVELSE AF PROJEKTETS FASER.....	4-1
4.1 Projektets formål og opdeling	4-1
4.2 Fase 1 – forprojekt med erfaringsindsamling	4-1
4.2.1 Generelt	4-1
4.2.2 Valg af bølgemodel	4-1
4.3 Fase 2 – opstilling af marint målesystem.....	4-5
4.3.1 Beskrivelse af målesystemet	4-5
4.3.2 Præsentation af målinger	4-7
4.3.3 Drift af målesystemet.....	4-9
4.4 Fase 3 – opstilling af bølgeprognosesystem.....	4-9
4.4.1 Opstilling af bølgemodel	4-9
4.4.2 Korrektion af bølgeprognoser på basis af bølgemålinger.....	4-12
4.4.3 Præsentation af bølgeprognoser og drift af bølgeprognosesystem.....	4-13
4.5 Fase 4 – evaluering og revision af bølgeprognosesystemet efter anvendelse i 20024-15	4-15
4.5.1 Generelt	4-15
4.5.2 Revision af bølgemodelsystem.....	4-15
4.5.3 Revision af korrektioner på basis af målinger	4-19
4.6 Fase 5 – formidling af projektets resultater	4-20
5 REFERENCER.....	5-1



BILAG

- A PSO-F&U Oplysningskema
- B Generel beskrivelse af DHI's bølgemodeller, MIKE 21 OSW og SW (på engelsk)
- C Generel beskrivelse af The Water Forecast (på engelsk)
- D A Third Generation Spectral Wave Model using an Unstructured Finite Volume Technique, Ole René Sørensen et al.
- E Time Series Analysis and Forecasting using Artificial Neural Networks, Vladan Babovic
- F Internal Note – Improving wave forecast data



KORT SAMMENFATNING

Opførelse og vedligeholdelse af havvindmølleparker medfører omfattende marine operationer. For at kunne udføre disse på en sikker og økonomisk måde kræves bl.a. detaljerede bølgeprognoser. Formålet med nærværende projekt har været at etablere et bølgeprognosesystem, der kan levere de relevante informationer med bedst mulig nøjagtighed.

Projektet er udført af DHI – Institut for Vand og Miljø og Tech-wise A/S med Elsam A/S som den projektansvarlige organisation under den såkaldte Public Service Obligation (PSO) ordning. Projektet er finansieret af Eltra med et beløb på kr 2,8 mill. Desuden har projektet draget nytte af samspillet med andre projekter, herunder udvikling af Tech-wises målesystem på Horns Rev og DHI's generelle prognoseservice, Vandudsigten.

Projektet har omfattet følgende faser:

- erfaringsindsamling
- opstilling af marint målesystem
- opstilling af numerisk bølgeprognosemodel
- revision af systemet efter 1. års drift
- formidling af projektets resultater

og har resulteret i følgende:

- et bølgeprognosesystem for Horns Rev Havvindmøllepark baseret på en numerisk bølgemodel med korrektion af 48-timers prognoser baseret på de aktuelle målinger. Systemet har været i drift siden den 1. maj 2002.
- opbygning af viden om bølgeprognosesystemer med korrektioner baseret på målinger, så et sådant system kan sættes op for andre lokaliteter. Således skal et system anvendes for Rødsand Havvindmøllepark fra primo maj 2003.
- generelle værktøjer til præsentation af bølgeprognoser
- præsentation af projektets resultater i to artikler, som fremsendes med henblik på publicering i tidsskriftet Coastal Engineering



EXECUTIVE SUMMARY

Construction and maintenance of offshore wind farms require a substantial number of marine operations. In order to carry these out in a safely yet economically manner detailed wave forecasts required. The purpose of the present project has been to establish a wave forecasting system being capable of delivering vital information on wave conditions for planning purposes.

The present project has been carried out by DHI Water & Environment and Tech-wise A/S with Elsam A/S as the project responsible organisation. It has been funded by Eltra as a PSO (Public Service Obligation) project with an amount of 2.8 mill Danish kroner. Furthermore the project has benefited from other projects including the development by Tech-wise of the measuring system at Horns Rev and the development of DHIs general forecast system, The Water Forecast (Vandudsigten).

The project has been divided into the following phases:

- collection of background material and experience from similar projects
- setting up a marine measuring system
- setting up a numerical wave forecast modelling system
- revision of the forecast system after its first year in operation
- dissemination of project results

The project has resulted in the following:

- a wave forecasting system for Horns Rev Offshore Wind Farm based on a numerical wave model with subsequent 48 hours forecast corrections based on online measurements. The system has been operating since May 1, 2002.
- general knowledge about setting up wave forecasting systems with forecasts corrected based on online measurements. Such a system is planned for Rødvand Offshore Wind Farm south of Lolland (Denmark). The system is planned to start operating at the beginning of May 2003.
- general tools for presentation of wave forecasts
- presentation of results from the project as two papers planned for publishing in the journal Coastal Engineering



1 INDLEDNING OG BAGGRUND

Regeringens havvindmølleplan sigter mod opstilling af vindmølleparker til søs med en kapacitet på 4000 MW inden år 2030. I 1998 pålagde Miljø- og Energiministeriet således elselskaberne at stå for opførelsen af fem demonstrationsparkere med en samlet effekt på 750 MW. Dette krav blev i 2002 reduceret til to demonstrationsparkere, Horns Rev og Rødsand, med en effekt på henholdsvis 160 MW og 158 MW.

Havvindmølleparken ved Horns Rev blev sat i drift i december 2002, mens havvindmølleparken ved Rødsand er under opførelse og forventes at blive taget i brug i oktober 2003.

Ved Horns Rev blev Elsam og Eltra pålagt at stå for opførelsen - Elsam som ejer og operatør af vindmølleparken, og Eltra som ansvarlig for etablering af forbindelsen til det overordnede elnet. Som de systemansvarlige er Elsam og Eltra ifølge elforsyningslovens §9 og §28 forpligtet til at udføre ”forsknings- og udviklingsaktiviteter, som er nødvendige for en fremtidig miljøvenlig og energieffektiv transmission og distribution af elektricitet”, den såkaldte Public Service Obligation (PSO) ordning. Nærværende projekt er udført og finansieret under denne ordning.

Opførelse og vedligeholdelse af havvindmølleparker medfører omfattende marine operationer. For at kunne udføre disse på en sikker og økonomisk måde kræves bl.a. detaljerede bølgeprognoser. Formålet med nærværende projekt har været at etablere et bølgeprognosesystem, der kan leve disse bølgeprognoser.

Systemet, der er baseret på numeriske modeller og on-site målinger, er sat op for Horns Rev havvindmøllepark, hvor det har været i drift siden maj 2002. Desuden vil det med mindre ændringer kunne anvendes ved andre havvindmølleparkere. Det skal således anvendes ved Rødsand/Nysted havvindmøllepark fra maj 2003.



2 PROJEKTETS ORGANISERING, FINANSIERING OG TIDSPLAN

2.1 Generelt

Ifølge elforsyningsloven (§9 og §28) er Elsam og Eltra som systemansvarlige for Horns Rev havvindmøllepark forpligtet til at udføre ”forsknings- og udviklingsaktiviteter, som er nødvendige for en fremtidig miljøvenlig og energieffektiv transmission og distribution af elektricitet”. Dette er den såkaldte Public Service Obligation (PSO) ordning. Nærværende projekt er finansieret under denne ordning.

2.2 Projektorganisation

Den projektansvarlige organisation er:

Elsam A/S
Overgade 45
7000 Fredericia

Projektansvarlig: Charles Nielsen
Regnskabsansvarlig: Jens Chr. Sørensen

mens de øvrige projektdeltagere er:

Tech-wise A/S (tidligere ELSAMPROJEKT A/S)
Kraftværksvej 53
7000 Fredericia

Projektansvarlig: J. W. Bonefeld
Faglig projektleder: Jan Pedersen
Nøglemedarbejder: Søren Neckelmann

og

DHI - Institut for Vand og Miljø (tidligere Dansk Hydraulisk Institut)
Agern Allé 11
2970 Hørsholm

Projektansvarlig: Vagner Jacobsen
Nøglemedarbejder: Morten Rugbjerg

Iøvrigt henvises til bilag A, som indeholder projektets oplysningskema.

2.3 Projektfinansiering

Projektet er finansieret under PSO-ordningen af Eltra med en bevilling på 2,8 mill kr. Detaljer fremgår af projektoplysningskemaet i bilag A.



Det skal bemærkes at udgifterne i forbindelse med driften at bølgeprognosesystemet for Horns Rev ikke er afholdt under nærværende projekt.

Sideløbende med nærværende projekt har DHI haft en række andre udviklingsprojekter, som har inkluderet videreudvikling af DHI's bølgemodeller og præsentation af resultater fra disse. Blandt disse kan nævnes udviklingen af DHI's on-line prognoseservice, Vandudsigten, og udvikling af DHI's modeller til at anvende fleksible net. Synergien mellem disse projekter og nærværende projekt har betydet, at de alle er nået meget længere end de ville have gjort hver for sig.

2.4 Projekttidsplan

Projektperioden har været planlagt til at strække sig over perioden 1. januar 2001 til 30. juni 2002. Det blev forlænget i to omgange, senest med brev dateret 18. december 2002 fra Eltra til Tech-wise A/S er projektet, hvor slutdatoen blev flyttet til 31. marts 2003 (med aflevering af en videnskabelig artikel inden 30. juni 2003).

Projektets vigtigste milepæl var 1. maj 2002, hvor bølgeprognosesystemet skulle være i drift, så det kunne anvendes ved opstilling og montage af vindmøllerne på Horns Rev. Denne deadline blev overholdt, idet bølgeprognosesystemet kørte i test fra slutningen af marts og var i normal drift fra 1. maj 2002.

Den endelige projektplan fremgår af tabel 2.1, mens den oprindelige tidsplan kan ses i bilag A (projektoplysningsskemaet). Beskrivelsen af de enkelte faser fremgår af kapitel 4

Tabel 2.1 Endelig projekttidsplan

	2001				2002				2003	
	1	2	3	4	1	2	3	4	1	2
Fase 1 – forprojekt										
Fase 2 – målesystem										
Fase 3 – bølgemodeller										
Fase 4 – evaluering										
Fase 5 – formidling										



3 PROJEKTETS RESULTATER

3.1 Generelt

Formålet med nærværende projekt har været at etablere et bølgeprognosesystem, som kan anvendes ved planlægning af og under marine operationer ved opførelse og vedligeholdelse af havvindmølleparker.

Det system, som er udviklet, består af

- et on-line marint målesystem
- en operationel numerisk bølgeprognosemodel
- en løbende korrektion af bølgeprognoseren baseret på den aktuelle måling
- præsentation af bølgeprognoseren overfor brugerne

En overordnet beskrivelse af systemet, som er anvendt ved Horns Rev Havvindmøllepark, og som skal anvendes ved Rødvand Havvindmøllepark, er givet i de følgende afsnit sammen med en oversigt over, hvorledes projektets resultater er formidlet. Endelig er en beskrivelse af de økonomiske implikationer ved anvendelse af bølgeprognosene ved opførelsen af Horns Rev Havvindmøllepark inkluderet.

3.2 Bølgeprognoser for Horns Rev Havvindmøllepark

Til anvendelse for alle, der skulle sejle, montere og foretage andre marine operationer i forbindelse med opførelse af Horns Rev Havvindmøllepark, har bølgeprognosser fra det system, som er udviklet under nærværende projekt, været tilgængelige fra den 1. maj 2002. Efter at alle vindmøller er sat i drift, hvilket for den sidste vindmølle vedkommende skete i midten af december 2002, er prognosesystemet fortsat med at leve tilbage til den efterfølgende vedligeholdelse.

Systemetopsætningen er illustreret i fig 3.1. Bølgeprognosesystemet indgår som en del af DHI's operationelle prognosesystem, Vandudsigten, hvilket bl.a. har givet en række fordele i forbindelse med overvågning af systemet. Figuren viser, hvorledes målinger fra målesystemet på Horns Rev anvendes til at korrigere bølgeprognoseren fra den specielle bølgemodel for Nordsøen og Horns Rev før den sendes videre til præsentation på en række websites. Bølgeprognosekorrektionen er foretaget én gang i timen på basis af den aktuelle måling, og er baseret på kunstige neurale netværk (eller Artificial Neural Networks, ANN).

Målingerne fra Horns Rev indsamlies på Tech-wises server før de sendes videre til Vandudsigten. Et eksempel på en webpræsentation af målingerne fra denne server sammen med den korrigerede prognose sendt fra Vandudsigten ses i fig 3.2. En tydeligere præsentation af de enkelte grafer fås på websiten ved klik på graferne.

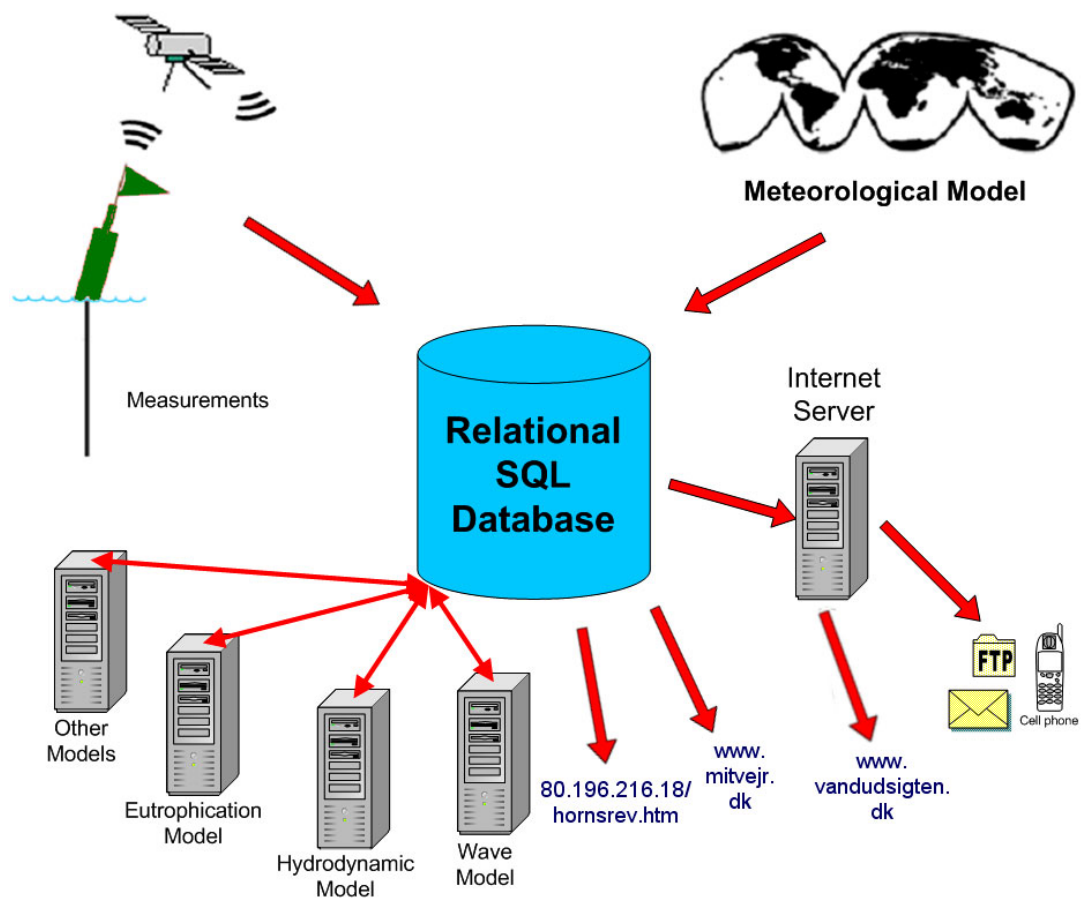


Fig 3.1 Dataflow i Vandudsigtens del af bølgeprøgnosesystemet for Horns Rev

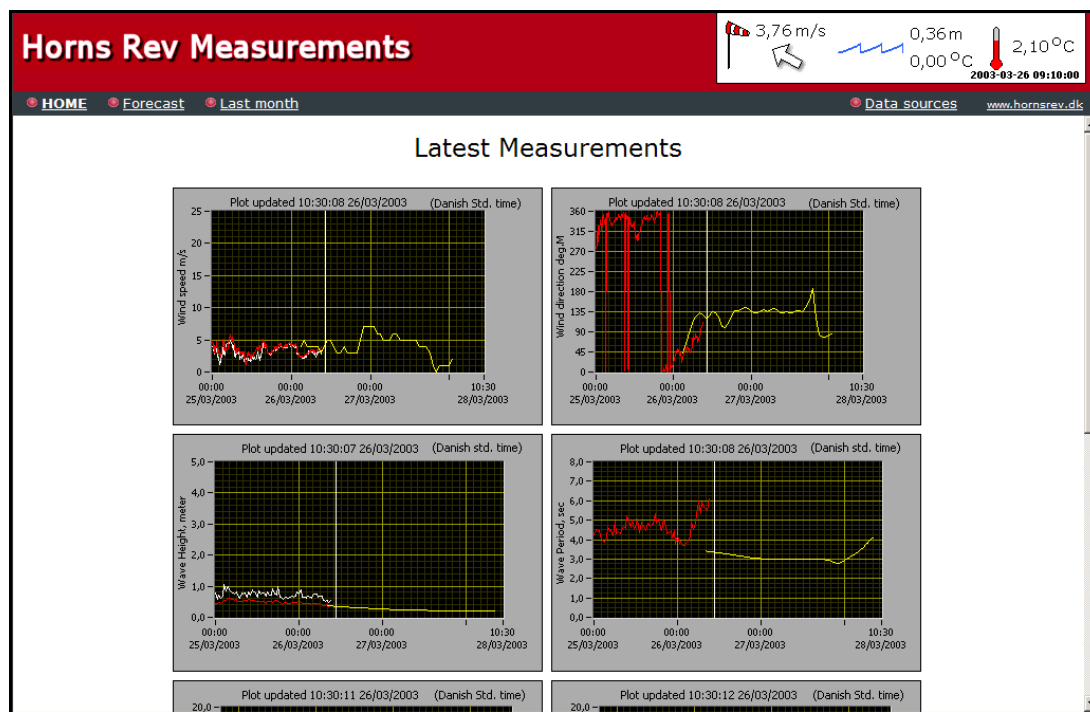


Fig 3.2 Bølgeprøgnosepræsentation på 80.196.216.18/hornsrev.htm



Udover at være tilgængelige på Tech-wises webserver på <http://80.196.216.18/hornsrev.htm>, har bølgeprognoser også været tilgængelige for kunder via Vejr2's website på www.mitvejr.dk og DHI's website på www.vandudsigten.dk.

Et eksempel på en korrigeredt bølgeprognose og den ukorrigerede prognose kan ses i fig 3.3. Her er illustreret, hvorledes en bølgemåling kl 12 (den 1. september 2002) har ”løftet” en bølgeprognose, som uden korrektion ville have forudsagt for små bølgehøjder. Dette kan ses ved sammenligning af den korrigerede prognose og de målinger, som blev foretaget efter kl 12.

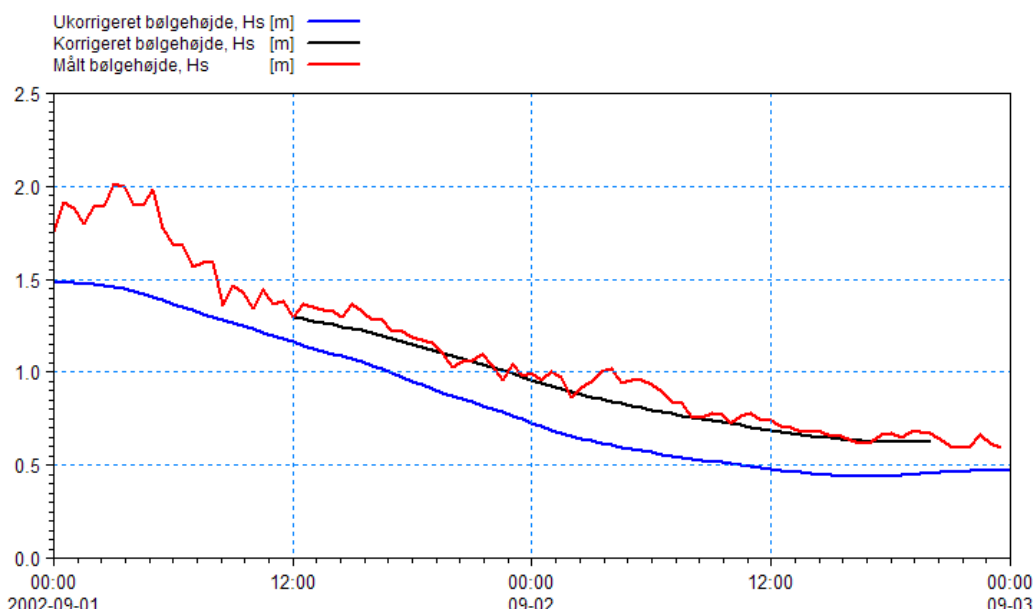


Fig 3.3 Eksempel på en ukorrigert og korrigert prognose fra den 1. september 2002 kl 12. Desuden er efterfølgende målinger vist.

Fra bølgeprognosemodellen er 5-døgns prognoser af følgende parametre beregnet to gange i døgnet, hvorefter de er gjort tilgængelige via alle eller nogle af ovennævnte websites:

- bølgehøjde (H_s), -periode (T_{02} og T_p) samt –retning
- dønninghøjde, -periode og –retning
- bølgespektre i udvalgte punkter

Førstnævnte bølgehøjde (H_s) indeholder både vindssø og dønninger.

Dønninger er inkluderet, da de viste sig at være af stor betydning for de marine operationer.

En detaljeret beskrivelse af målesystemet, bølgemodellen og korrektionsproceduren er inkluderet i afsnit 4.



3.3 Bølgeprognosesystemet for andre havvindmølleparker

Prognosesystemet, som anvendt for Horns Rev Havvindmøllepark, kan sættes op ved andre havvindmølleparker, hvis følgende er tilstede:

- on-line bølgemålinger
- en bølgeprognosemodel
- en periode med samtidige målinger og prognoser til ”oplæring” af ANN-korrektionsproceduren

I forbindelse med montering og efterfølgende vedligeholdelse vil systemet blive sat op for Rødsand/Nysted Havvindmøllepark syd for Lolland. Målinger foretages af Energi E2, mens Vandudsigtens generelle bølgeprognose for de indre danske farvande vil blive anvendt som bølgemodel. Bølgeprognosser sammen med prognosser for bl.a. strøm, vandstand, vind og vandtemperatur vil blive præsenteret via Vandudsigtens website. Et eksempel på en præsentationsside kan ses i fig 3.4. Systemet skal være operationelt fra starten af maj 2003.

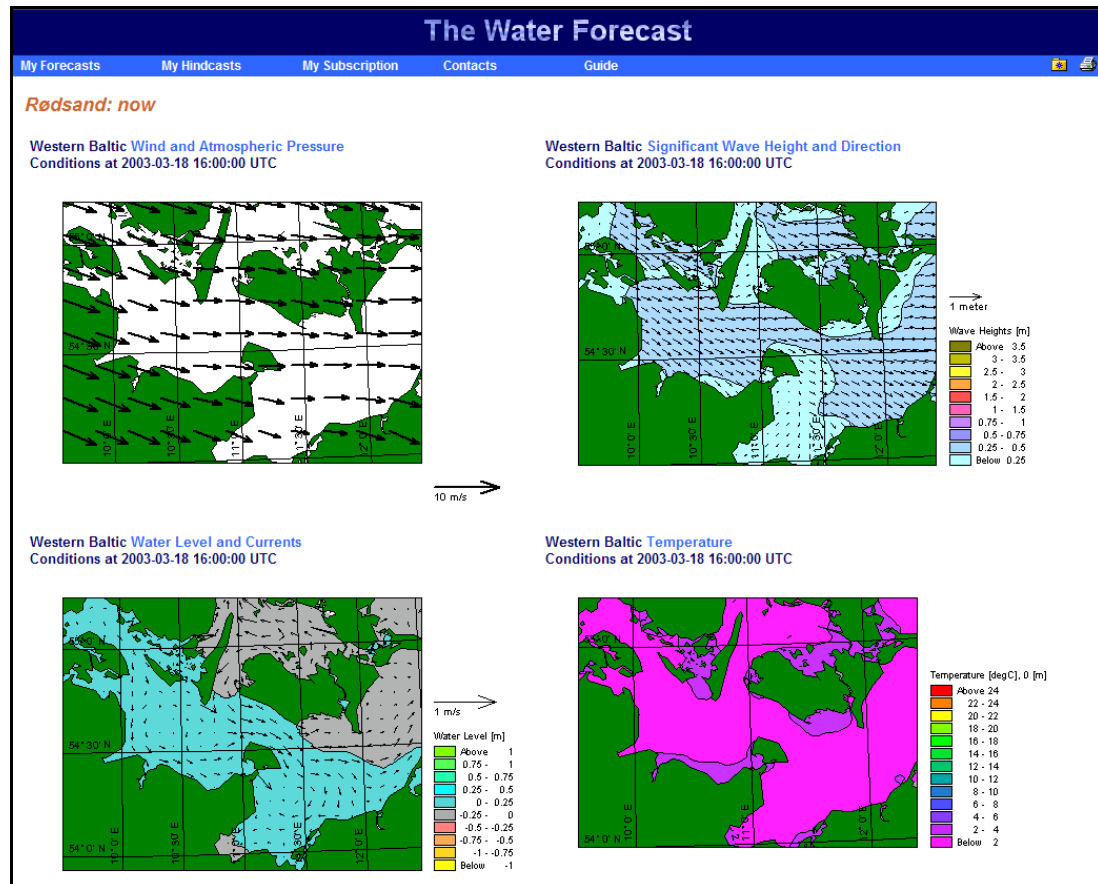


Fig 3.3 Eksempel på præsentation for Rødsand Havvindmøllepark på Vandudsigtens website



3.4 Formidling af projektets resultater

Den viden, som er opsamlet hen igennem projektet, de tekniker, som er udviklet, samt selve bølgeprognoserne formidles på følgende måder:

- Bølgeprognoserne for Horns Rev er tilgængelige på tre websites:
80.196.216.18/hornsrev.htm, www.mitvejr.dk og www.vandudsigten.dk.
- Bølgeprognoser for andre havvindmølleparker vil kunne gøres tilgængelige på www.vandudsigten.dk. Således vil bølgeprognosesystemet blive anvendt for Rødsand Havvindmøllepark syd for Lolland fra primo maj 2003.
- Udviklingen af bølgemodellen med fleksibelt net er beskrevet i en videnskabelig artikel ("A Third Generation Spectral Wave Model using an Unstructured Finite Volume Technique" - se bilag D), som sendes til tidsskriftet Coastal Engineering for offentliggørelse
- Udviklingen af bølgeprognosesystemet vil blive beskrevet i en videnskabelig artikel (med den tentative titel "Wave Forecasting for Offshore Wind Farms"), som forventes sendt til tidsskriftet Coastal Engineering medio 2003 for offentliggørelse
- Den generelle beskrivelse af projektet er givet i nærværende rapport

3.5 Økonomiske fordele ved anvendelse af bølgeprognosesystemet

Ved afslutningen af projektet er dets økonomiske implikationer ved anvendelsen af bølgeprognosesystemet ved opførelsen af Horns Rev Havvindmøllepark vurderet.

De to mest almindelige konsekvenser som følge af fejlskøn over vejrforholdene (bølger og vind) vil være:

- mobilisering til en plads, hvor det konstateres, at der ikke kan arbejdes
- forbliven i havn selv om forholdene tillader, at der kan arbejdes

Derudover kan tænkes situationer, hvor et fartøj bliver fanget i en hurtig vejromskifring og må nødankre på pladsen.

Et eksempel på betydningen af en detaljeret lokal prognose, som udarbejdet gennem dette projekt, haves fra en af de udenlandske underentreprenører på Horns Rev. Vedkommende havde forud for opgaven sikret sig en bølgeprognose dækende den relevante del af Nordsøen fra vedkommendes lokale meteorologiske institut (en tilsvarende prognose kan findes på DMI's hjemmeside over Tyskebugt). En sådan prognose gældende for et større område og uden en detaljeret modellering af bathymetri i lokalområdet giver alt for grove estimer og kan i praksis ikke benyttes uden lokalt fortolkningskendskab. Resultatet for denne entrepenør var, at kun ca. halvdelen af de mulige arbejdsdage i den første måned af installationsperioden blev udnyttet, dvs. en udnyttelsesgrad på ca. 50%. Efter en evaluering af forholdene blev entrepenøren bedt om at benytte den i dette projekt udarbejdede prognose, hvorefter udnyttelsesgraden steg til tæt ved 100 %.



Med totale offshore installationsomkostninger på omkring 350 mio. kr. (Elsam og Eltra) for Horns Rev Havvindmøllepark, vil selv små forbedringer af udnyttelsestiden have store økonomiske konsekvenser. De gunstige vejrforhold, der herskede i installationsperioden på Horns Rev, taget i betragtning, vurderes det, at den detaljerede bølgeprognose forbedrede udnyttelsesgraden med 10-15 % svarende til omkostninger i størrelsesordenen 30-50 mio. kroner.



4 DETALJERET BESKRIVELSE AF PROJEKTETS FASER

4.1 Projektets formål og opdeling

Opførelse og vedligeholdelse af havvindmølleparker medfører omfattende marine operationer. For at kunne udføre disse på en sikker og økonomisk måde kræves bl.a. detaljerede bølgeprøgnoser. Formålet med nærværende projekt har været at etablere et bølgeprøgnosesystem, der kan levere disse bølgeprøgnoser, og at gøre dette system operationelt for Horns Rev havvindmøllepark.

Projektet har været opdelt i følgende 5 faser:

1. forprojekt med erfarringsindsamling og identifikation af forskellige prognoseteknikker
2. opstilling af et marint målesystem på Horns Rev til indsamling af bl.a. vind- og bølgedata
3. opstilling af et numerisk bølgeprøgnosesystem efter de i fase 1 identificerede teknikker og indeholdende korrektioner af prøgnoserne baseret på aktuelt målte bølgeforsyninger
4. evaluering og revision af det opstillede bølgeprøgnosesystem
5. formidling af projektets resultater

De enkelte faser er beskrevet nedenfor.

4.2 Fase 1 – forprojekt med erfarringsindsamling

4.2.1 Generelt

Et tidligere eksempel på forudsigelse af hydrografiske parametre i danske farvande er installationen af de 60.000 tons tunge tunnelementer i Drogdenrenden i Øresund fra august 1997 til januar 1999. En strømprøgnose baseret på en kombination af deterministiske modeller, on-line målinger og anvendelsen af neurale netværk sikrede en succesrig installation af samtlige elementer uden fordyrende downtime (se ref /1/). Bl.a. med dette eksempel i mente blev nærværende projekt igangsat.

4.2.2 Valg af bølgemodel

I foråret 2001 besluttede DHI at gå ind på markedet for prøgnoseydelser indenfor vandområdet leveret via Internettet. Vandudsigten, som servicen kaldes, startede den 1. juni 2001. På www.vandudsigten.dk og www.waterforecast.com leveres 5-døgnsprediktioner for Nordsøen, indre danske farvande og Østersøen for bølger, strøm, vandstand, salinitet, vandtemperatur, ilt og klorofyl. En kort beskrivelse af Vandudsigten er inkluderet i bilag C. Således eksisterede hele den bagvedliggende organisation for operationelle ydelser fra dette tidspunkt på DHI inklusiv en bølgemodel dækkende



Nordsøen og Horns Rev. Bølgemodellen var dog ikke detaljeret nok omkring Horns Rev til at opfylde nærværende projekts nøjagtighedskriterier.

For at kunne opnå en tilstrækkelig nøjagtighed var en detaljeret model omkring Horns Rev nødvendig. Ved bestemmelsen af designbølgehøjder for vindmøllefundamenterne (se ref. /2/) blev en kombination af to bølgemodeller anvendt:

- en regional model med et kvadratisk beregningsnet på 55,56 km i hele modelområdet og 18,52 km langs Vestkysten og i Skagerrak (se fig 4.1). Bølgemodellen var en fuldt spektral og tidsvarierende model, MIKE 21 OSW.
- en række lokale modeller - én for hver af de 8 hovedkompasretninger – med et rettangulært beregningsnet på 200 m x 50 m dækkende Horns Rev (se fig 4.2). Denne model var en parametreret (dvs ikke fuldt spektral) og stationær model, MIKE 21 NSW.

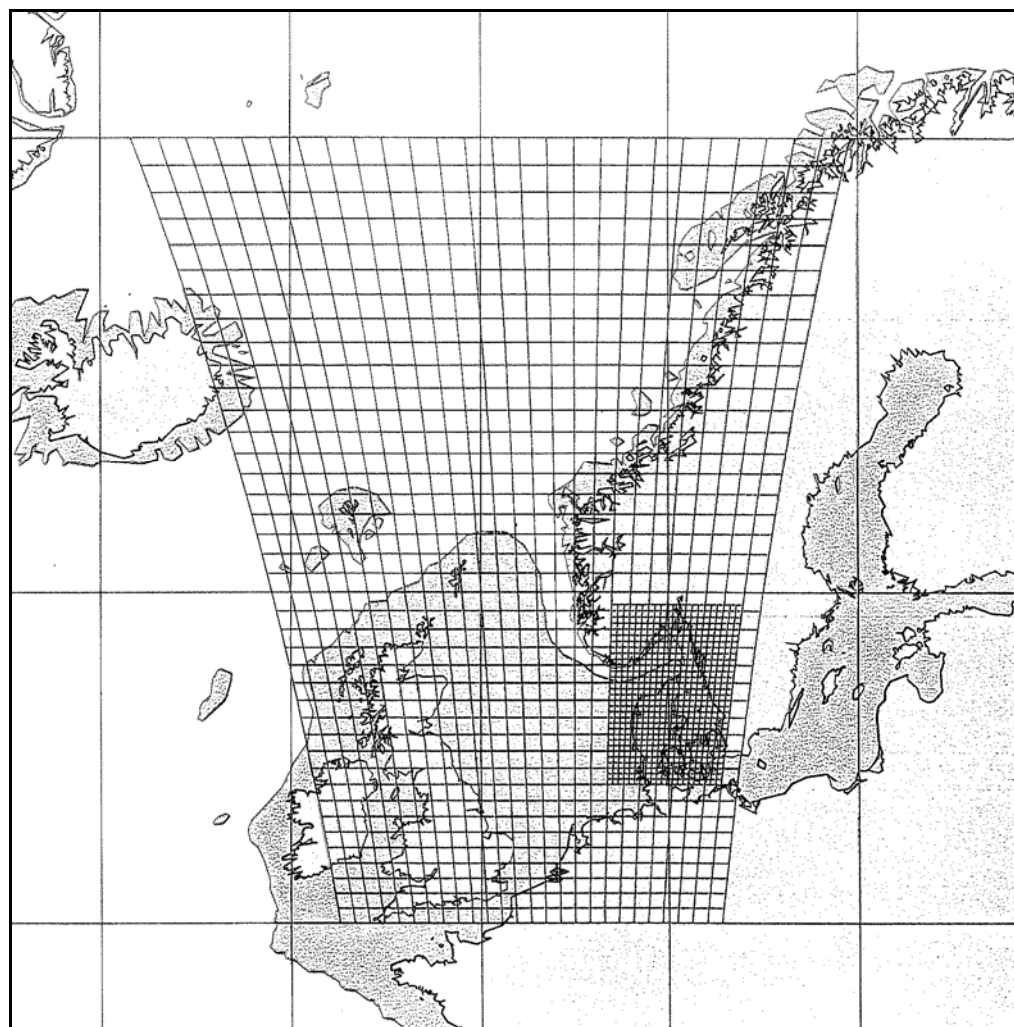


Fig 4.1 Beregningsnet for regionale bølgemodeller anvendt ved beregning af designbetingelser for vindmøllefundamenterne på Horns Rev havvindmøllepark.

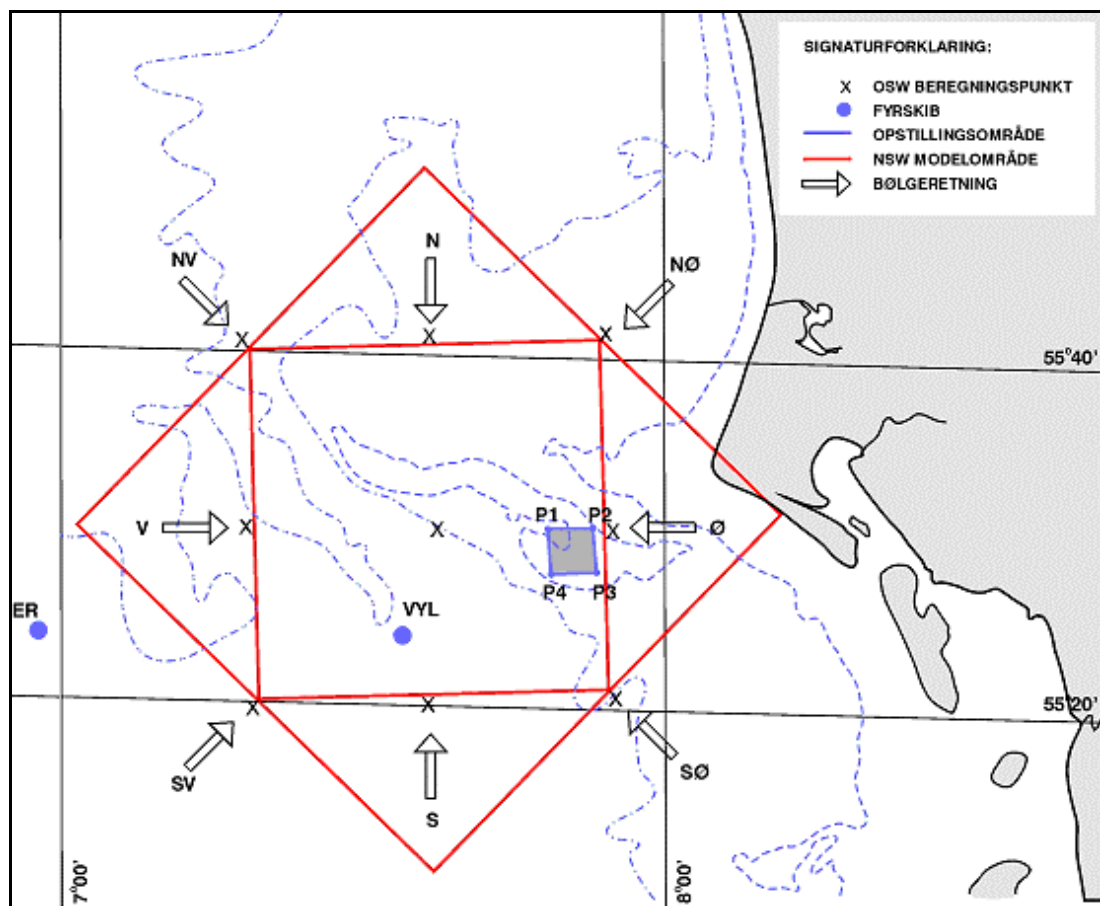


Fig 4.2 Beregningsnet for lokale bølgemodeller anvendt ved beregning af designbetingelser for vindmøllefundamenterne på Horns Rev havvindmøllepark

Årsagen til at denne kombination af bølgemodeller var valgt var, at det gav mulighed for en meget detaljeret beskrivelse af bølgeforholdene i opstillingsområdet. Metoden kræver imidlertid, at der skal anvendes forskellige lokalmodeller (MIKE 21 NSW-modeller) alt efter fra hvilken retning bølgerne nærmer sig Horns Rev i den regionale model (MIKE 21 OSW).

På det tidspunkt, da valget af bølgemodeller til nærværende projekt skulle foretages, viste en ny mulighed sig, idet DHI var begyndt på udvikling af modeller med fleksible net. Dette vil sige net bestående af trekantede (eller firkantede) af varierende størrelse indenfor modelområdet. Ved at anvende en enkelt model dækende hele interesseområdet kunne alle problemer med overførsel af data fra den regionale model til en den relevante lokale model undgås. Det besluttedes derfor at gøre nærværende projekt til et pilotprojekt for anvendelse af en fuldt spektral og tidsvarierende bølgemodel med fleksibelt net. Modellen betegnes MIKE 21 SW.

Fig. 4.3 og fig. 4.4 viser det anvendte MIKE 21 SW beregningsnet. Bemærk, at der er tale om en enkelt model; fig 4.4 viser blot et udsnit af det totale modelområde, som er vist i fig 4.3.

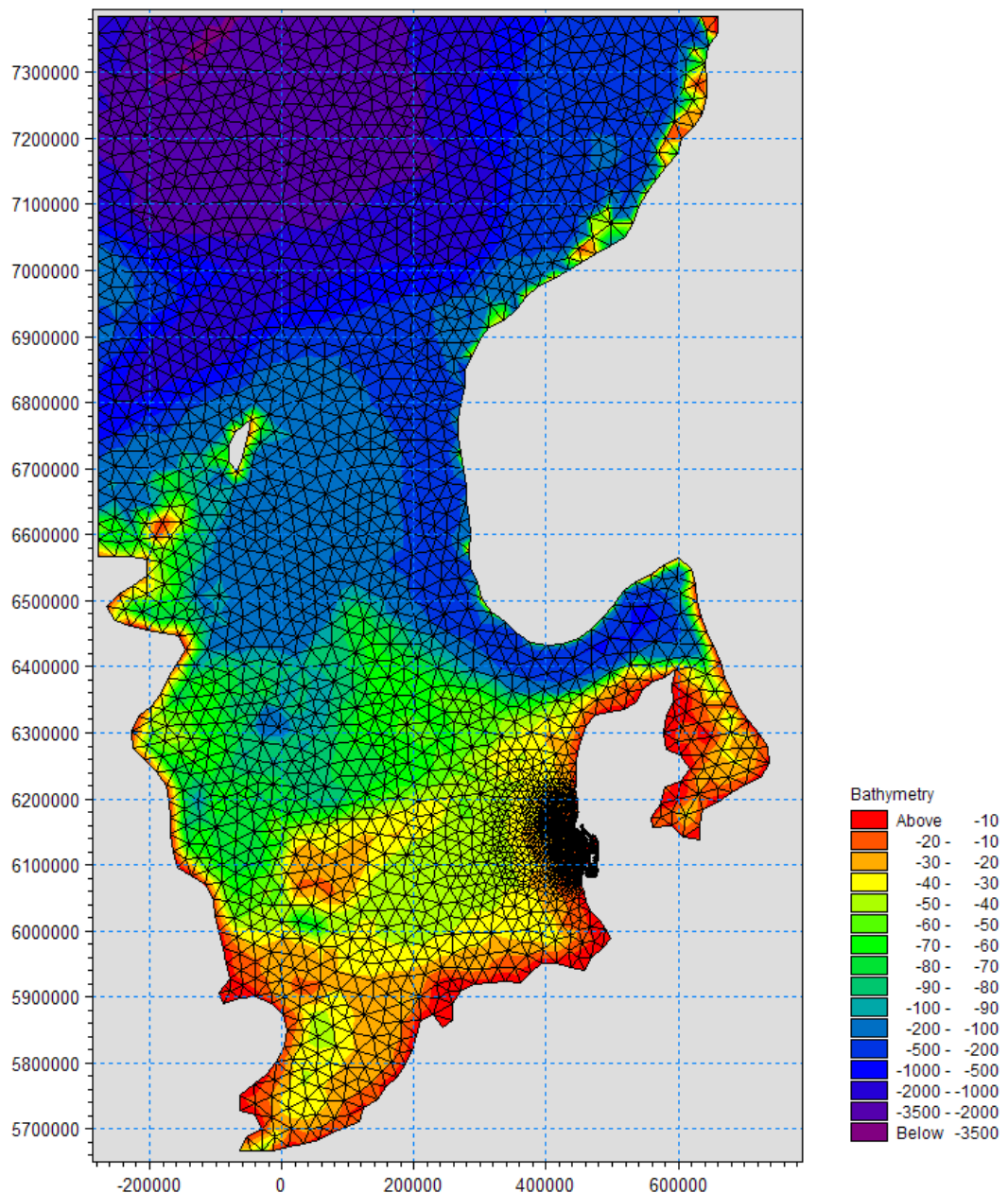


Fig 4.3 Beregningsnet for bølgemodel med fleksibelt net. Akserne viser UTM-koordinater (zone 32)

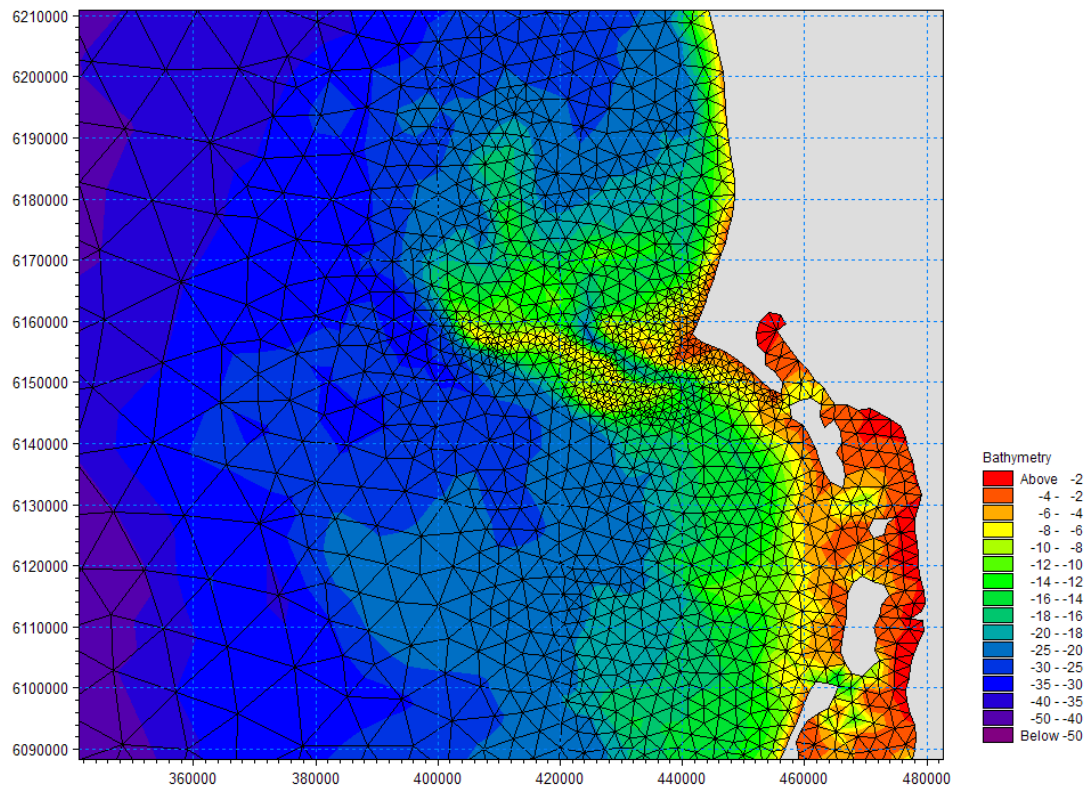


Fig 4.4 Detaljer i beregningsnettet for bølgemodel med fleksibelt net omkring Horns Rev. Akserne viser UTM-koordinater (zone 32)

4.3 Fase 2 – opstilling af marint målesystem

4.3.1 Beskrivelse af målesystemet

Målesystemet blev bygget op omkring allerede tilstedeværende komponenter der blev etableret i forbindelse med PSO-2000 projektet ”Måleprogram for vind, bølger og strøm på Horns Rev”, ELTRA projekt nr. EG-05 3248.

Installationsmæssigt er der primært to begrænsende faktorer for hvornår materiellet kan operere offshore – vindstyrken og bølgehøjden. Fokus blev derfor lagt på måling af disse to parametre. Bølgetilstanden repræsenteres ved den såkaldte signifikante bølgehøjde H_s , den maksimale bølgehøjde H_{max} i måletidsrummet samt den tilhørende gennemsnitlige bølgeperiode, og vindstyrken ved 10-minutters middelvinden i 62 og 15 meters højde samt vindretningen.

I forhold til det eksisterende system var en række ændringer nødvendige, idet systemet oprindeligt var etableret til at levere data hjem lejlighedsvis ved manuelt at kalde op til målestationerne og downloade data. Dette betød i praksis at dataoverførsel blev foretaget en til to gange om ugen. For at kunne benyttes til nærværende projekt var en total omprogrammering og restrukturering af systemet nødvendig, således at data automatisk kunne hjemtages med en frekvens på minimum en gang i timen. Omprogrammering af opkaldssoftware og andre systemændringer blev foretaget af Tech-wise.

Det endelige system er vist skematisk på fig. 4.5.

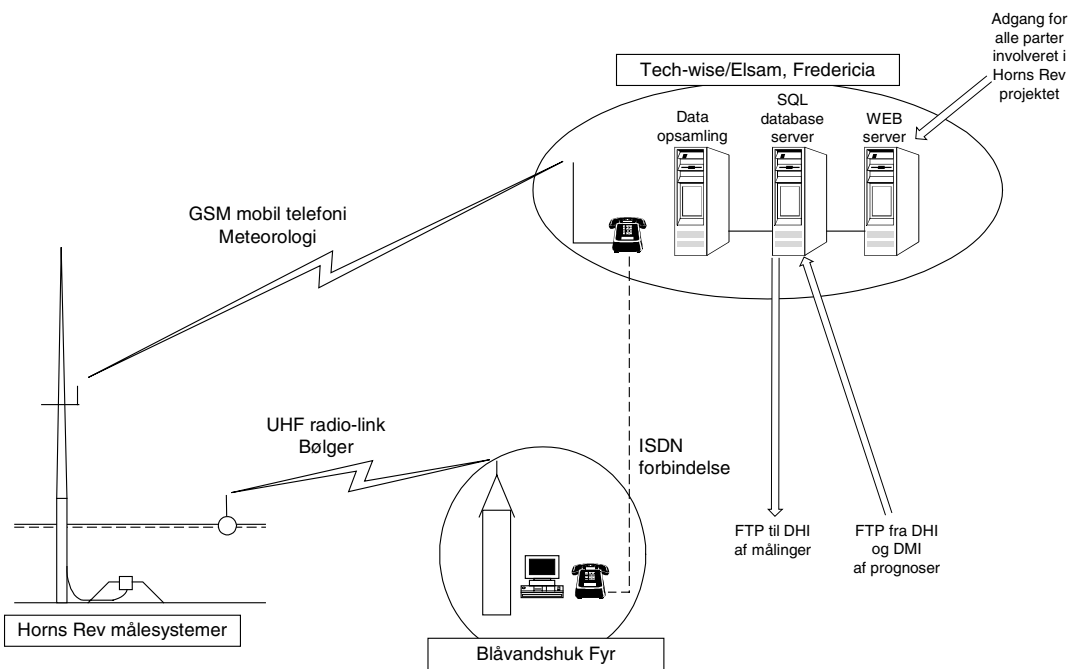


Fig 4.5 Skematisk opbygning af målesystem.

Selve processen omkring datahjemtagning og udarbejdelse af opdateret prognose på baggrund af nyeste målinger er som følger:

1. Dataopsamlings-PC'en kontakter via GSM mobil telefoni målemasten og downloader de seneste data fra den interne datalogger.
2. Dataopsamlings-PC'en downloader via FTP de seneste bølgeregistreringer fra opsamlingsenheden placeret på Blåvandshuk Fyr.
3. Nyeste data gemmes i SQL database, hvorfra de via FTP overføres til DHI (bølger) og DMI (vind)
4. Ca. 15 minutter senere downloades fra DHI en, på baggrund af de modtagne målinger, opdateret bølgeprognose (ANN korrektion).
5. De opdaterede prognoser gemmes i SQL databasen.
6. Ved udtræk fra databasen generes nye plot over målinger og prognoser til præsentation på <http://80.196.216.18/hornsrev.htm>, som er en til installationsfasen specifikt oprettet WEB-side der er frit tilgængelig

Ovenstående proces gentages en gang hver time døgnet rundt.

Et væsentligt aspekt i ovenstående er timingen mellem de enkelte sekvenser, specielt timingen mellem overførsel af data mellem de 3 involverede parter (Tech-wise, DHI og DMI).



4.3.2 Præsentation af målinger

I fig 4.6 er vist tidsserieplot af hhv. vindstyrke og signifikant bølgehøjde fra installationsperiodens start i marts 2002 og indtil nu. Datadækningsgraden for de to målinger er hhv. 99.9 % og 92.4 %.

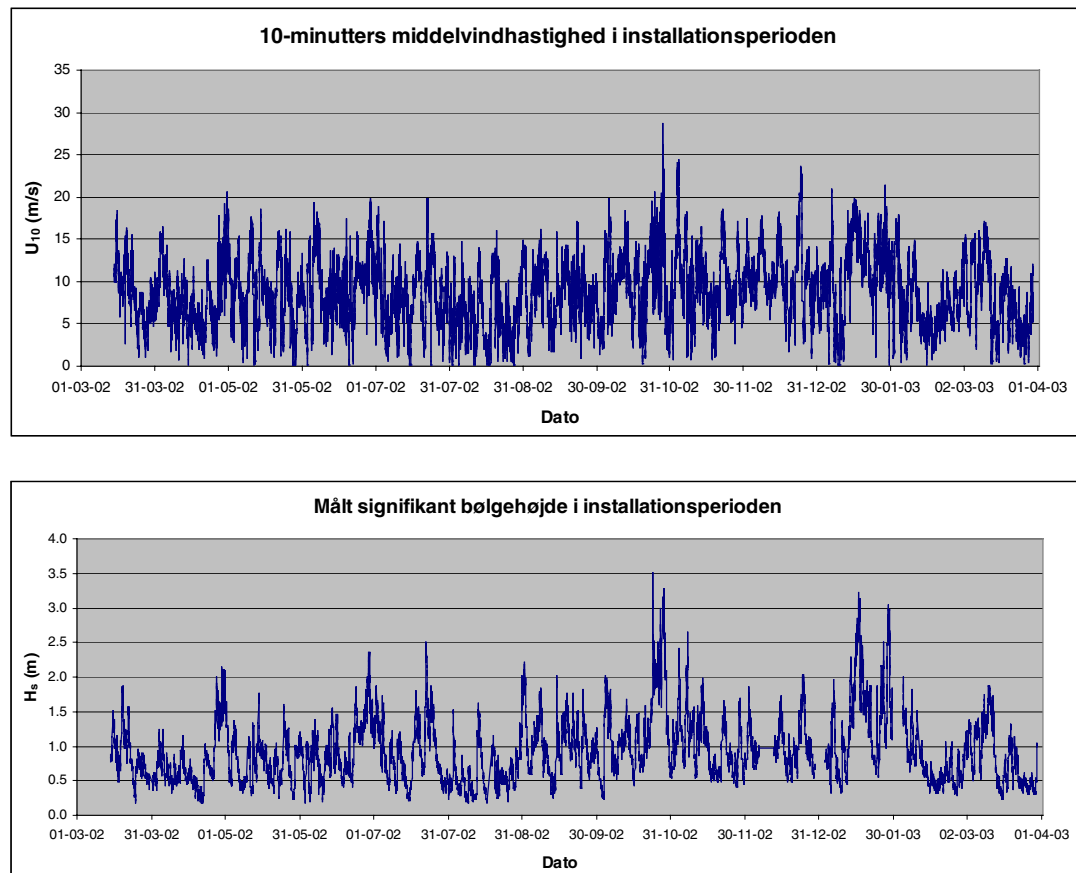
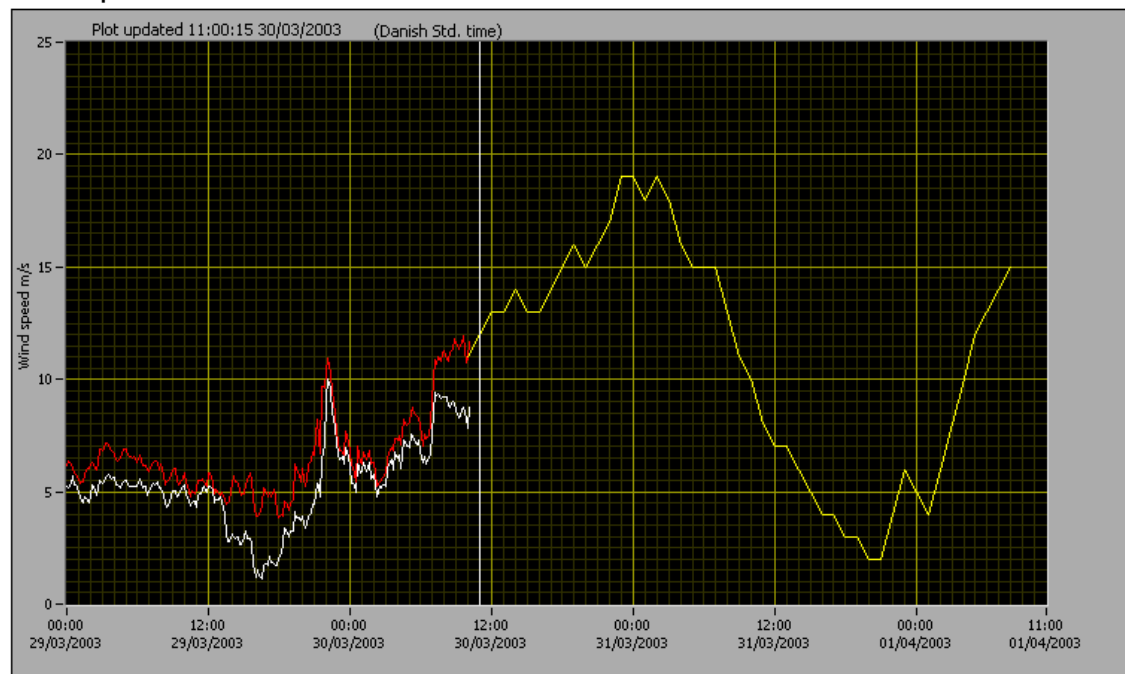


Fig 4.6 Dækningsgrad for målinger

Målingerne præsenteres overfor entrepenører og andre brugere som tidsserier over det forløbne 1½ døgn sammen med en 48 timers prognose på projektets hjemmeside (<http://80.196.216.18/hornsrev.htm>). Eksempler på præsentationen af hhv. vindstyrke og bølgehøjde målinger (sammen med 48 timers prognose) er vist i fig 4.7.



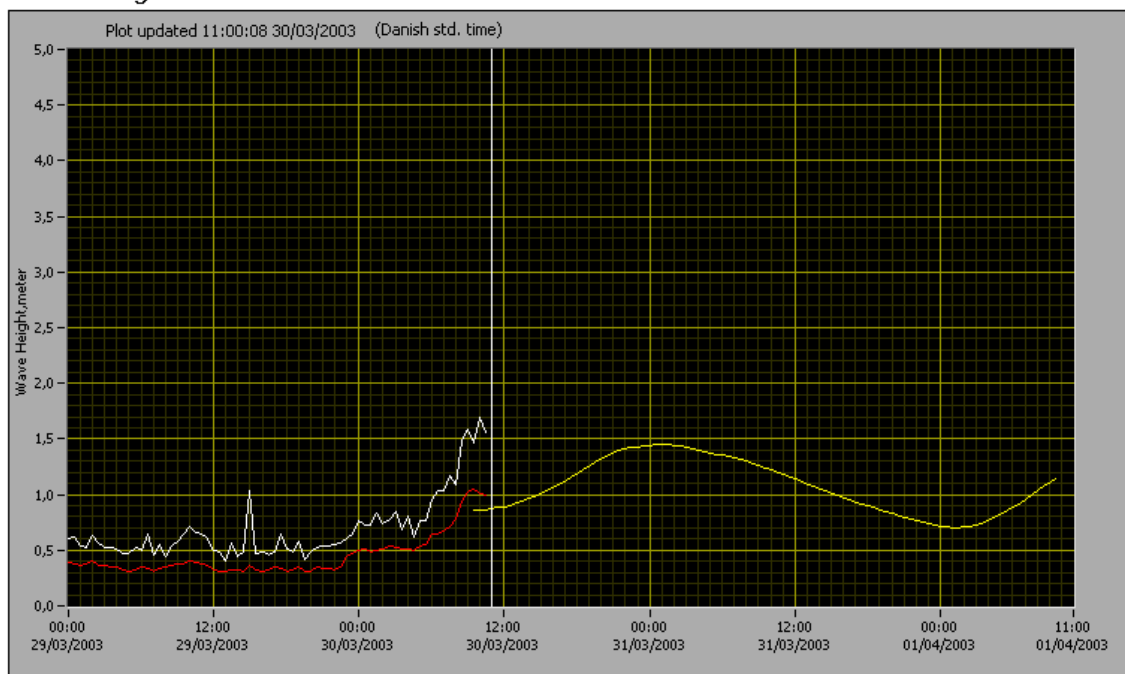
Wind Speed Forecast for Horns Rev



Description:

Red: Measured wind speed at level 62 (10 min avg)
White: Measured wind speed at level 15 (10 min avg max(15SW,15NE))
Yellow: Latest wind speed forecast (1h avg)

Wave Height at Horns Rev



Description:

White: Measured Hmax
Red: Measured Hs
Yellow: Latest Hs forecast

Fig 4.7 Eksempler på præsentationer på <http://80.196.216.18/hornsrev.htm>



4.3.3 Drift af målesystemet

Med de mange overførsler af data samt timingen af disse imellem de forskellige parter, har det krævet en del ressourcer at holde systemet kørende. Løbende er der blevet udført modifikationer for at forbedre systemets robusthed over nedbrud, som følge af udfald af kommunikationslinier eller nedbrud af udstyr. Da det udviklede system har været intensivt benyttet af de fleste af de entrepenører der arbejdede med opførelsen af vindmølleparken på Horns Rev, har det været essentielt at systemet fungerede.

4.4 Fase 3 – opstilling af bølgeprognosesystem

4.4.1 Opstilling af bølgemodel

Som beskrevet i afsnittet 4.2 (fase 1) blev DHI's fuldt spektrale og tidsvarierende bølgemodel med fleksibelt beregningsnet, MIKE 21 SW, valgt som bølgemodel. MIKE 21 SW er således en videreudvikling af den offshore bølgemodel, MIKE 21 OSW, som har været anvendt på DHI i en lang årerække. En generel beskrivelse (på engelsk) af MIKE21 OSW og MIKE 21 SW er inkluderet i bilag B. Desuden er det teoretiske grundlag beskrevet meget grundigt i en videnskabelige artikel inkluderet i bilag C.

Det område, som er dækket af bølgemodellen er vist i fig 4.3 og 4.4.

Til beregning af en 5-døgns bølgeprognose kræves følgende input til modellen:

- havdybder i alle beregningspunkter
- vindhastighed og –retning i alle beregningspunkter for hvert tidstrin i den 5 døgn lange beregningsperiode.

Mens havdybderne er tilgængelige fra søkort og opmålinger omkring Horns Rev, er vinddata tilgængelige via DHI's genrelle prognoseservice, Vandudsigten. Her modtages to gange dagligt en 5-dages vindprognose for Nordsøen, indre danske farvande og Østersøen fra det meteorologiske firma Vejr2 A/S.

Som output fra modellen produceres for hver halve time i de 5 døgn:

- bølgehøjde (H_s), -periode (T_{02} og T_p) samt –retning
- dønninghøjde, -periode og –retning
- bølgespektre i udvalgte punkter

Førstnævnte bølgehøjde (H_s) indeholder både vindsø og dønninger.

At inkludere dønningparametre som output fra modellen er nyt i forhold til tidligere bølgemodelberegninger på DHI. Der findes ikke nogen entydig beskrivelse af dønninger, hvorfor flere beregningsmåder er blevet afprøvet. Disse er tilpasset efter feedback fra brugerne på Horns Rev. Beregningen af dønningparametrene er beskrevet nærmere i afsnit 4.5.

Opdeling af bølger i dønninger og vindsø kan visualiseres v.h.a. et plot af bølgespektret, som viser fordelingen af bølger på bølgeperioder og –retninger på et givet tidspunkt. Et



eksempel kan ses i fig 4.8, hvor der ses en kombination af dønninger med periode omkring 10 sekunder fra nordvest og vindgenereret ø fra syd-sydvest med periode på 7 sekunder.

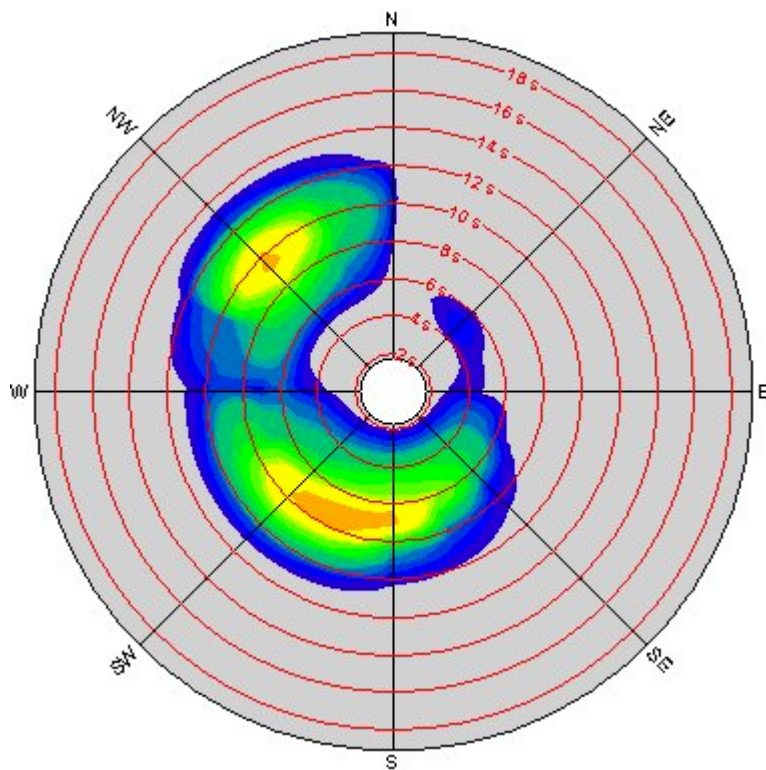


Fig 4.8 *Bølgespektrum med vindø fra SSV og dønninger fra NV. Fra Jyske Rev den 29. april 2002 kl 00 UTC.*

En vigtig del af opsætningen af en bølgemodel er tilpasning af en række modelparametre, således at modellen beregninger passer med målinger fra området. Resultatet af denne modelkalibrering og –validering er vist som en del af den videnskabelige artikel i bilag C. Her er modelberegninger sammenlignet med målinger fra bl.a. Horns Rev og Fjaltring.

Et eksempel på et vindfelt (model input) og de tilhørende bølgemodelresultater er vist i fig 4.9 og 4.10.

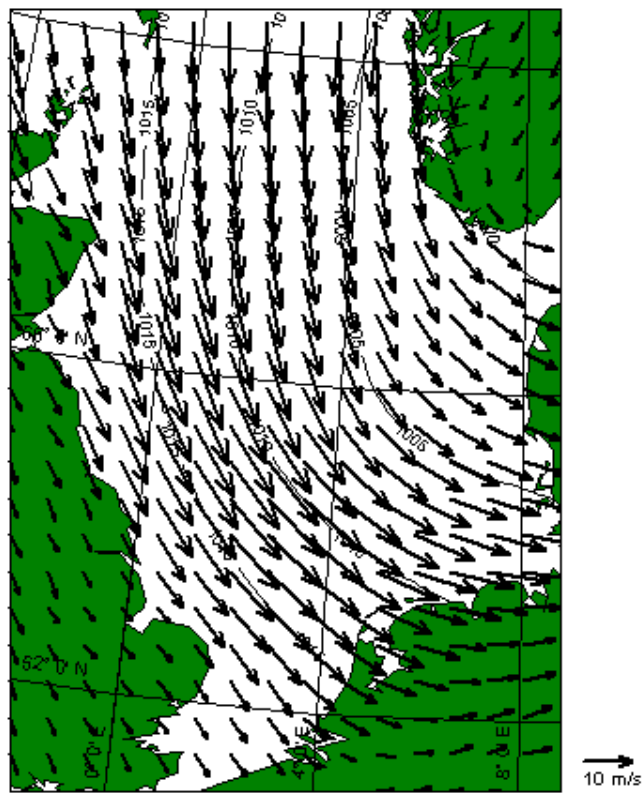


Fig 4.9 Vindfelt i Nordsøen den 28. juni 2002 kl 03 UTC

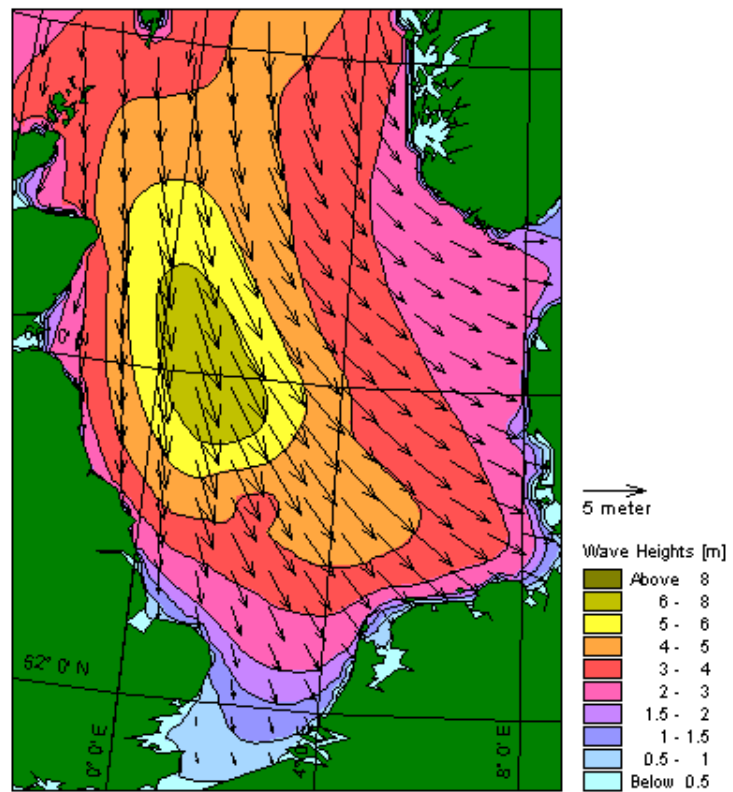


Fig 4.10 Bølgefelt i Nordsøen den 28. juni 2002 kl 03 UTC



4.4.2 Korrektion af bølgeprognoser på basis af bølgemålinger

En bølgeprognose, som beregnes på basis af en vindprognose, er ikke en ”perfekt” prognose, idet hverken vindprognosen eller den efterfølgende bølgeprognoseberegning med bølgemodellen er perfekte. Fra målestasjonen ved Horns Rev ved man imidlertid, hvad bølgehøjden er her og nu. Ved at korrigere bølgeprognosen på basis af den målte bølgehøjde kan en væsentligt forbedret prognose opnås.

Til korrektion af bølgeprognosene for Horns Rev er anvendt tekniker kendt som ”kunstige neurale netværk” (Artificial Neural Networks, ANN, på engelsk). En general beskrivelse af anvendelse af kunstige neurale netværk i forbindelse med prognoser er inkluderet i bilag E.

Et kunstigt neutralt netværk er (som det er anvendt i nærværende projekt) en række matematiske funktioner med en række parametre, som optimeres til på den bedste måde at forudsige en variabel (bølgehøjden) baseret på en række variable (en målt bølgehøjde og en modelleret bølgehøjdeprognose). Funktionerne og parametrene findes ved at genemgå en lang række situationer, hvor alle variable er kendt – den såkaldte oplæring.

Efter at have afprøvet en lang række kombinationer af funktioner, blev nogle få udvalgt bl.a. på basis af kendskab til de fysiske processer, som styrer bølgehøjdevariationen. En beskrivelse af de valgte funktioner og parametre (kaldet ANN-korrektionen) kan ses i bilag F.

I fig 4.11 er forbedringen ved anvendelse af ANN-korrektionen illustreret. Mens en ukorrigert prognose i middel har en fejl (spredning) på 0.26 m – 0.28 m indenfor de første 24 timer i en prognose, så varierer fejlen på den korrigerede prognose fra 0 m – 0.24 m. Den grønne kurve viser, hvor stor fejlen vil være, hvis målingen foretaget til tiden 0 timer blev brugt som prognose for de efterfølgende 24 timer.

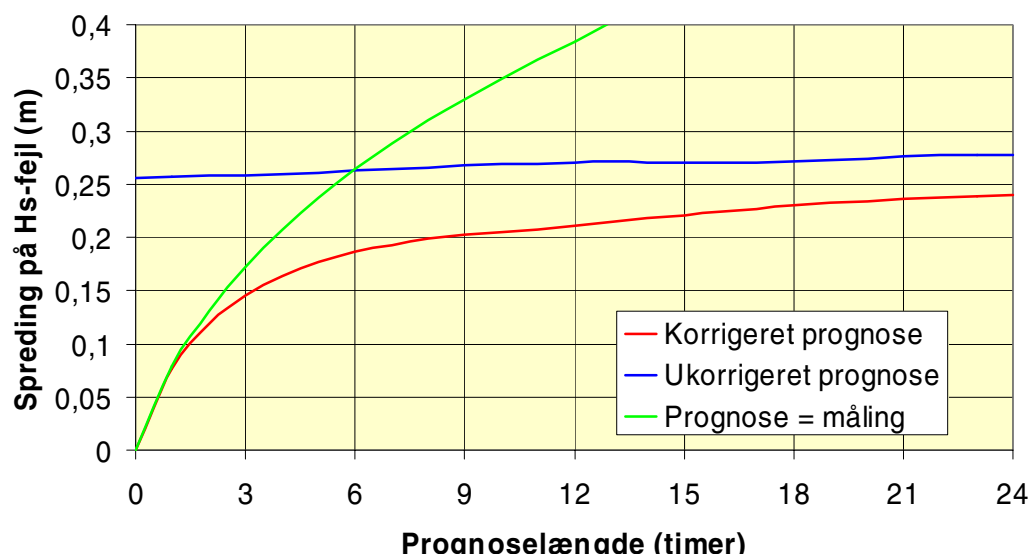


Fig 4.11 Fejlmål med og uden anvendelse af ANN-korrektion



4.4.3 Præsentation af bølgeprøgnoser og drift af bølgeprøgnosesystem

Resultaterne af bølgeprøgnosene er præsenteret overfor brugerne sammen med andre prognoseparametre via tre websites:

- 80.196.216.18/hornsrev.htm, som er sat op af Tech-wise
- www.vandudsigten.dk, som er sat op af DHI
- www.mitvejr.dk, som er sat op af Vejr2

En skematisk beskrivelse af dataflowet i bølgeprøgnosesystemet er vist i fig 4.12. Det skal bemærkes, at ANN-korrektionen af bølgehøjdeprøgnosene kun er vist på 80.196.216.18/hornsrev.htm, men at den også vil kunne vises på de andre websites når ønsket.

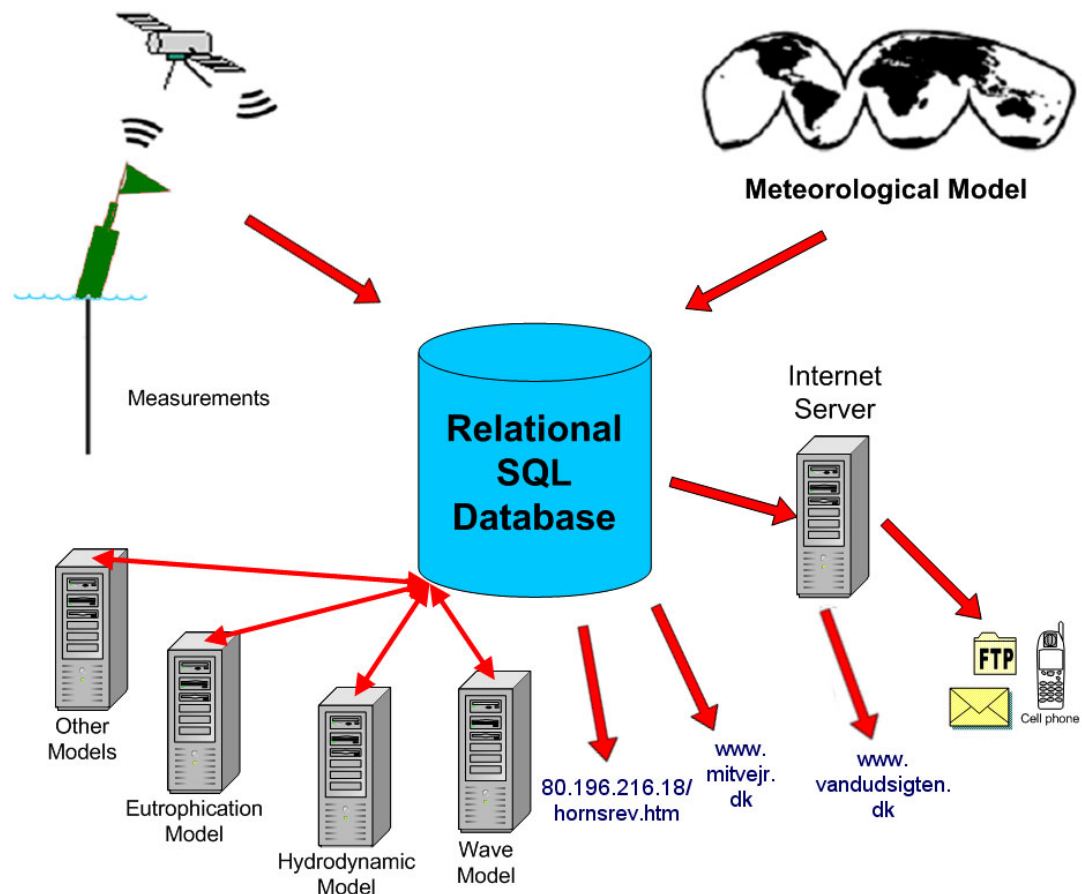


Fig 4.12 Dataflow for bølgeprøgnosesystem

80.196.216.18/hornsrev.htm

På denne Internetadresse er den ANN-korrigerede bølgeprøgnose præsenteret sammen med målinger og en vindprøgnose. Et eksempel ses på fig 4.3

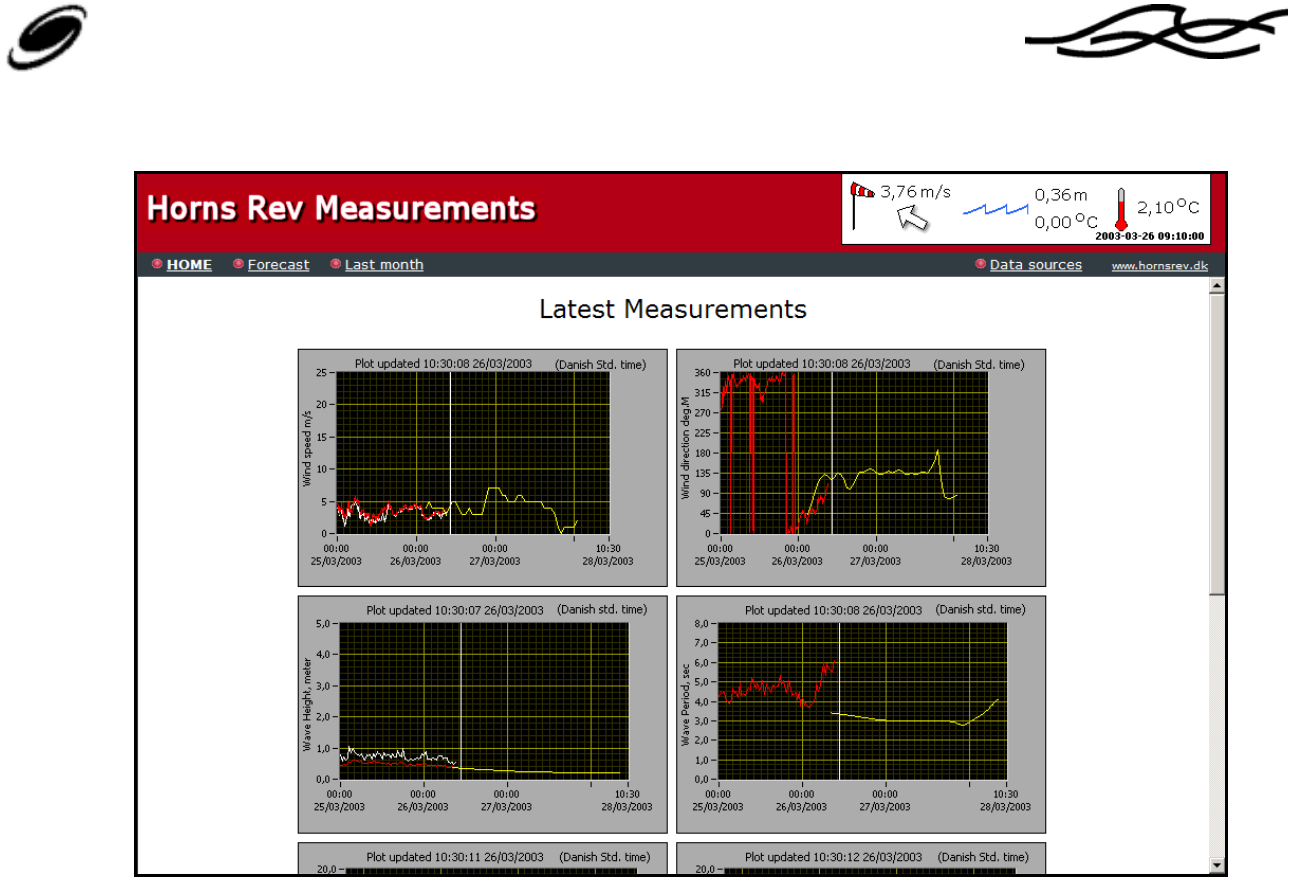


Fig 4.13 Bølgepræsentation på 80.196.216.18/hornsrev.htm

www.vandudsigten.dk

På denne Internetadresse kan bølgepræsenterne ses sammen med præsenterne for andre ”vand”-relaterede parametre såsom vandstand, strømhastighed og –retning. Desuden kan præsenterne for vindhastighed og –retning vises. Denne website er DHI’s brugertilpassede website. Et eksempel kan ses på fig 4.14, hvor en animering af bølgeforsvare (til venstre) er vist sammen med en animering af vindforholdene (til højre).

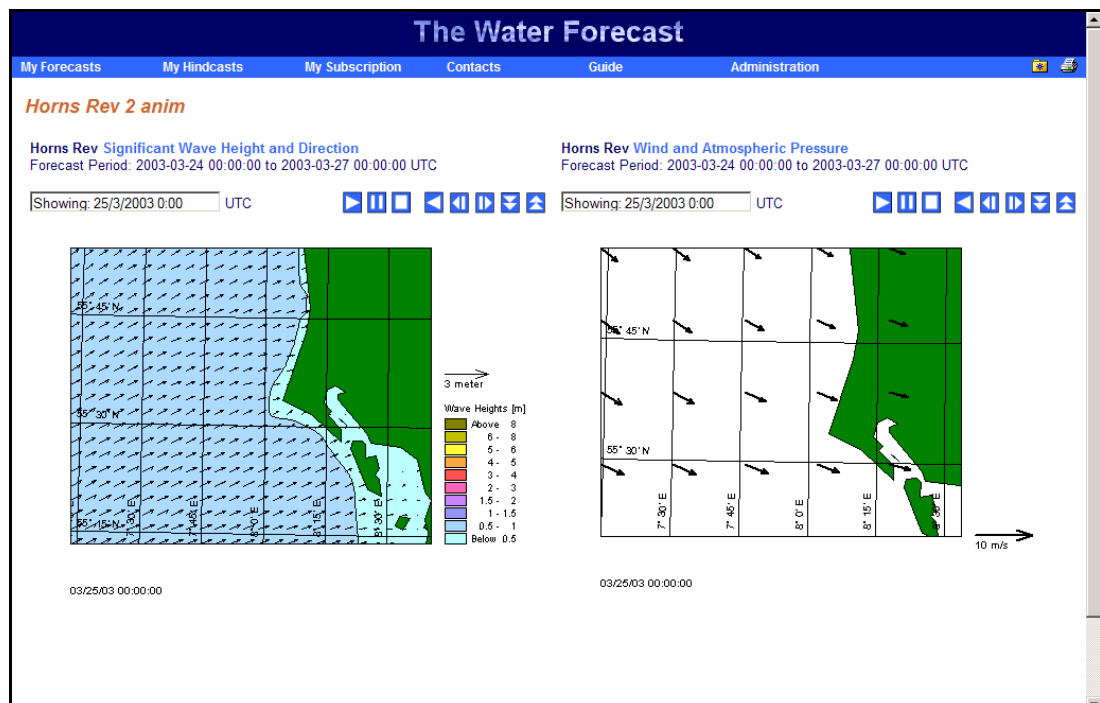


Fig 4.14 Bølgepræsentation på www.vandudsigten.dk



www.mitvejr.dk

På denne Internetadresse kan bølgeprognoserne ses sammen med andre meteorologiske parametre. Denne website er Vejr2's brugertilpassede website. Et eksempel kan ses på fig 4.15.

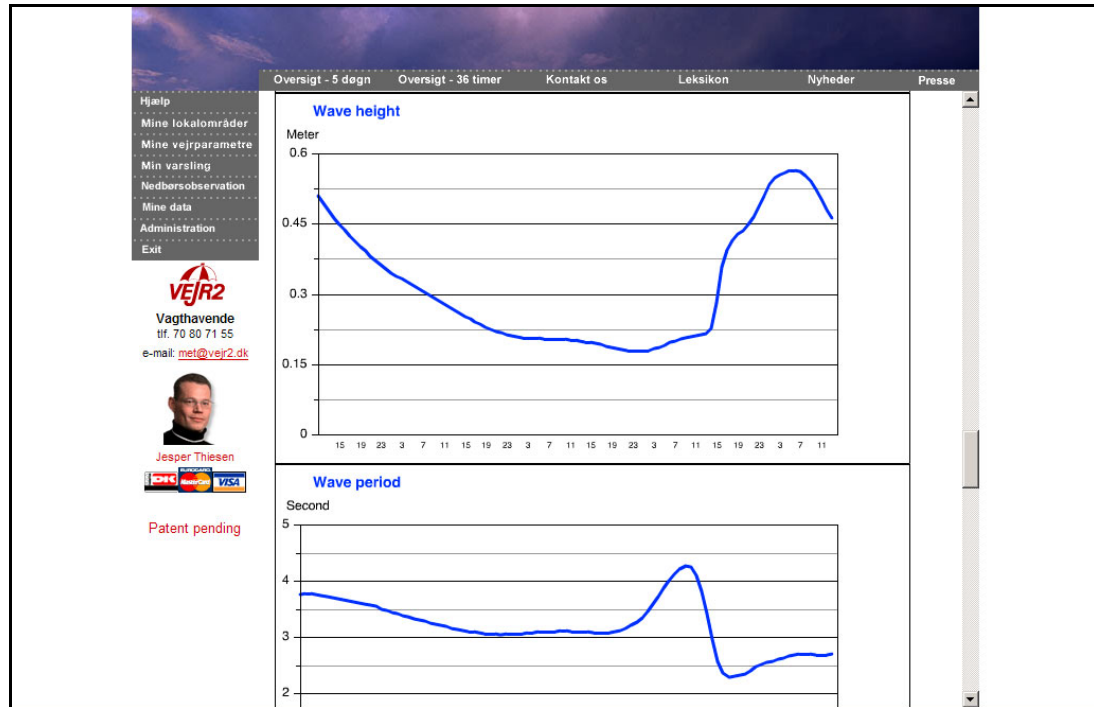


Fig 4.15 Bølgepræsentation på www.mitvejr.dk

4.5 Fase 4 – evaluering og revision af bølgepræsentationen efter anvendelse i 2002

4.5.1 Generelt

Efter igangsættelse af den operationelle bølgevarsling den 1. maj 2002 blev brugernes erfaringer indsamlet. På basis af disse blev bølgepræsentationen revideret som beskrevet i de følgende afsnit.

4.5.2 Revision af bølgemodelsystem

Brugerne af bølgepræsentationen gav udtryk for, at de beregnede bølgehøjder passede tilfredsstillende, mens de beregnede dønninghøjder var for små. Mens der eksisterer en generel måde at beregne en bølgehøjde på baseret på et bølgespektrum, gør det samme sig ikke gældende for dønninghøjden. Det blev derfor besluttet at revidere dønninghøjdeberegningen fra en modifieret version af UK Met Offices metode til følgende metode (se ref /3/): Bølgekomponenter (se fig 4.6), som medtages ved beregningen af dønninghøjde, -periode og -retning, skal opfylde følgende kriterium

$$\frac{U_{10}}{C} \cdot \cos(\theta - \theta_w) \leq 0.83$$



hvor U_{10} er vindhastigheden (midlet over 10 minutter)
C er fasehastigheden for den enkelte bølgekomponent
 θ er retningen for den enkelte bølgekomponent
 θ_w er vindretningen

Denne nye metode giver væsentligt højere dønninghøjder. Et eksempel på et bølgehøjdekart (med kombineret windsø og dønninger) og et dønninghøjdekart ses i fig. 4.16 og 4.17. Bemærk, at mens de primært vindgenererede bølger ikke ændrer retning, når de passerer hen over Horns Rev, påvirkes de lange dønninger kraftigt ved passage af Horns Rev.

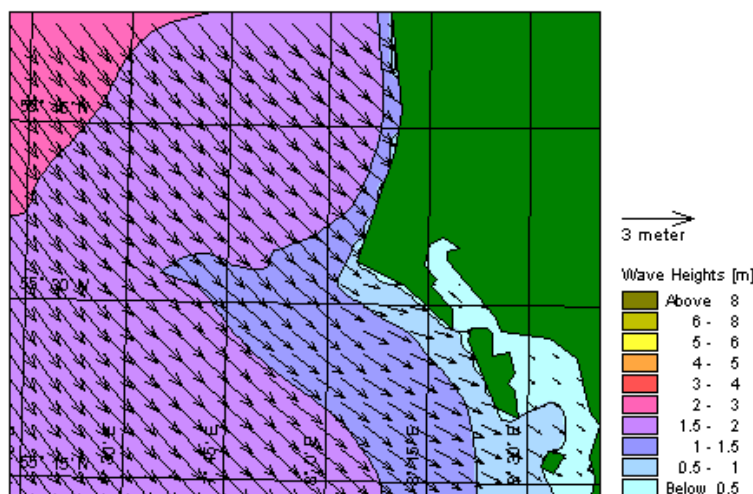


Fig 4.16 Bølgeprognose for Horns Rev den 19. marts 2003 kl 13 UTC

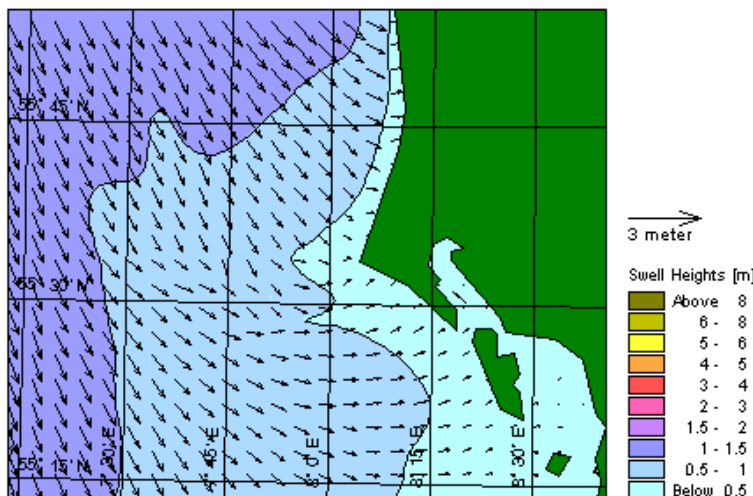


Fig 4.17 Dønningprognose for Horns Rev den 19. marts 2003 kl 13 UTC

Bølgemodellen som beskrevet i fase 3 dækker Nordsøen og en del af Norske Havet. Bølger, der genereres af vinden i dette område kan i visse situationer nå Horns Rev som dønninger. Der er imidlertid bølger, som genereres ude i Nordatlanten, og som også kan ende som dønninger ved Horns Rev. Disse sidstnævnte bølger er ikke inkluderet i det set-up, som er beskrevet i fase 3. Da visse typer af operationer er meget følsomme overfor dønninger, blev det besluttet at etablere en bølgeprognosemodel for Nordatlanten.



Denne model beregner således bølgehøjden på den nordlige og nordvestlige rand af den model, som blev etableret i fase 3 (se fig. 4.3).

Nordatlantmodellen er baseret på MIKE 21 SW med en havdybder som vist i fig 4.18. Modellen kører som en del af Vandudsigten og bruger som input en 5-døgns vindprædikt fra den såkaldte AVN-model fra National Centers for Environmental Prediction, USA. Et eksempel på et vindfelt og det tilhørende bølgefelt er vist i fig 4.19 og 4.20.

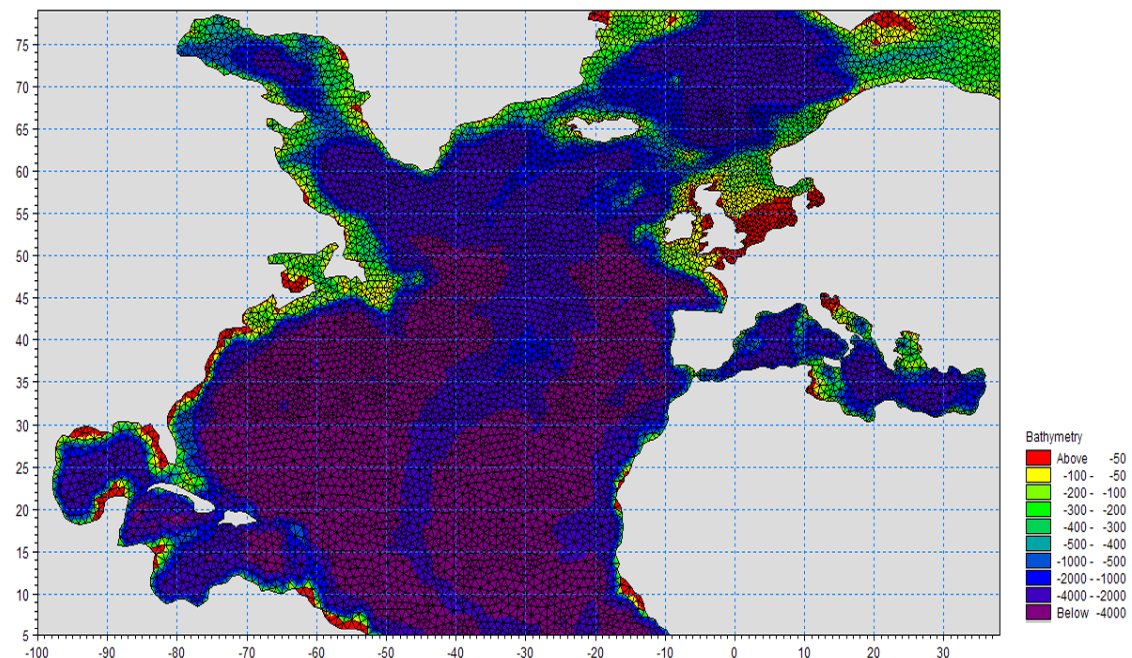


Fig 4.18 Beregningsnet for Nordatlantisk bølgemodel med fleksibelt net.

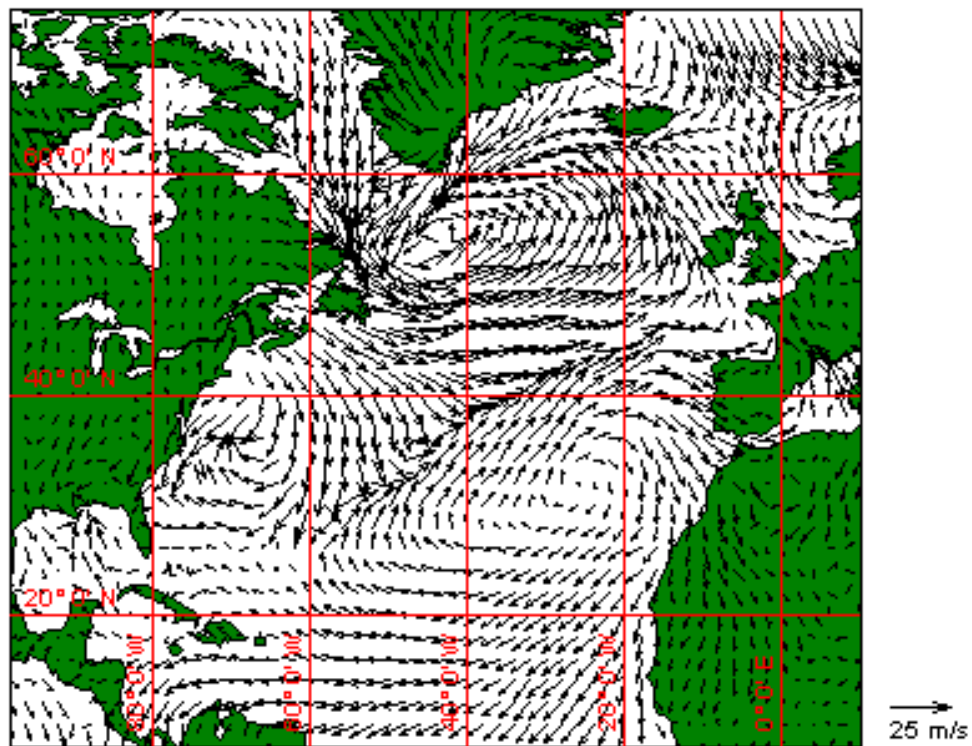


Fig 4.19 Vindfelt i Nordatlanten den 27. februar 2003 kl 00 UTC

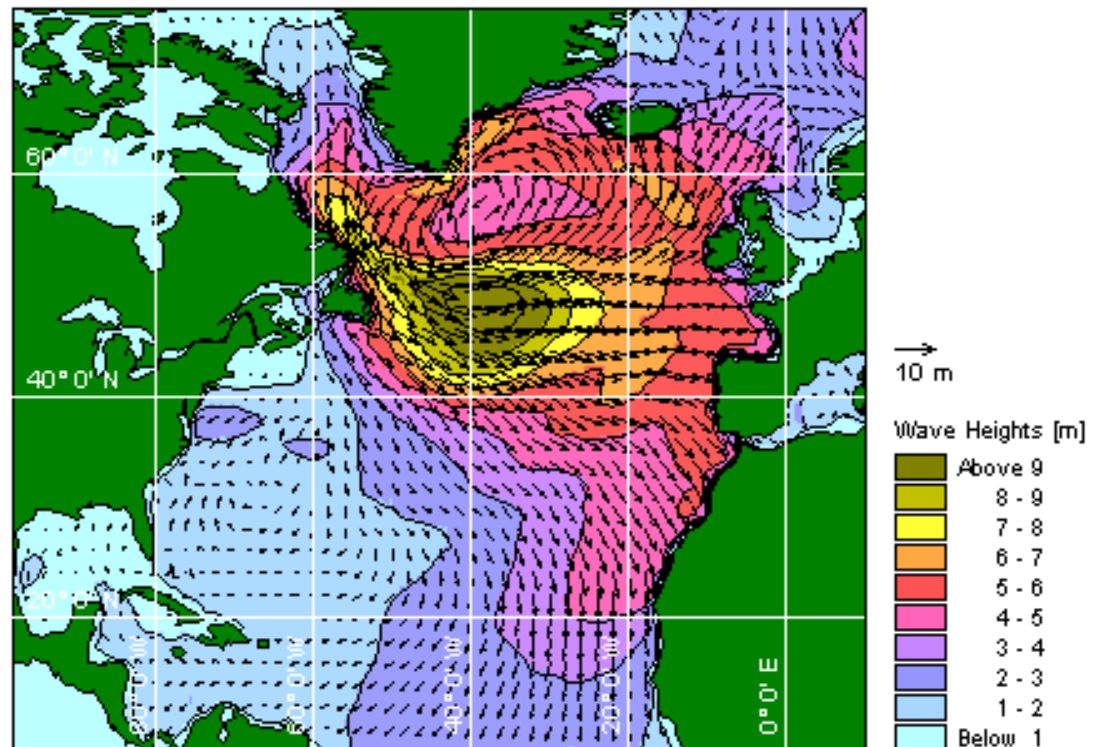


Fig 4.20 Bølgefelt i Nordatlanten den 27. februar 2003 kl 00 UTC



4.5.3 Revision af korrektioner på basis af målinger

Det blev besluttet at revidere ANN-korrektionen efter anvendelsen i år 2002 på grund af følgende:

- DHI skiftede leverandør af vindprognoser fra DMI til Vejr2. Selvom vindprognosene er forholdsvis ens, vil eventuelle afvigelser påvirke ANN-korrektionen
- det viste sig, at den i 2002 anvendte ANN-korrektion indeholdt en meget stor grad af udglatning af prognosen. Dette gav godt nok den mindste fejl på spredningen, men betød også, at alle store udsving som f.eks. store bølgehøjder ofte blev kraftigt reduceret

En genberegning af parametrene i ANN-korrektionen inklusiv en fjernelse af udglatningen af prognosen gav en spredning på fejlen som vist i fig 4.21.

Ved sammenligning med fig 4.9 (fejlen ved den første ANN-korrektion) ses umiddelbart en større fejl ved den nye korrektion. Dette skyldes primært ønsket om ikke at fjerne de store bølgehøjder i prognoserne ved udglatning, idet de høje bølger må anses for meget vigtige for brugerne.

Fig 4.22 viser hvorledes en ukorrigert prognose for den 1. september 2002 kl 12 bliver korrigert på basis af målingen kl 12, og hvorledes denne korrektion kom til at passe med de efterfølgende målinger.

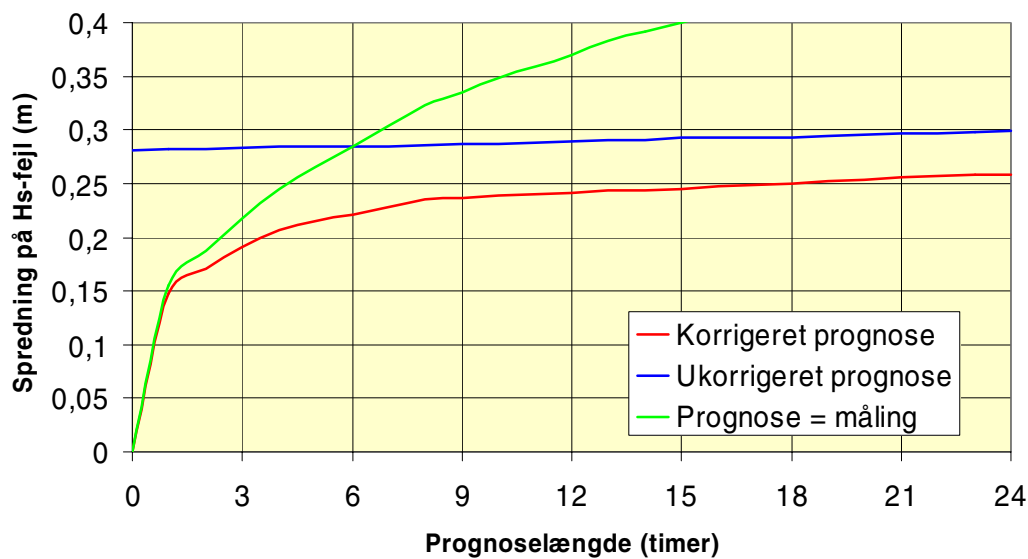


Fig 4.21 Fejmål med og uden anvendelse af ANN-korrektion med genberegnede parametre

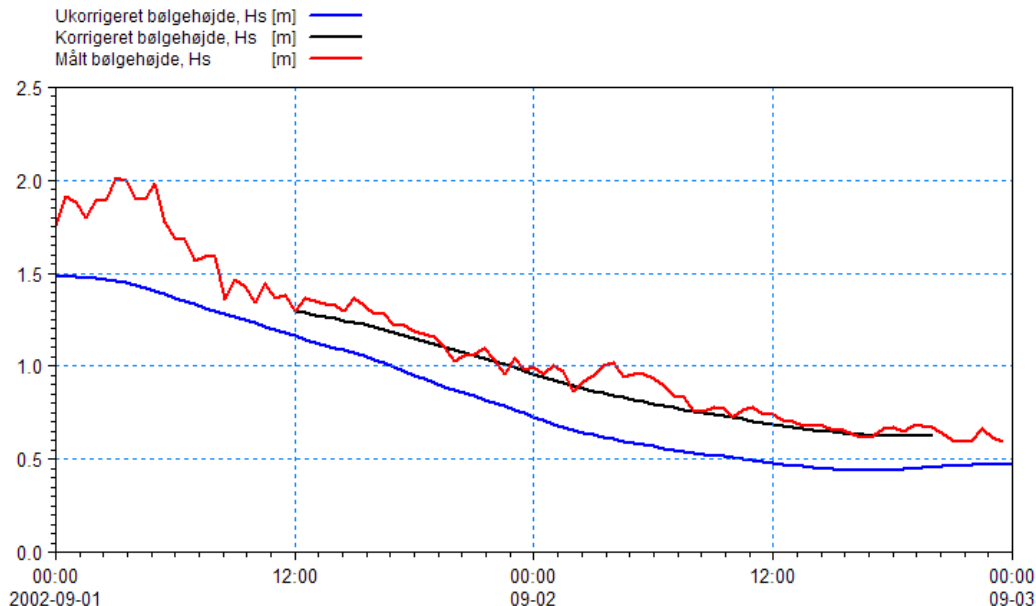


Fig 4.22 Eksempel på en ukorrigert og korrigert prognose fra den 1. september 2002 kl 12. Desuden er efterfølgende målinger vist.

4.6 Fase 5 – formidling af projektets resultater

Den viden, som er opsamlet hen igennem projektet, de tekniker, som er udviklet, samt selve bølgeprognoserne formidles få følgende måder:

- Bølgeprognoserne for Horns Rev er tilgængelige på tre websites: 80.196.216.18/hornsrev.htm, www.mitvejr.dk og www.vandudsigten.dk.
- Bølgeprognoser for andre havvindmølleparker vil med mindre modifikationer kunne ses på www.vandudsigten.dk. Således vil bølgeprognosesystemet blive anvendt for Rødsand havvindmøllepark syd for Lolland fra primo maj 2003.
- Udviklingen af bølgemodellen med fleksibelt net er beskrevet i en videnskabelig artikel ("A Third Generation Spectral Wave Model using an Unstructured Finite Volume Technique" - se bilag D), som sendes til tidsskriftet Coastal Engineering for offentliggørelse
- Udviklingen af bølgeprognosesystemet vil blive beskrevet i en videnskabelig artikel (med den tentatieve titel "Wave Forecasting for Offshore Wind Farms"), som forventes sendt til tidsskriftet Coastal Engineering medio 2003 for offentliggørelse
- Den generelle beskrivelse af projektet er givet i nærværende rapport



5 **REFERENCE**

- /1/ Jensen, H.R., Babovic, V., Rasmussen, E.B. (2000), *Real-time current forecasts for tunnel element towing in Øresund, Denmark*, Øresund Link Immersed Tunnel Conference 2000, Copenhagen, 2000.
- /2/ Dansk Hydraulisk Institut, *Havvindmøllefundamenter ved Horns Rev, Hydrografiske Data, Revision 1*, Rapport til ELSAMPROJEKT A/S, November 1999.
- /3/ Young, I.R., *Wind Generated Ocean Waves*, Elsevier Ocean Engineering Book Series, Volume 2, 1999.



B I L A G



B I L A G A

PSO-F&U Oplysningseskema

**5. Årsopdelt finansieringsplan (Artsopdelt budget anføres i punkt 14):**

Beløb i 1.000 DKK	År 2001		År 2002		År 2003		År 2004	
	Eltra	Øvrig	Eltra	Øvrig	Eltra	Øvrig	Eltra	Øvrig
Total budget	1800		1000					

6. Dato:**Projektansvarliges underskrift:**

7. Finansiering og mandskabsindsats:

Organisation/virksomhed/institution (Øvrig finansiering skal specificeres)	PSO		Egen-finansiering	Øvrig finansiering	Total i 1.000 DKK	Timer
	Elkraft	Eltra				
ELSAMPROJEKT		870			870	940
DHI		1930			1930	2500
Total (beløb i 1.000 DKK):					2800	3440

Hvis egenfinansieringen for hele projektet eller for projektdeltageres andele udgør mindre end 25 % af de samlede projektudgifter, inkl. et (beregnet) overhead på 100 % af lønomkostningerne, skal der anføres en særskilt begrundelse herfor.



8. Projektbeskrivelse:

Et eksempel på anvendelse af prognosetechnikken, dvs. forudsigelse af hydrografiske parametre, i danske farvande er installationen af de 60.000 tons tunnelementer til Øresundsforbindelsen. Prognose baseret på en kombination af deterministiske modeller, online-målinger og anvendelsen af neurale netværk sikrede en succesrig installation af samtlige elementer uden fordyrende downtime. For havmøllerne kan et prognose system baseret på lignende principper anvendes, idet dog bølgerne og ikke strømmen er den mest afgørende parameter. Horns Rev bliver det første opstillingsområde og tænkes derfor anvendt som eksempel i projektet, men den generelle metodik kan anvendes også for Læsø og andre installationsområder. Formålet med et prognosesystem vil være at minimere omkostninger/downtime i forbindelse med de omfattende marine operationer.

Forskellige typer af forecast teknologier kan anvendes:

- 1) Deterministisk forecast baseret på forudsagte vindfelter og tilhørende bølgemodellering.
- 2) Deterministisk modellering som under 1) men med assimilering af måledata i modelsystemet.
- 3) Deterministisk modellering plus dataassimilering samt korrektion af forudsigelser baseret på neurale netværks-teknologier.
- 4) Neurale netværk baseret udelukkende på målinger.

Følgende mulige modeltyper undersøges:

- a) Opdatering af inputparametre (metoden svarer til 2).
- b) Opdatering af tilstandsvvariable (Kalman-filtre).
- c) Opdatering af modelparametre (her blot nævnt som eventualitet, idet metoden ikke har fundet udbredt anvendelse i hydrodynamiske modeller).
- d) Opdatering af outputvariable (fejlforudsigelse(prediction)).

Formålet med det foreliggende projekt er at bestemme den optimale forecast-teknologi, vurdere dens nøjagtighed samt de økonomiske gevinstre, der kan opnås ved dens anvendelse. Til udviklingsprojektet omkring bølgeforecast foreligger der følgende "byggesten":

- Bølgemodel - MIKE 21 OSW3G - for Nordsøen.
- Lokal bølgemodel MIKE 21 NSW for området ved Horns Rev.
- Tryk og vindfelter (input til bølgemodel, drivende kræfter).
- Havbundsbathymetri for Nordsøen og Horns Rev-området.
- Marint målesystem.
- Kunstige neurale netværksteknologier (Artificial Neural Networks, ANN).

Projektet tænkes udført i 5 faser med følgende indhold:

1. fase: Forprojekt – erfarsingsindsamling, identifikation af forskellige typer af forecast-teknikker til forudsigelse af bølgeforhold, herunder granskning af muligheder/begrænsninger.
Udarbejdelse af endelig projektbeskrivelse, tidsplan og budget.
2. fase: Opkoppling af marint målesystem ved Horns Rev til online-transmission af bølgedata.
3. fase:
 - a. Opkoppling af bølgemodeller til vindfelter i 'forecast mode' og til assimilering af måledata.
 - b. Indbygning af ANN i forecast og "træning" af systemet under brug af allerede eksisterende måledata fra Horns Rev.
 - c. Testning/kalibrering af de forskellige forecast-teknikker.
 - d. Korrektioner på dele af forecast-systemet med henblik på konfidens i de 'forecastede' bølgeparametre.
4. fase: Vurdering af de forskellige forecast-teknikkers anvendelighed og nøjagtighed. Vurderingen vil blive baseret på sammenligning med eksisterende data fra målekampagnen forestået af ELSAMPROJEKT 1999-2000.
5. fase: Implementering og tilretning ved drift af den operative bølgeprognosemodel for Horns Rev i byggeperioden medio 2001 til ultimo 2002, så modellen er klar til rutinemæssig brug efter idriftsættelsen.

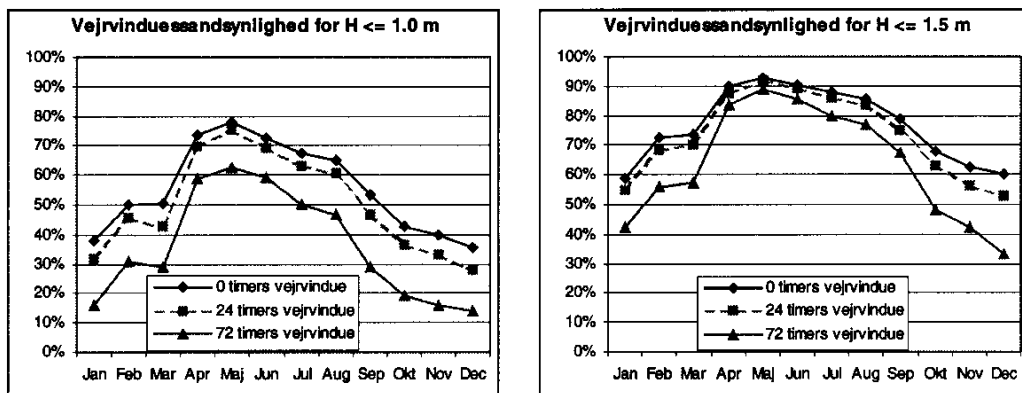
Målet med implementering af et forecast-system er på så nøjagtig en måde som muligt at kunne angive bølgebetingelserne inden for visse tidsrammer. Et sådant systems nøjagtighed vil i sagens natur have større fejl, jo længere tidshorizonten er. Det er derfor også en vigtig del af projektet at få vurderet den mulige fejl i estimererne, således at man kan lave en bedre risikovurdering og økonomisk optimering af de marine operationer og disses planlægning.

9. Projektets relevans:

Havmølleplanen sigter mod 4000 MW opstillet til søs. Havmøllepålægget til elværkerne angiver, at 750 MW skal være installeret med udgangen af 2008. Dette har resulteret i, at de første to projekter på hver 150 MW; havmølleparkerne på Horns Rev og Rødsand; er godt på vej. Horns Rev-parken forventes at blive den første med planlagt idriftsættelse ultimo 2002.

I forbindelse med de planlagte vindmølleparker vil der være omfattende marine operationer i forbindelse med installationer af fundamenter, møller, kabler m.v. Udover problematikken med montagen af de ca. 80 møller i hver park er det store spørgsmål de betingelser, hvorunder den efterfølgende drift og vedligehold skal foregå.

Erfaringerne fra målemasten på Horns Rev har vist, at det er muligt at foretage mandskabsoverførsel fra båd til faststående konstruktion i bølgehøjder op til 1,0-1,5 m - afhængig af bølgeperiode og strømforhold. Hvis der skal foretages større reparationer eller udskiftninger af store enkeltkomponenter som f.eks. vinger, gear eller generatorer, er det påkrævet, at søtilstanden igennem en længere periode (vejrvindue) er under det kritiske bølgehøjdeniveau. For kritiske bølgehøjder på henholdsvis 1,0 og 1,5 m viser nedenstående figurer vejrvinduessandsynligheden som funktion af årstiden.



Da det er forbundet med meget store omkostninger, dels at skulle indstille en igangværende operation, dels at "miste" et vindue med tilhørende produktionstab til følge, er en prognose for bølge- og vindforhold af yderste vigtighed, når man tager de meget lave vejrvinduessandsynligheder i vinterhalvåret i betragtning. En nøjagtig prognose vil endvidere gavne arbejdssikkerheden, idet forhåndsviden om varigheden af bølgeforskifter kan indgå i arbejdsplanlægningen, således at risikofyldte mandskabsoverførsler undgås.

Overordnet styres bølgeforskifterne af de atmosfæriske parametre såsom vindhastighed, vindretning og tryk samt de lokale geografiske forhold. Prognoser på disse parametre alene har tidligere været brugt (bruges) til forudsigelse af bølger. Modeller - baseret på denne metodik - viser dog temmeligt store unøjagtigheder, idet bølger og ændringer af bølger foregår i et noget "trægere" system. Disse unøjagtigheder forsøges minimeret gennem assimilering af målte bølger samt anvendelse af neurale netværk i ansøgte projekt.

Bølgeprognosemodellen, som bliver specielt udviklet med Horns Rev som eksempel, vil med relativt få ændringer kunne benyttes til de øvrige havmølleprojekter samt øvrige projekter, hvori kendskab til bølgetilstanden spiller en væsentlig rolle for projektets gennemførelse.

Projektet vil - gennem afprøvning af det udviklede system i en periode på ca. 1½ år samt implementering af informationer om operationelle kriterier og priser - give et godt estimat på opnåelige besparelser ved anvendelse af en sofistikeret prognosemodel.

**10. Værtsorganisationens F&U-strategi inden for området, inkl. projektets sammenhæng med andre gennemførte og planlagte projekter. Der skal oplyses om ansøgte eller modtagne bevillinger til beslægtede projekter:**

Det er Elsams klare mål at blive den førende udvikler og entreprenør for dansk energi- og miljøpolitik inden for produktion af kraftvarme og vedvarende energi. Elsam vil målrettet og løbende udbygge den erhvervede kompetence inden for miljøvenlig produktion af el og varme, og Elsam vil aktivt søge at øge engagementet i miljøvenlige energianlæg i ind- og udland.

Projektet er en integreret del af det samlede demonstrationsprojekt på Horns Rev.

11. Arbejdsfordeling og projektledelse:

Arbejdet gennemføres som en del af Elsams havmølleprojekter, hvad angår organisation og projektledelse.

ELSAMPROJEKT A/S og DHI vil i samarbejde udføre de under §8 "Projektbeskrivelse" listede faser 1, 2, 4 og 5. Fase 3 vil blive udført af DHI.

12. Plan for formidling og udnyttelse af projektets resultater:

Projektets resultater – bølgeprognosemodellen – skal direkte anvendes ved planlægning af installation, service, vedligeholdelses- og reparationsopgaver på Horns Rev-parken.

Modellens anvendelighed vil løbende blive moniteret, og der vil blive ført statistik på eventuelle fejlfrekvenser, som rapporteres tilbage til prognosemodellen.

Det forventes, at selv lang tid efter at være taget i brug, vil det være nødvendigt med modelforbedringer.

Resultaterne vil gennem DHI's marine prognosesystemer blive anvendelige for øvrige havmølleprojekter. Resultaterne formidles direkte til øvrige operatører af havmølleparker.

13. Omfang af offentliggørelse:

Projektets resultater formidles direkte til de involverede parter. Herudover vil projektets hovedresultater og konklusioner blive sammenskrevet i 'papers' til fremlæggelse på nationale/internationale konferencer med fokus på marine og meteorologiske prognosesystemer.

14. Budget

Omkostningsart	Beløb i 1.000 DKK
Lønomkostninger	2.590.000
Apparater, udstyr, materialer	200.000
Eksterne ydelser	
Rejse- og opholdsudgifter	10.000
Andet	
Total budget	2.800.000
Eventuelle indtægter og restanlægsværdi ved projektafslutning	

15. Anvisningsoplysninger:

Pengeinstitut, navn: Danske Bank

Adresse: Gothersgade 18, 7000 Fredericia

Reg.nr.: 3206

Kontonr.: 114122

SE-nr.: 61126228

16. Projektplan: Faseopdeling af projektet og angivelse af tilhørende målbare resultater i form af faglige milepæle.

1. fase: Forprojekt. Granskning af forskellige typer af forecast-teknikker til forudsigelse af bølgeforsigt. Resultatet er en projektbeskrivelse, tidsplan og budget for udarbejdelse af marint prognosesystem for Horns Rev.
2. fase: Opkobling af marint målesystem ved Horns Rev til online-transmission af bølgedata. Resultatet er online-overførsel af måledata fra de marine sensorer på Horns Rev.
3. fase: Opkobling af bølgemodeller, "træning" af systemet, testning/kalibrering og korrektioner. Resultatet er et kalibreret, numerisk modelsystem til forudsigelse af bølgeparametre på Horns Rev.
4. fase: Vurdering af forecast-systemets anvendelighed og nøjagtighed. Resultatet er en evaluering, hvor der fokuseres på økonominisk optimering af de marine operationer og disses planlægning under anvendelse af prognosesystemet.
5. fase: Implementering og tilretning ved drift af den operative bølgeprognosemodel for Horns Rev i byggeperioden medio 2001.

Resultatet er et færdigt marint prognosesystem klar til rutinemæssig brug efter idriftsættelsen af havmølleparken.

17. Tidsplan

Startdato: 01/01/2001

Slutdato: 30/06/2002

	År 2000				År 2001				År 2002			
	1	2	3	4	1	2	3	4	1	2	3	4
Aktiviteter/milepæle/betaling												
Fase 1 – forprojekt					■	■						
Fase 2 – online system					■	■						
Fase 3 – bølgemodeller					■	■	■	■				
Fase 4 – evaluering						■	■	■				
Fase 5 – implementering						■	■	■				



Aktivitetens varighed



Milepæl



B I L A G B

***Generel beskrivelse af DHI's bølgemodeller,
MIKE 21 OSW og SW (på engelsk)***



Short Description of MIKE 21 SW - Spectral Wave Model

MIKE 21 SW is a new generation spectral wind-wave model based on unstructured meshes. The model simulates the growth, decay and transformation of wind-generated waves and swell in offshore and coastal areas.



*MIKE 21 SW is a state-of-the-art numerical tool for prediction and analysis of wave climates in offshore and coastal areas
© BIOFOTO/Klaus D. Bentzen*

MIKE 21SW solves the spectral wave action balance equation formulated in either Cartesian or spherical co-ordinates. Effects of wave generation, dissipation and nonlinear wave-wave interactions are described by various kinds of state-of-the-art source functions. The numerical representation of the geographical domain is obtained using an unstructured mesh composed of triangular elements and an efficient cell-centered finite volume method. The time integration is performed using an efficient multi-sequential integration scheme.

MIKE 21 SW includes two different formulations:

- Directionally decoupled parametric formulation
- Fully spectral formulation

The directionally decoupled parametric formulation is based on a parameterization of the wave action conservation equation. Following Holthui-



jsen et al (1989) the parameterization is made in the frequency domain by introducing the zeroth and first moment of the wave action spectrum as dependent variables. A similar formulation is used in the MIKE 21 NSW Nearshore Spectral Wind-Wave Module.

The fully spectral formulation is based on the wave action conservation equation as described in e.g. Komen et al (1994) and Young (1999), where the directional-frequency wave action spectrum is the dependent variable. A similar formulation is used in the MIKE 21 OSW Offshore Spectral Wind-Wave Module.

Application Areas

MIKE 21 SW is used for the assessment of wave climates in offshore and coastal areas - in hindcast and forecast mode.

A major application area is the design of offshore, coastal and port structures where accurate assessment of wave loads is of utmost importance to the safe and economic design of these structures. Measured data is often not available during periods long enough to allow for the establishment of sufficiently accurate estimates of extreme sea states. In this case, the measured data can then be supplemented with hindcast data through the simulation of wave conditions during historical storms using MIKE 21 SW.

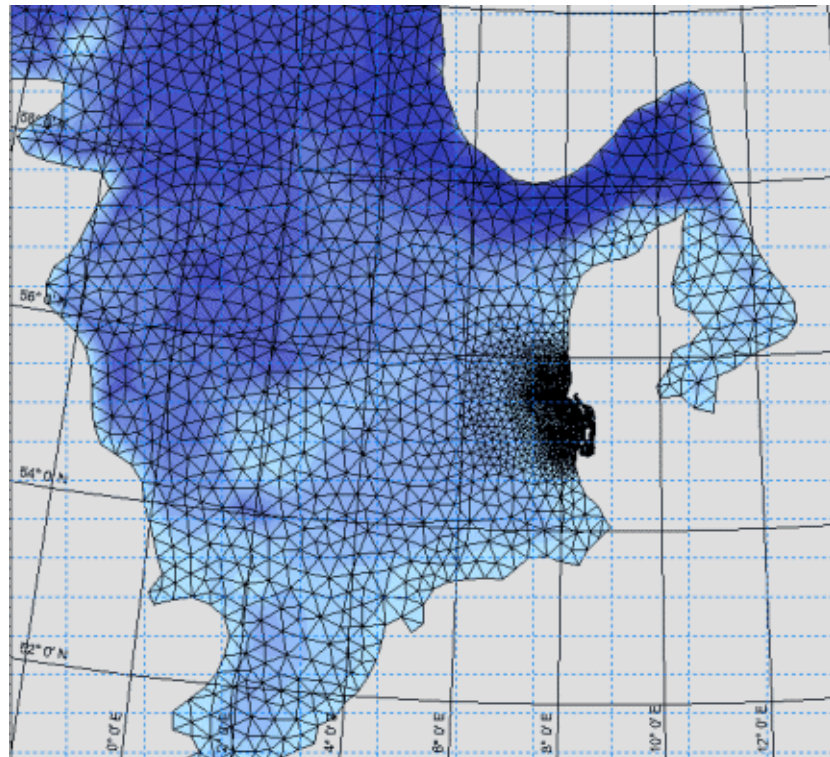
MIKE 21 SW is also used for the calculation of the sediment transport, which for a large part is determined by wave conditions and associated wave-induced currents. The wave-induced current is generated by the gradients in radiation stresses that occur in the surf zone. MIKE 21 SW can be used to calculate the wave conditions and associated radiation stresses.



Illustration of typical application areas

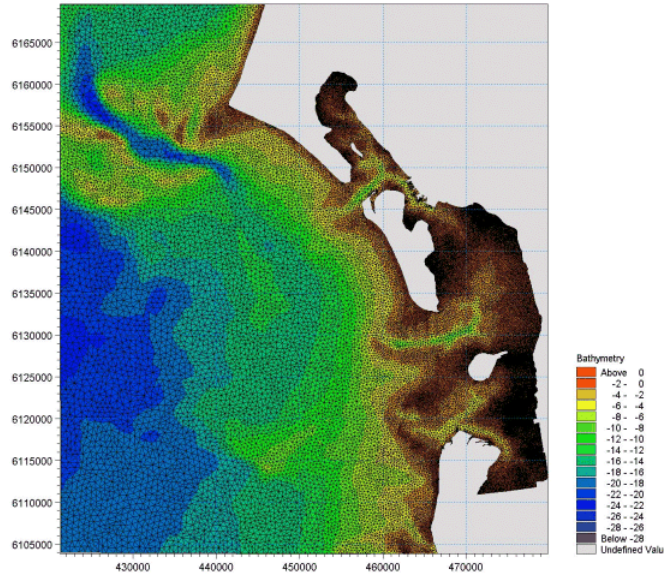


MIKE 21 SW is particularly applicable for simultaneous wave prediction and analysis on regional scale (like the North Sea, see figure below) and local scale (west coast of Jutland, Denmark, see figure below). Coarse spatial and temporal resolution is used for the regional part of the mesh and a high-resolution boundary- and depth-adaptive mesh is describing the shallow water environment at the coastline.



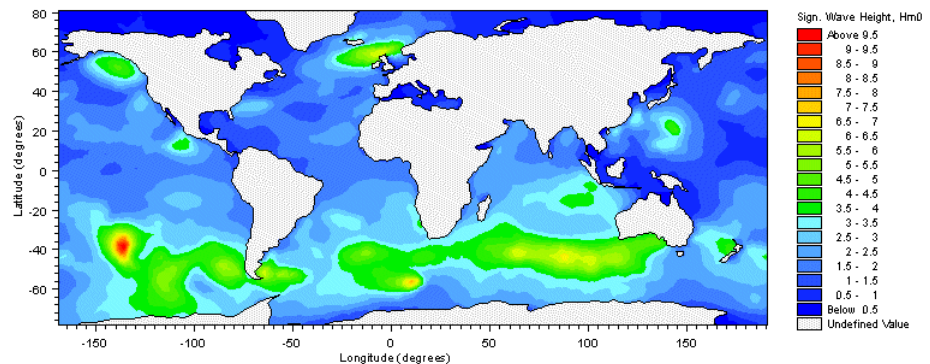
Example of a computational mesh for detailed wave prediction at the west coast of Jutland, Denmark

Assessment of wave conditions in nearshore and coastal areas which most often involves transformation of known offshore wave statistics (derived from e.g. measurement, regional/global models, remote sensing data etc) is most efficiently performed using the directionally decoupled parametric formulation.



Example of a computational mesh used for transformation of offshore wave statistics using the directionally decoupled parametric formulation

MIKE 21 SW can also be applied on global scale as illustrated in the figure below.



Example of global application of MIKE 21 SW

Computational Features

The main features of the new generation MIKE 21 SW Spectral Wave Model are as follows:



-
- Fully spectral and directionally decoupled parametric formulations
 - Source functions based on state-of-the-art 3rd generation formulations
 - Optimal degree of flexibility in describing bathymetry and ambient flow conditions using depth-adaptive and boundary-fitted mesh
 - Coupling with hydrodynamic flow model for modelling of wave-current interaction and time-varying water depth
 - Cell-centered finite volume method
 - Multi-sequential time integration scheme
 - Extensive range of model output parameters (wave, swell, air-sea interaction parameters, radiation stress tensor, spectra etc)



MIKE 21 OSW OFFSHORE SPECTRAL WIND-WAVE MODULE

MIKE 21 OSW is a fully spectral wind-wave model, which describes the growth, decay and transformation of wind-generated waves in offshore areas as well as in coastal areas. The model comprises the following phenomena:

- wind induced wave growth
- nonlinear wave-wave interactions
- wave breaking
- bottom friction
- shoaling
- refraction

MIKE 21 OSW is a time-dependent discrete spectral wind-wave model formulated in terms of the energy density spectrum with a discrete resolution of frequencies and directions. The model includes two different descriptions of physical processes governing the wind-wave generation and decay:

- state-of-the-art 3rd generation formulation
- 2nd generation formulation

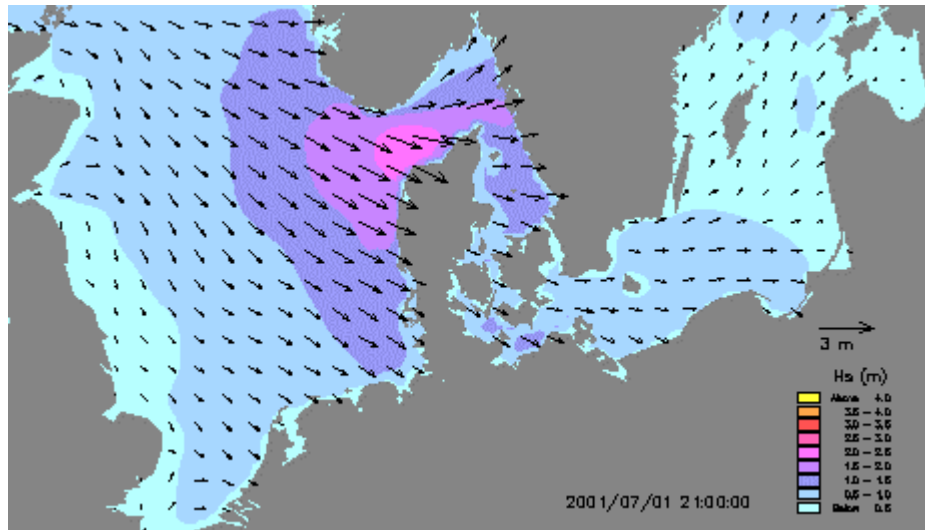
The 3rd generation model is based on the internationally developed WAM Cycle 4 model (Komen et al, 1994) originally developed for deep-water applications on global and regional scales.

DHI has extended its application into shallower water areas, Johnson and Kofoed-Hansen (2000). The 2nd generation model is based on the well-proven formulation by Resio (1981) and has successfully been applied in large number of projects. The 2nd generation model typically requires less computational effort than the 3rd generation model.



Application Areas

A major application area is the design of offshore structures where accurate assessment of wave loads is of utmost importance to the safe and economic design of these structures. Measured data is often not available during periods long enough to allow for the establishment of sufficiently accurate estimates of extreme sea states. In this case, the measured data can then be supplemented with hindcast data through the simulation of wave conditions during historical storms using MIKE 21 OSW.



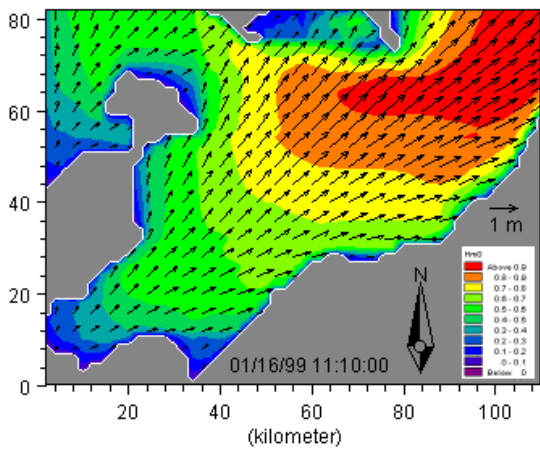
MIKE 21 OSW application in the North Sea and Baltic Sea. The chart shows a computed wave field illustrated by the mean wave direction and significant wave height.



Another application area comprises establishment of design wave conditions for offshore windfarms and marine pipelines in coastal areas. Also wave forecast in connection with assessment of operational conditions can be performed using MIKE 21 OSW.



For detailed analysis of the wave climate in coastal and shallow water the fully spectral MIKE 21 OSW model is often used in connection with a nearshore wave model like the Near-Shore Spectral Wind-Wave Module, MIKE 21 NSW. The high-resolution nearshore models require wave conditions along the offshore model boundary. Based on information about the wind conditions, the boundary conditions can be determined by applying MIKE 21 OSW for the offshore area.



Coastal application of MIKE 21 OSW in Feme Belt located between Denmark and Germany. The chart shows a computed wave field illustrated by the mean wave direction and significant wave height.

Model equations

The MIKE 21 OSW model is based on the numerical integration of the spectral energy balance equation formulated in Cartesian co-ordinates

$$\frac{DF}{Dt} = S_{in} + S_{nl} + S_{ds} + S_{bot} + S_{brk}$$

The left-hand side describes the wave propagation in time and space using linear wave theory. The right-hand side represents the superposition of source functions describing various physical phenomena.

Symbol List

$F(f, \theta, x, y, t)$: spectral energy density ($\text{m}^2/\text{Hz}/\text{rad}$)

S_{in} : wind input (m^2)

S_{nl} : nonlinear energy transfer (m^2)

S_{ds} : dissipation due to white-capping (m^2)

S_{bot} : bottom friction (m^2)

S_{brk} : bottom-induced wave breaking (m^2)

x, y : spatial co-ordinates (m)

t : time (s)

f : frequency (Hz)

θ : wave propagation direction (rad)

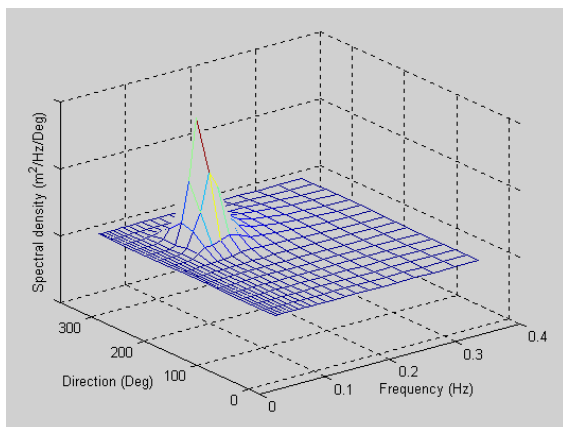
The wind input is (as default in MIKE 21 OSW 3G) based on Janssen's (1989, 1991) quasi-linear theory of wind-wave generation, where the momentum transfer from the wind to the sea not only depends on the wind stress, but also the sea state itself. The nonlinear energy transfer, (through the resonant four-wave interaction) is approximated by the DIA approach, Hasselmann et al (1985). The source function describing the dissipation due to white-capping is also based on the theory of Hasselmann (1974) and Janssen (1989). The bottom friction dissipation is modelled using the approach by Johnson and Kofoed-Hansen (2000), which depends on the wave and sediment properties. The source function describing the bottom induced wave breaking is based on the well-proven approach of Battjes and Janssen (1978).

A detailed description of the various source functions is available in Komen et al (1994), which also includes the references listed above.



Solution methods

MIKE 21 OSW is a discrete spectral wind-wave model, where the spectral energy density is calculated in a number of discrete bins or mesh points of a rectangular Eulerian grid for a number of discrete frequencies and directions. The numerical integration of the spectral energy balance equation is divided into two steps, namely, a propagation step and a source function integration. The propagation step is solved using either a first-order Eulerian upwind scheme (as originally used in the WAM model) or a second order semi-Lagrangian, Brink-Kjær et al (1984). The integration of the source functions is based on a semi-implicit method suggested by Komen et al (1994) and Hersbach (1998). For both source function formulations (2nd and 3rd generation) a parametric (or diagnostic) model is used dynamically to describe the high frequency tail of the directional wave spectrum. The discrete (or prognostic) model thus covers the resolved frequency range using the parametric model as a trigger source function.



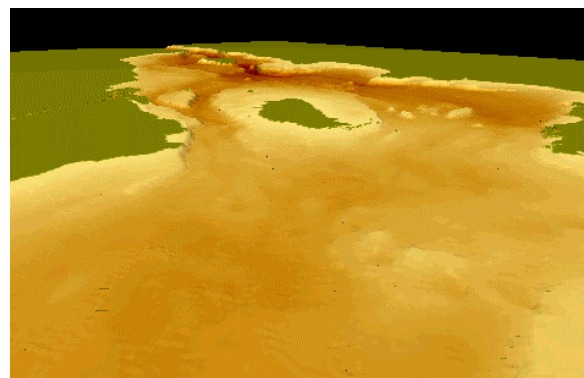
Directional-frequency wave spectrum resolved by 28 logarithmic-distributed frequencies and 12 evenly spaced wave directions.

Model input

The necessary input data can be divided into following groups:

- Basic model parameters:
 - model grid size and extent
 - time step and length of simulation
 - type of output required and its frequency
 - type of model and transport schemes

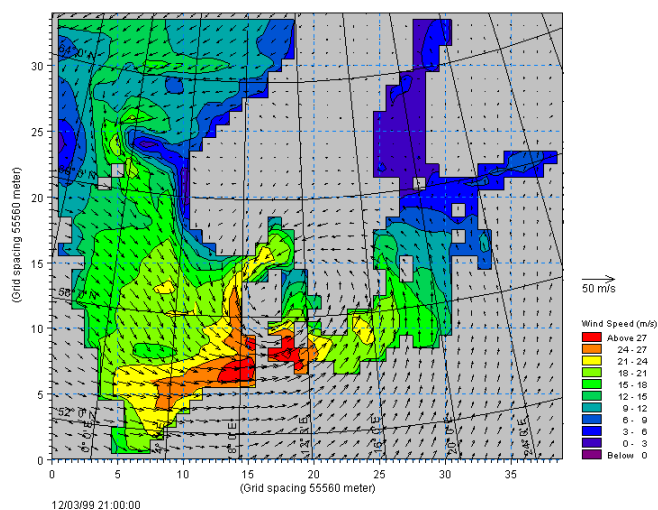
- Bathymetry
- Wind data



An example of coastal area bathymetry.

- Calibration parameters
 - white-capping dissipation
 - wind input (momentum transfer)
 - bottom friction
 - bottom-induced wave breaking
- Initial conditions
 - cold-start
 - hot-start
- Boundary conditions
 - open boundaries
 - closed boundaries

Along all essential boundaries, the time and spatially varying directional-frequency wave energy spectrum should be specified.

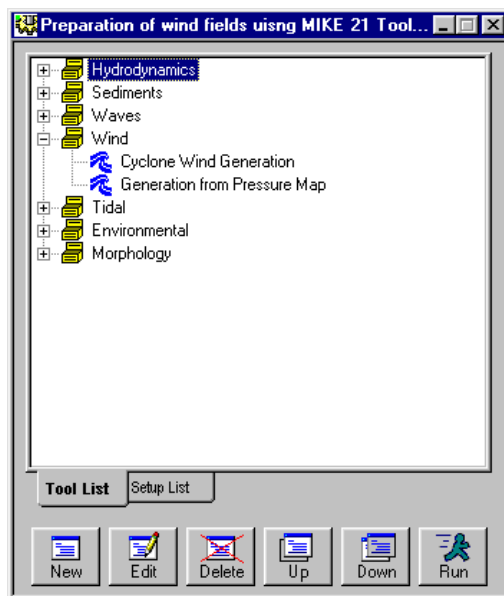


The chart shows a hindcast wind field in the North Sea and Baltic Sea as wind speed and direction.



The main task in preparing the input data for the MIKE 21 OSW model is to generate a bathymetry and to select and prepare the time- and space-varying wind fields. The wind field can be given as wind speed and direction or wind velocity components, and can be given either as constants for the entire computational domain or as a 2D map. As the wind is the main driving force in MIKE 21 OSW accurate hindcast or forecast wind fields is of uttermost importance for the wave prediction.

If wind data is not available from an atmospheric meteorological model, the wind fields can be determined by using the wind-generating programs available in MIKE 21 Toolbox, see below.



Graphical user interface of the MIKE 21 Toolbox including tools for generation of wind fields.

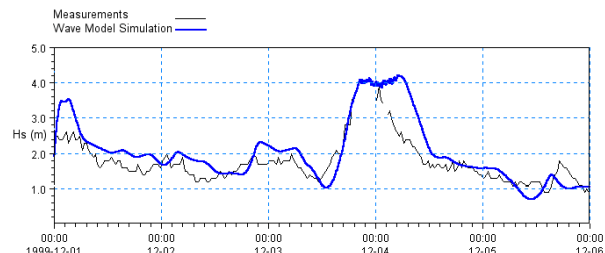
Model output

At each grid point and for each time step two types of output can be obtained from MIKE 21 OSW:

- Basic output including directional-frequency wave spectra at selected grid points and or areas
- Derived output including following characteristic integral measures:
 - significant wave height, H_m0
 - peak wave period, T_p
 - averaged wave period, T_{01}
 - zero-crossing wave period, T_{02}

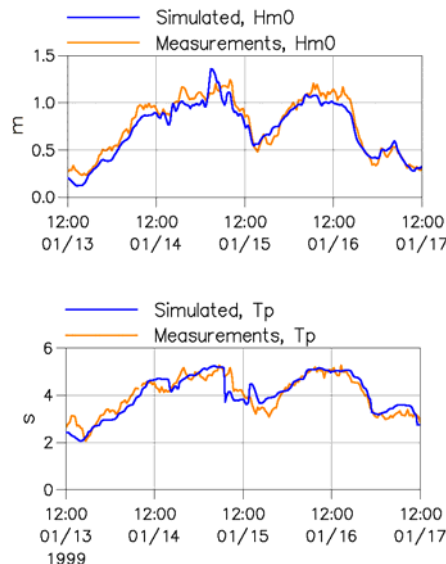
- wave energy period, T_{10}
- peak wave direction, θ_p
- mean wave direction, θ_m
- directional standard deviation, σ

Also the significant wave height in the two Cartesian directions (x and y) can be saved for plotting of wave directions as vectors.



Comparison between measured and simulated significant wave height in the Baltic Sea.

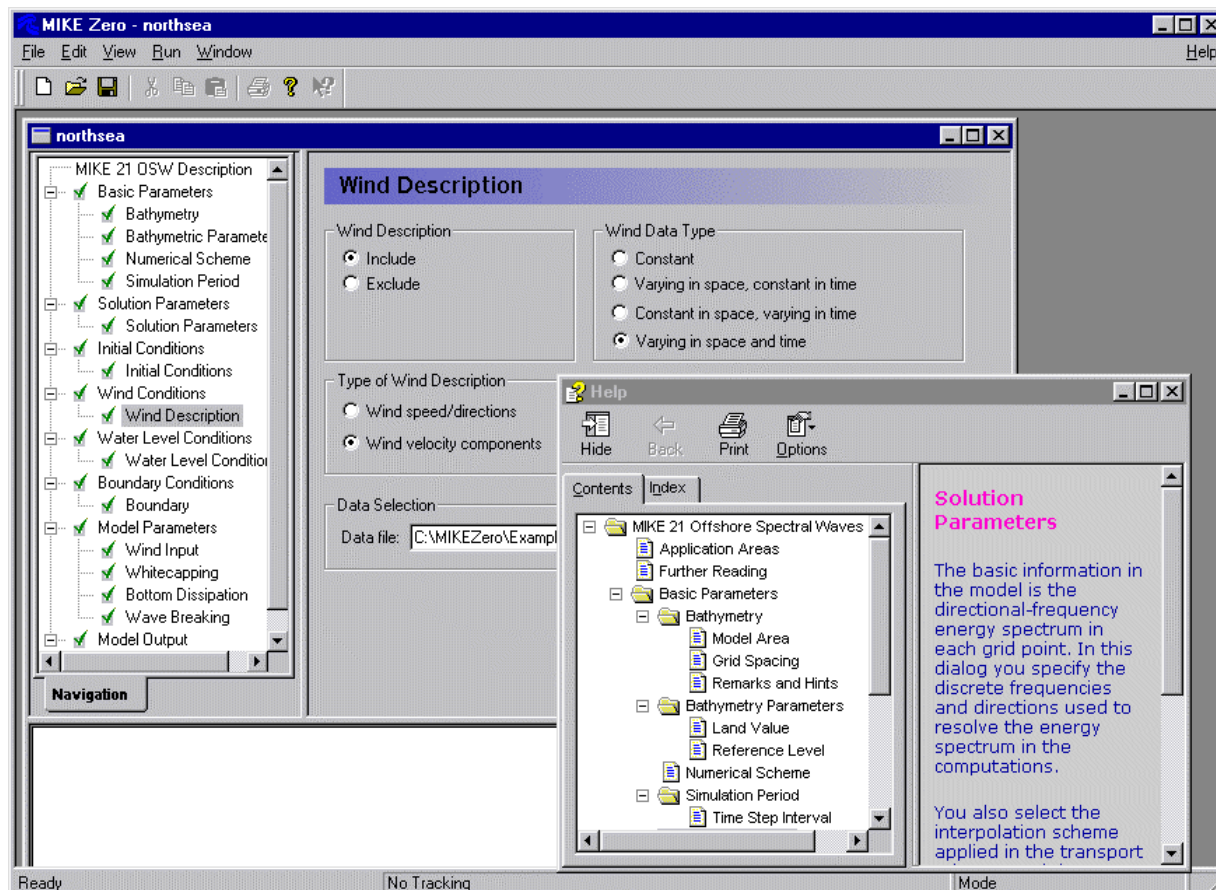
All output data can be post-processed, analysed and presented in various graphical formats using the pre- and post-processing module, MIKE 21 PP.



Comparison between measured and simulated significant wave height and peak wave period in a coastal area application (Femer Belt, Denmark) of MIKE 21 OSW.

Graphical user interface

MIKE 21 OSW is operated through a fully Windows integrated Graphical User Interface (GUI) and is compiled as a true 32-bit application. Support is provided at each stage by an Online Help system.



The graphical user interface of the MIKE 21 OSW model including an example of the Online Help system.

Hardware and operating system requirement

As MIKE 21 OSW is based on a fully Windows integrated GUI and compiled as a 32-bit application implies that the module can only be executed under Windows 95/98/ME and Windows 2000/NT. Microsoft Internet Explorer 4.0 (or higher) is required for network license management as well as for accessing the Online Help. The hardware requirements for executing MIKE 21 OSW are therefore similar to those recommended for utilising Windows 95/98/ME and Windows 2000/NT. These are:

	Minimum:	Recommended:
Processor:	Pentium II, 200 MHz	Pentium II/III, 400 MHz (or more)
Memory (RAM):	64 MB	128 MB (or more)
Hard disk:	1 GB	10 GB
Monitor:	VGA	SVGA, resolution 1024x768
Graphic card:	4 MB RAM, 24 bit true colour	4 MB RAM (or more), 24 bit true colour
CD-ROM drive:	10 x speed	20 x speed

Support

News about new features, applications, papers, updates, patches, etc are available at the MIKE 21 web site located at

<http://www.dhisoftware.com/MIKE21>

For further information on MIKE 21 OSW please contact the Software Support Centre at DHI:

DHI Software Support Centre

DHI Water & Environment
Agern Allé 11
DK-2970 Hørsholm
Denmark

Tel: +45 4516 9333

Fax: +45 4516 9292

Web: www.dhisoftware.com

e-mail: software@dhi.dk



FEMA Approval of MIKE 21

The US Federal Emergency Management Agency (FEMA) has per May 2001 officially approved MIKE 21 for use in coastal Flood Insurance Studies.

The three modules, which are the hydro-dynamic module, near-shore spectral wind-wave module and offshore-spectral wind-wave module, have been accepted for coastal storm surge, coastal wave heights, and coastal wave effect usage.

For more information please check www.fema.gov/nfp and www.dhisoftware.com.



FEMA approval of MIKE 21 OSW

References

Brink-Kjær, O., Knudsen, J., Rodenhuis, G.S. and Rugberg, M., (1984). Extreme wave conditions in the central North Sea. In: Proc. of Offshore Technology Conference, pp 283-293.

Johnson, H.K., and Kofoed-Hansen, H., (2000). Influence of bottom friction on sea surface roughness and its impact on shallow water wind wave modelling. *J. Phys. Oceanogr.*, **30**, 1743-1756.

Johnson, H.K., Vested, H.J., Hersbach, H. Højstrup, J. and Larsen, S.E., (1999). On the coupling between wind and waves in the WAM model. *J. Atmos. Oceanic Technol.*, **16**, 1780-1790.

Kitaigorodskii, S.A., Krasitskii, V.P. and Zaslavskii, M.M., (1975). On Philips' theory of equilibrium range in the spectra of wind-generated gravity waves. *J. Phys. Oceanogr.*, **5**, pp 410-420.

Komen, G.J., Cavalieri, L., Doneland, M., Hasselmann, K., Hasselmann S. and Janssen, P.A.E.M., (1994). Dynamics and modelling of ocean waves. Cambridge University Press, UK, 560pp.

Resio, D.T., (1981). The estimation of wind-wave generation in a discrete spectral model. *J. Phys. Oceanogr.*, **11**, pp 510-525.

References on applications

Brink-Kjær, O., Kej, A., Cardone, V. and, Pushparatnam, E., (1986). Environmental Conditions in the South China Sea Offshore Malaysia: Hindcast Study Approach. In: Proc. Offshore Technology Conference. 13pp.

Kofoed-Hansen, H., Johnson, H.K., Højstrup, J. and Lange, B., (1998). Wind-wave modelling in waters with restricted fetches. In: Proc of 5th International Workshop on Wave Hindcasting and Forecasting, 27-30 January 1998, Melbourne, FL, USA, pp. 113-127.

Kofoed-Hansen, H., Johnson, H.K., Astrup, P. and Larsen, J., (2001). Prediction of waves and sea surface roughness in restricted coastal waters. In: Proc of 27th International Conference of Coastal Engineering, pp.1169-1182.

Al-Mashouk, M.A., Kerper, D.R. and Jacobsen, V., (1998). Red Sea Hindcast study: Development of a sea state design database for the Red Sea.. *J Saudi Aramco Technology*, **1**, 10pp.

Rugbjerg, M., Nielsen, K., Christensen, J.H. and Jacobsen, V., (2001). Wave energy in the Danish part of the North sea. In: Proc of 4th European Wave Energy Conference, 8pp.



MIKE 21 OSW can also be applied for wave forecast in ship route planning and improved service for conventional and fast ferry operators.

B I L A G C

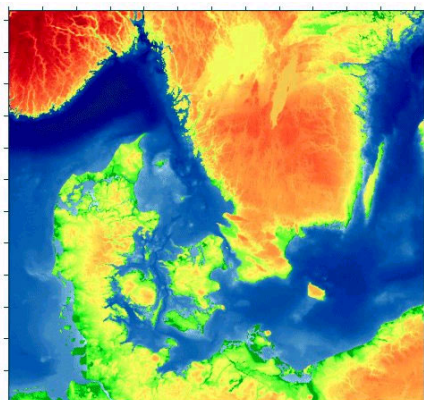
***Generel beskrivelse af Vandudsigten – The Water Forecast
(på engelsk)***

Weather Forecasting is a well-established activity, which has been servicing the public for more than a century. Recent developments in operational hydrography and hydrology have made it possible to produce similar forecasting for water systems. DHI has produced a webbased prototype for a comprehensive water forecasting system. The scope of this system with special emphasis on Offshore Wind Farms is presented below.

Who Are the Users?

Potential users of a Water Forecast are shown below (in no way a complete list):

- The Municipality water engineer responsible for hoisting the “blue flag” and for warnings of storm water overflow occurrences for the benefit of bathers along selected beaches
- The professional fisherman, who checks the local current, salt and temperature conditions in order to indicate the whereabouts of the fish
- The yachtsman, who wants to know the weekend’s wind and current conditions before planning his sailing activities
- The boat owner, who wishes to know the water level to make sure that his boat remains safely on the shore
- Trolling fishers wanting to know where the thermocline is in order to locate the salmon



- The angler in summer who wants to know where the cold water will hit the shore to increase his chances of finding the salmon
- The marine farmer, who wishes to know how salt and temperature vary, aiming at an optimum feeding of the fish
- The county biologist, who wishes to issue a timely warning to the public of an occurrence of poisonous algae.
- The Danish environmental authorities wishing to inform the public of next week’s oxygen depletion in Kattegat

- The offshore wind farm construction company, who wants to have forecasts before transporting construction elements to the sea site



© N.E.G. MECOM

- The captain of the diving vessel Stromboli of Malmö, who wishes to satisfy himself that the water is clear enough for the divers to locate the wreck
- The county engineer, who wishes to know the height of the waves before he stands on the quay and finds the waves to high for him to inspect or repair the measurement buoy
- The county engineer carefully watching the oil spill to be able to take preventive measures before it reaches Rødsand.
- The ferry company using currents and waves to optimise the route planning
- The rescue company needing to know the floating route of the man-over-board
- The windsurfer needing to know today’s best beach for his activities

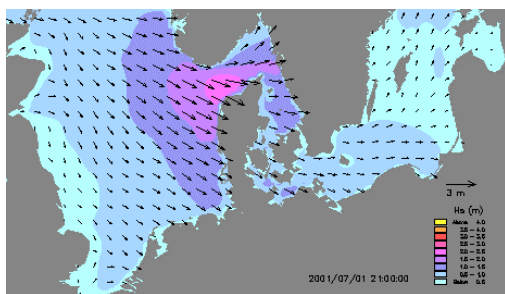
A Prototype Forecasting System

The Water Forecast describes the hydrography and water environment of the Baltic, the Danish waters and the North Sea for 72 hours until midnight the next day. The simulations are updated once pr. day and ready about noon UTC

At present, the water conditions are described for a 124 times 124 grid point. A facility for zooming out to get an overall view of the entire North Sea and Baltic as well as for zooming in to get a close view of coastal areas, lakes or rivers is being planned. Alarms for oil spills and for the bathing water quality will also be included.

Water Forecasts

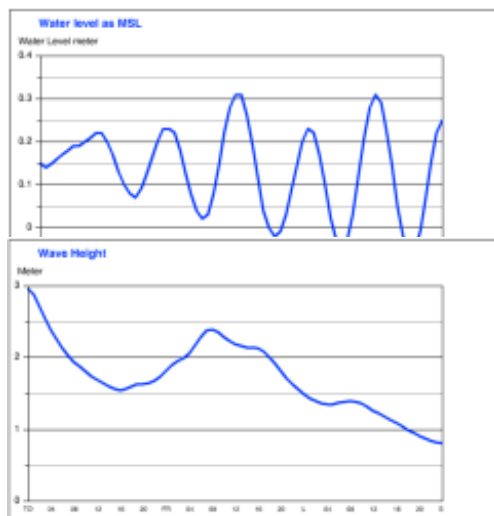
Software tools now exist which can model waves as well as hydrodynamics, advection/dispersion and numerous biological and chemical variables in 3 dimensions and down to the desired resolution.



The models are combined with data continuously collected from the area and with meteorological forecast to give water forecasts of the following variable:

- wave height, wave period and wave direction
- water level, current speed and current direction
- temperature and salinity
- dissolved oxygen and chlorophyll-a

The forecasts are presented in single points (see example below) and as animated maps (see above). However, the data presentation may also be customised to individual needs.



Detailed Wave Forecasts

DHI is together with Tech-wise developing detailed local wave forecasting techniques

especially for use during the construction period and for the following maintenance of offshore wind farms. The technique is scheduled for use at Horns Rev, Denmark, from the spring of 2002.

Weather Forecasts

DHI collaborates with a weather forecasting centre through which detailed local weather forecasts similar to the water forecasts are available.

The DHI Models

Wave conditions are forecast using DHI's MIKE 21 OSW model, which is based on the internationally developed and used WAM model. The hydrodynamic model used for forecasting of water levels, currents, temperature and salinity is DHI's MIKE 3, which is also implemented for the Danish Environmental authorities in the Danish Seas Model. Finally, dissolved oxygen and chlorophyll-a is forecast using DHI's MIKE 21 EU model.

Access to Prototype

All data are available in an English version at www.waterforecast.com and in a Danish version at www.vandudsigtten.dk.

You may also contact DHI for a personal test subscription by sending an email to:
vandvagt@dhi.dk

Further Information

For further information including subscription rates please contact:

Karl Iver Dahl-Madsen (kdm@dhi.dk)
 DHI Water & Environment
 Agern Allé 11
 DK-2970 Hørsholm
 Denmark
 Tel: +45 45 16 92 00
 Fax: + 45 45 16 92 92

B I L A G D

A Third Generation Spectral Wave Model using an Unstructured Finite Volume Technique, (på engelsk)

A THIRD-GENERATION SPECTRAL WAVE MODEL USING AN UNSTRUCTURED FINITE VOLUME TECHNIQUE

Ole René Sørensen, Morten Rubjerg, Lars Steen Sørensen
and Henrik Kofoed-Hansen

DHI Water & Environment, Agern Allé 11, DK 2970 Hørsholm, Denmark

Abstract

A new third-generation spectral wave model is presented for prediction of the wave climates in offshore and coastal areas. The essential topic of the present paper is new numerical techniques for solution of the governing equations. The discretisation in the geographical space and the spectral space is based on cell-centered finite volume technique. In the geographical space, an unstructured mesh is applied. Due to the high degree of flexibility, unstructured meshes are very efficient to deal with problems of different characteristic scales. In coastal areas, a fine grid is required to resolve the important physical phenomena and to resolve the complex bottom topographies, while in offshore areas coarser resolution is usually sufficient. The time integration is performed using a fractional step approach, where an efficient multisequence explicit method is applied for the propagation process. Results presented shown for a storm in the North Sea and compared to observations.

1. Introduction

Third-generation wave models are used extensively for prediction of the growth, decay and transformation of wind-generated waves and swell in the deep ocean and shelf seas. Recently, these models have been extended for application in coastal areas. The main focus has so far been on the formulation of the source functions describing the different physical phenomena, which are important in shallow water. The essential topic of the present paper is new numerical techniques for solution of the governing equations.

Traditionally, third-generation spectral wave models are solved using either an Eulerian or a semi-Lagrangian approach and rectangular structured meshes. Examples of such models are the WAM model (WAMDI Group, 1988), the WAVEWATCH III model (Tolmann, 1991 and Tolmann and Chalikov, 1996), the PHIDIAS model (Van Vledder et al., 1994), the MIKE 21 OSW model (Johnson and Kofoed-Hansen, 1998)

and the SWAN model (Booij et al., 1999 and Ris et al., 1999). Even with the computers of today, third-generation spectral wave models are very computational demanding. To resolve the characteristic scales of the important physical phenomena in the coastal areas, a fine mesh is required. In the breaking zone, a resolution of the order of 10 m is needed. A high resolution is also needed to resolve the complex bottom topographies in shallow water environments, such as barrier islands, reefs, submerged bars, and channels. The need for high-resolution local models can be achieved by using the nesting technique, where a local model with a fine mesh is embedded in a coarse mesh model. Usually, only a one-way transfer of boundary condition from the coarse mesh model to the fine mesh model is used. With the goal of reducing the computational effort, it is desirable to introduce more flexible meshes as an alternative to nested models. Control of node distribution allows for optimal usage of nodes and adaption of mesh resolution to the relevant physical scales. Flexible meshes can be accomplished in a number of ways, e.g. multi-block curvilinear meshes, overlapping meshes, local mesh refinement and unstructured meshes. Only a few examples of third-generation spectral model using flexible meshes have been presented. Recently, the possibility of using curvilinear meshes has been implemented in the SWAN model, however, so far only in a single-block mode. Benoit el al. (1996) developed the model TOMAWAC based on semi-Lagrangian approach, where an unstructured finite element technique was used for the spatial discretisation of the dependent variables.

In this paper, a new Eulerian model based on unstructured meshes is developed. The unstructured mesh approach has been chosen because it gives the maximum degree of flexibility. In coastal regions, the effect of tides, surges and currents can be very important for accurate prediction of the wave conditions. In the presents of dynamic depths and currents, the conserved quantity is wave action and the dynamics of the gravity waves can be described by the conservation equation for wave action density. For small-scale applications, the basic conservation equations are usually formulated in Cartesian co-ordinates, while spherical polar co-ordinates are used for large-scale applications. The source functions implemented in the new model are based on state-of-the-art third-generation formulations.

The spatial discretisation of the conservation equation for wave action is performed using an unstructured finite volume (FV) method. During the last decade, FV methods have been successfully applied for modelling of non-linear transport problems and compressible flow problems. The time integration is based on a fractional step approach, where the propagation step is solved using an explicit method. The use of explicit method can introduce a severe restriction on the time step for a given spatial discretisation due to the CFL stability condition. In order to relax the restriction on the time step, a multisequence explicit integration scheme is applied.

This paper is structured as follows: In Chapter 2, the governing equations are described. The numerical solution techniques for the spatial discretisation and the time integration are presented in Chapter 3. In Chapter 4 the model is verified. Finally, Chapter 5 draws up the conclusion.

2. Governing Equations

In the present model, the wind waves are represented by the action density spectrum $N(\sigma, \theta)$. The independent phase parameters have been chosen as the relative (intrinsic) angular frequency, $\sigma = 2\pi f$, and the direction of wave propagation, θ . The relation between the relative angular frequency (as observed in a frame of reference moving with the current velocity) and the absolute angular frequency, ω , (as observed in a fixed frame) is given by the linear dispersion relation

$$\sigma = \sqrt{gk \tanh(kd)} = \omega - \bar{k} \cdot \bar{U} \quad (1)$$

where g is the acceleration of gravity, d is the water depth and \bar{U} is the current velocity vector and \bar{k} is the wave number vector with magnitude k and direction θ . The action density, $N(\sigma, \theta)$, is related to the energy density $E(\sigma, \theta)$ by

$$N = \frac{E}{\sigma} \quad (2)$$

2.1 Wave Action Balance Equation

The governing equation is the wave action balance equation formulated in either Cartesian or spherical co-ordinates (see Komen et al. (1994) and Young (1999)). In horizontal Cartesian co-ordinates, the conservation equation for wave action can be written as

$$\frac{\partial N}{\partial t} + \nabla \cdot (\bar{v}N) = \frac{S}{\sigma} \quad (3)$$

where $N(\bar{x}, \sigma, \theta, t)$ is the action density, t is the time, $\bar{x} = (x, y)$ is the Cartesian co-ordinates, $\bar{v} = (c_x, c_y, c_\sigma, c_\theta)$ is the propagation velocity of a wave group in the four-dimensional phase space \bar{x} , σ and θ , and S is the source term for the energy balance equation. ∇ is the four-dimensional differential operator in the \bar{x} , σ , θ -space. The four characteristic propagation speeds are given by

$$(c_x, c_y) = \frac{d\bar{x}}{dt} = \bar{c}_g + \bar{U} \quad (4a)$$

$$c_\sigma = \frac{d\sigma}{dt} = \frac{\partial \sigma}{\partial d} \left[\frac{\partial d}{\partial t} + \bar{U} \cdot \nabla_{\bar{x}} d \right] - c_g \bar{k} \cdot \frac{\partial \bar{U}}{\partial s} \quad (4b)$$

$$c_\theta = \frac{d\theta}{dt} = -\frac{1}{k} \left[\frac{\partial \sigma}{\partial d} \frac{\partial d}{\partial m} + \bar{k} \cdot \frac{\partial \bar{U}}{\partial m} \right] \quad (4c)$$

Here, s is the space co-ordinate in wave direction θ , and m is a co-ordinate perpendicular to s . $\nabla_{\bar{x}}$ is the two-dimensional differential operator in the \bar{x} -space. The magnitude of the relative group velocity \bar{c}_g is given by

$$c_g = \frac{\partial \sigma}{\partial k} = \frac{1}{2} \left(1 + \frac{2kd}{\sinh(2kd)} \right) \frac{\sigma}{k} \quad (5)$$

In spherical co-ordinates, the conserved property is the action density $\hat{N}(\bar{x}, \sigma, \theta, t)$. Here, $\bar{x} = (\phi, \lambda)$ is the spherical co-ordinates, where ϕ is the latitude and λ is the longitude. The action density \hat{N} is related to the normal action density N through $\hat{N} d\sigma d\theta d\phi d\lambda = N d\sigma d\theta dx dy$, or

$$\hat{N} = NR^2 \cos \phi \quad (6)$$

where R is the radius of the earth.

2.2 Source Functions

The source term, S , on the right side of Eq (3) represents the superposition of source functions describing various physical phenomena

$$S = S_{in} + S_{nl} + S_{ds} + S_{bot} + S_{surf} \quad (7)$$

Here, S_{in} represents the generation of energy by the wind, S_{nl} is the wave energy transfer due to non-linear wave-wave interaction, S_{ds} is the dissipation of wave energy due to whitecapping, S_{bot} is the dissipation due to bottom friction and S_{surf} is the dissipation of wave energy due to depth-induced breaking.

The wind input, S_{in} , is based on Janssens's quasi-linear theory of wind wave generation (Janssen, 1989, 1991), and implemented as in WAM Cycle 4 (see Komen et al., 1994). The non-linear energy transfer through the four-wave interaction is represented by the discrete interaction approximation (DIA) proposed by Hasselmann et al. (1985). The source function describing the dissipation due to whitecapping, S_{ds} , is based on the theory of Hasselmann (1974), tuned according to Janssen (1989) and Janssen and Günter (1992).

The rate of dissipation due to bottom friction is given by

$$S_{bot}(\sigma, \theta) = -C_f \frac{k}{\sinh(2kd)} E(\sigma, \theta) \quad (8)$$

where C_f is a friction coefficient. A number of expressions for the friction coefficient have been proposed in the literature, see Johnson and Kofoed-Hansen (2000). Here we use the formulation suggested by Weber (1991). The friction coefficient is determined as the product of a friction factor and the rms orbital velocity at the bottom. The friction factor is calculated using the expression by Jonsson (1966) and Jonsson and Carlson (1976). In the expression by Jonsson, the friction coefficient is determined as function of the bottom roughness length scale, k_N , and the orbital displacement at the bottom.

Depth-induced breaking occurs when waves propagate into very shallow areas, and the wave height can no longer be supported by the water depth. The formulation of wave breaking is based on the breaking model by Battjes and Janssen (1978). Eldeberky and Battjes (1995) proposed a spectral formulation of the breaking model, where the spectral shape was not influenced by breaking. The source function due to depth-induced breaking can be written

$$S_{\text{surf}}(\sigma, \theta) = -\frac{\alpha Q_b \bar{\sigma} H_m^2}{8\pi} \frac{E(\sigma, \theta)}{E_{\text{tot}}} \quad (9)$$

where $\alpha \approx 1.0$ is a calibration constant, Q_b is the fraction of breaking waves, $\bar{\sigma}$ is the mean relative frequency, E_{tot} is the total wave energy, and $H_m = \gamma d$ is the maximum wave height. The value of the breaker parameter, γ , varies from 0.5 to 1.0

3. Numerical Method

The frequency spectrum is split up into a deterministic prognostic part for frequencies lower than a cut-off frequency and an analytical diagnostic part for frequencies higher than the cut-off frequency. A dynamic cut-off frequency depending on the local wind speed and the mean frequency is used as in the WAM Cycle 4 model (see WAMDI Group (1988) and Komen et al. (1994)). Above the cut-off frequency limit of the prognostic region, a parametric tail is applied

$$E(\sigma, \theta) = E(\sigma_{\max}, \theta) \left(\frac{\sigma}{\sigma_{\max}} \right)^{-m} \quad (10)$$

where m is a constant. In the present model $m = 5$ is applied. The diagnostic tail is used in the calculation of the non-linear transfer and in the calculation of the integral parameters used in the source functions. The deterministic part of the spectrum is determined solving Eq (3) using numerical methods.

3.1 Space Discretisation

The discretisation in geographical and spectral space is performed using a cell-centered finite volume method. In the geographical domain, an unstructured mesh is used. The spatial domain is discretised by subdivision of the continuum into non-overlapping elements. The elements can be of arbitrarily shaped polygons, however, in this paper only triangles are considered. The action density, $N(\bar{x}, \sigma, \theta)$ is represented as a piecewise constant over the elements and stored at the geometric centres. In frequency space, a logarithmic discretisation is used

$$\sigma_1 = \sigma_{\min} \quad \sigma_l = f_\sigma \sigma_{l-1} \quad \Delta\sigma_l = \sigma_{l+1} - \sigma_{l-1} \quad l = 2, N_\sigma$$

where f_σ is a given factor, σ_{\min} is the minimum discrete angular frequency and N_σ is the number of discrete frequencies. In the directional space, an equidistant discretisation is used

$$\theta_m = (m-1)\Delta\theta \quad \Delta\theta_m = 2\pi/N_\theta \quad m = 1, N_\theta$$

where N_θ is the number of discrete directions. The action density is represented as piecewise constant over the discrete intervals, $\Delta\sigma_l$ and $\Delta\theta_m$, in the frequency and directional space.

Integrating Eq (3) over area A_i of the i th element, the frequency increment $\Delta\sigma_l$ and the directional increment $\Delta\theta_m$ give

$$\begin{aligned} \frac{\partial}{\partial t} \int_{\Delta\theta_m} \int_{\Delta\sigma_l} \int_{A_i} N d\Omega d\sigma d\theta - \int_{\Delta\theta_m} \int_{\Delta\sigma_l} \int_{A_i} \frac{S}{\sigma} d\Omega d\sigma d\theta = \\ \int_{\Delta\theta_m} \int_{\Delta\sigma_l} \int_{A_i} \nabla \cdot (\bar{F}) d\Omega d\sigma d\theta \end{aligned} \quad (11)$$

where Ω is an integration variable defined on A_i and $\bar{F} = (F_x, F_y, F_\sigma, F_\theta) = \bar{v}N$ is the convective flux. The volume integrals on the left-hand side of Eq (11) are approximated by one-point quadrature rule. Using the divergence theorem, the volume integral on the right-hand can be replaced by integral over the boundary of the volume in the \bar{x}, σ, θ -space and these integrals are evaluated using a midt-point quadrature rule. Hence, Eq (11) can be written

$$\begin{aligned} \frac{\partial N_{i,l,m}}{\partial t} = -\frac{1}{A_i} \left[\sum_{p=1}^{NE} (F_n)_{p,l,m} \Delta l_p \right] - \\ \frac{1}{\Delta\sigma_l} [(F_\sigma)_{i,l+1/2,m} - (F_\sigma)_{i,l-1/2,m}] - \frac{1}{\Delta\theta_m} [(F_\theta)_{i,l,m+1/2} - (F_\theta)_{i,l,m-1/2}] + \frac{S_{i,l,m}}{\sigma_l} \end{aligned} \quad (12)$$

where NE is the total number of edges in the cell (NE = 3 for triangles). $(F_n)_{p,l,m} = (F_x n_x + F_y n_y)_{p,l,m}$ is the normal flux through the edge p in the geographical space with length Δl_p . $\bar{n} = (n_x, n_y)$ is the outward pointing unit normal vector of the boundary in the geographical space. $(F_\sigma)_{i,l+1/2,m}$ and $(F_\theta)_{i,l,m+1/2}$ are the flux through the face in the frequency and directional space, respectively.

The convective flux is derived using a first-order upwinding scheme. In the geographical space, the normal flux at the edge between element i and j is given by

$$F_n = c_n \left(\frac{1}{2}(N_i + N_j) - \frac{1}{2} \frac{c_n}{|c_n|} (N_i - N_j) \right) \quad (13)$$

where c_n is the propagation speed normal to the cell face

$$c_n = \frac{1}{2} (\bar{c}_i + \bar{c}_j) \cdot \bar{n} \quad (14)$$

The numerical diffusion introduced using first-order upwinding schemes can be significant, see e.g. Tolman (1991, 1992). In small-scale coastal applications and application dominated by local wind, the accuracy obtained using these schemes are considered to be sufficient. However, for the case of swell propagation over long distances, higher-order upwinding schemes may have to be applied.

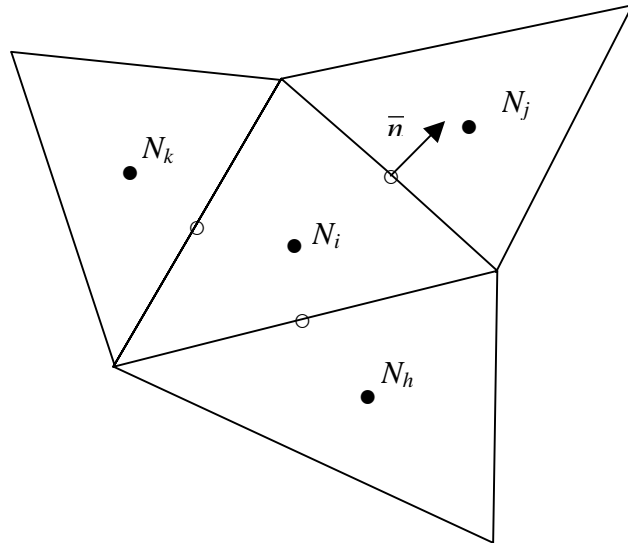


Fig. 1. • centroid point and ○ midpoint of edges.

3.2 Time Integration

The integration in time is based on a fractional step approach. Firstly, a propagation step is performed calculating an approximate solution N^* at the new time level ($n+1$) by solving Eq (3) without the source terms. Secondly, a source terms step is performed calculating the new solution N^{n+1} from the estimated solution taking into account only the effect of the source terms.

Propagation step

The propagation step is carried out by an explicit Euler scheme

$$N_{i,l,m}^* = N_{i,l,m}^n + \Delta t \left(\frac{\partial N_{i,l,m}}{\partial t} \right)^n \quad (15)$$

where $(\partial N_{i,l,m} / \partial t)^n$ is given by Eq (12) with $S_{i,l,m} = 0$ and Δt is the global time step. To overcome the severe stability restriction, a multisequence integration scheme is employed following the idea by Vislmeier and Hänel (1995). Here, the maximum time step is increased by locally employing a sequence of integration steps, where the number of steps may vary from element to element. Using the explicit Euler scheme, the time step is limited by the CFL condition stated as

$$Cr_{i,l,m} = \left| c_x \frac{\Delta t}{\Delta x_i} \right| + \left| c_y \frac{\Delta t}{\Delta y_i} \right| + \left| c_\sigma \frac{\Delta t}{\Delta \sigma_l} \right| + \left| c_\theta \frac{\Delta t}{\Delta \theta_m} \right| < 1 \quad (16)$$

where $Cr_{j,l,m}$ is the Courant number and Δx_i and Δy_i are characteristic length scale in the x and y -directions for the i th element. The maximum local Courant number, $Cr_{max,i}$, is determined for each element in the geographical space, and the maximum local time step, $\Delta t_{max,i}$, for the i th element is then given by

$$\Delta t_{max,i} = \Delta t / Cr_{max,i} \quad (17)$$

To ensure accuracy in time, the intermediate levels have to be synchronised. Therefore, the fraction, f_g , of the local time step to the global time step is chosen as powers of $1/2$

$$f_g = \left(\frac{1}{2} \right)^{g-1}, \quad g = 1, 2, 3, \dots \quad (18)$$

The local time step, Δt_i , is then determined as the time step with the maximum value of the level index, g , for which

$$\Delta t_i f_g < \Delta t_{\max,i} \quad (19)$$

Two neighbouring elements are not allowed to have an index difference greater than one. The edges get the lowest index of the two elements they support.

The calculation is performed using a group concept, in that groups of elements are identified by their index, g . The computational speed-up using the multisequence integration compared to the standard Euler method increases with increasing number of groups. However, to get accurate results in time, the maximum number of groups must be limited. In the present work, the maximum number of levels is 32.

Source term step

The source term step is performed using an implicit method

$$N_{i,l,m}^{n+1} = N_{i,l,m}^* + \Delta t \left[\frac{(1-\alpha)S_{i,l,m}^* + \alpha S_{i,l,m}^{n+1}}{\sigma_l} \right] \quad (20)$$

where α is a weighting coefficient that determines the type of finite difference method. Using a Taylor series to approximate S^{n+1} and assuming the off-diagonal terms in the functional derivative $\partial S / \partial E$ to be negligible such that the diagonal part $\partial S_{i,l,m} / \partial E_{i,l,m} = \gamma$, Eq (20) can be simplified as

$$N_{i,l,m}^{n+1} = N_{i,l,m}^n + \frac{(S_{i,l,m}^* / \sigma_l) \Delta t}{(1 - \alpha \gamma \Delta t)} \quad (21)$$

For growing waves ($\gamma > 0$), an explicit forward difference is used ($\alpha = 0$), while for decaying waves ($\gamma < 0$), an implicit backward difference ($\alpha = 1$) is applied.

Especially for small fetches, stability problems may occur. Hence, a limiter on the maximum increment of spectral energy between two successive time steps is introduced. The limiter proposed by Hersbach and Janssen (1999) is applied.

3.4 Boundary Conditions

At the land boundaries in the geographical space, a fully absorbing boundary condition is applied. The incoming flux components (the flux components for which the propagation velocity normal to the cell face is positive) are set to zero. No boundary condition is needed for the outgoing flux components. At an open boundary, the incoming flux is needed. Hence, the energy spectrum has to be specified at an open boundary. In the frequency space, the boundaries are fully absorbing. No boundary conditions are needed in the directional space.

4. Numerical Experiments

In order to verify the accuracy of the numerical approach, a large number of test cases have been conducted. These include simple tests of both depth-induced and current-induced shoaling and refraction of monochromatic, long-crested waves for which analytical solutions can be obtained. The agreement with the analytical solutions was excellent. In the present paper, we will focus on a real test case.

4.1 Storm of 29 January 2002 in the North Sea

The storm of 29 January 2002 was severe. The storm was caused by a depression travelling from England towards the eastern part of the North Sea. The storm produced prolonged strong westerly winds with a maximum 10 m wind speed of approximately 26 m/s. The simulation period chosen for the numerical simulations runs from 00 UTC 22 January 2002 to 00 UTC 31 January 2002.

The computational domain covers part of the Norwegian Sea, the North Sea, the Inner Danish Waters, the Baltic Sea and the Gulf of Botnia. Special emphasis is devoted the prediction of the wave conditions at Horns Rev (reef) in the south eastern part of the North Sea. At this site, a 168 MW offshore wind farm with 80 turbines have been established. The numerical model has been used to forecast the wave conditions during the construction in 2002, and is subsequently being used in connection with maintenance. An unstructured mesh containing 8985 triangular elements is used: in the Norwegian Sea the element size is approximatively 800 km^2 , in the North Sea, the Baltic Sea, and the Gulf of Botnia the element size is approximatively 200 km^2 , in the inner Danish Waters the element size is approximatively 50 km^2 and finally in the Horns Rev area a very fine mesh with an element size of 1.5 km^2 is applied. The mesh is shown in Fig 2 and a close-up of the mesh in the area at Horns Rev is shown in Fig 3. A fine mesh is required in the area at Horns Rev due to the complex topography characterized by a system of reefs (see Fig 4). The overall time step in the simulation is

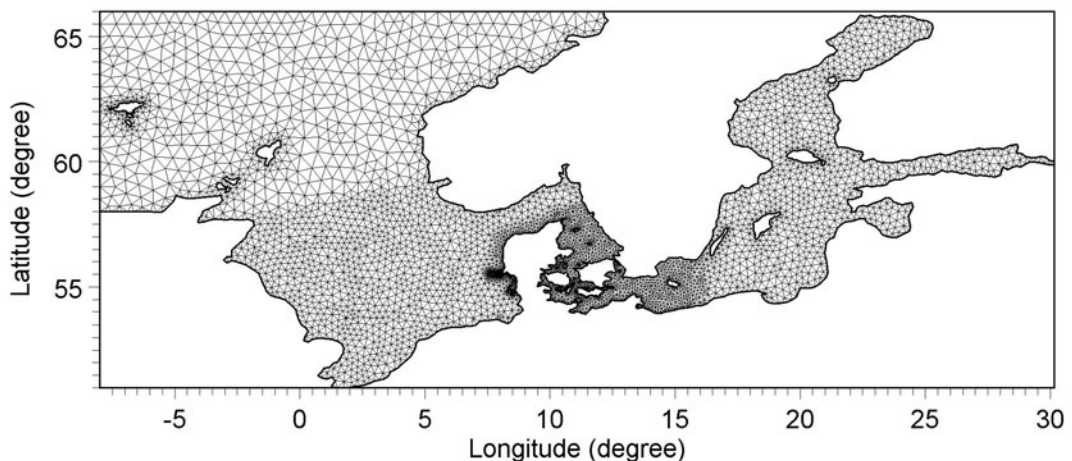


Fig. 2. The mesh.

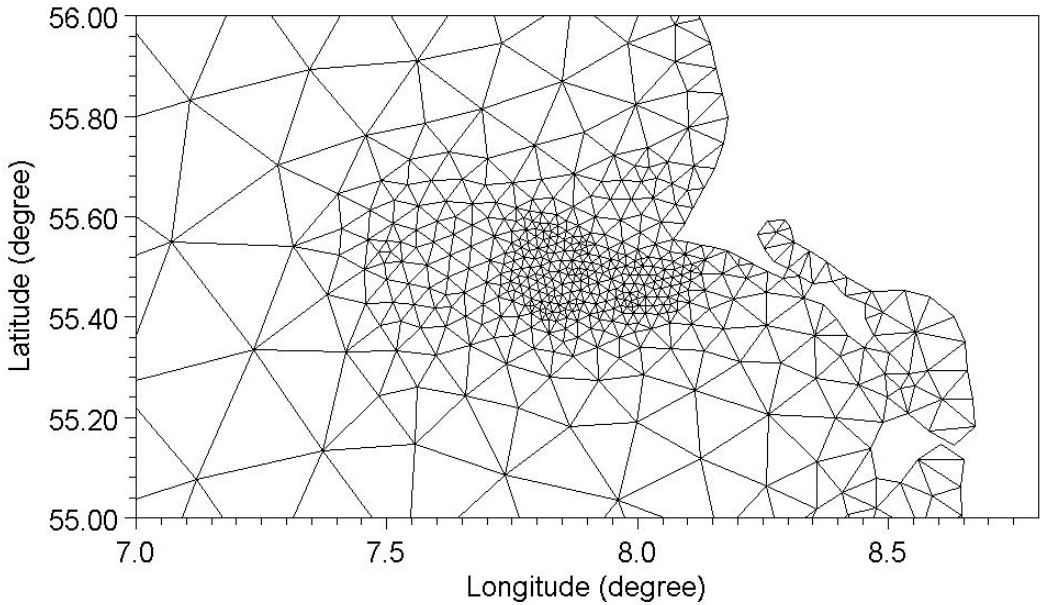


Fig. 3. Close-up of the mesh at Horns Rev.

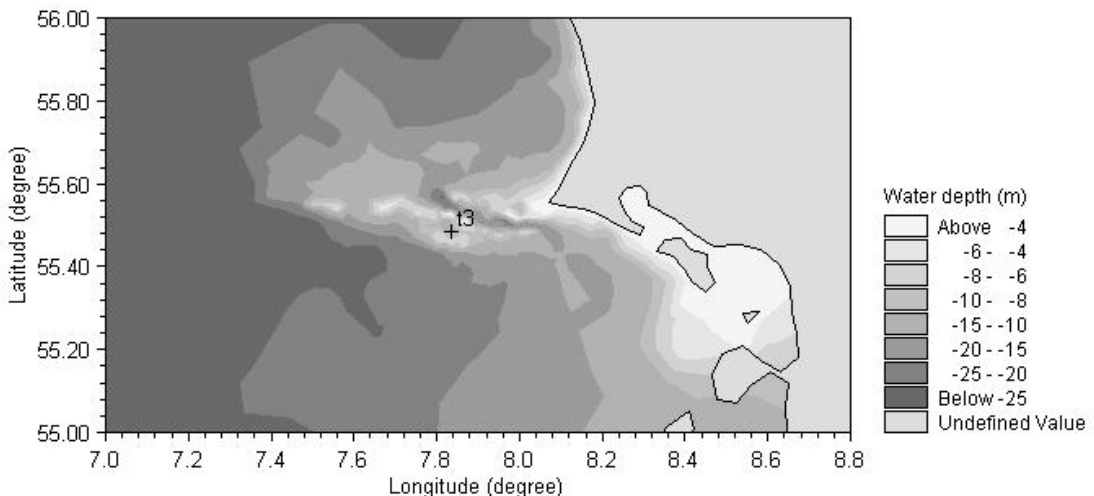


Fig. 4. Close-up of the bathymetry at Horns Rev. The location of the buoy is shown on the plot (t3).

600 s. A logarithmic frequency discretisation with 25 frequencies is used. The lowest discrete frequency is $f_{min} = 0.40$ Hz and the ratio between successive frequencies is chosen as $f_\sigma = 1.115$. The number of discrete directions is chosen as 16. The maximum level index in the propagation step is 32 and the averaged number of levels in the propagation step is 6. Hence, a speed-up of a factor 6 for the propagation is obtained

using the multisequence integration scheme compared to using a standard Euler scheme.

The wind data for the storm of January 2002 has been provided from Vejr2's meteorological ETA model. The data consist of 10 m wind speed and the wind direction every 3 hours. At Horns Rev, the tidal range is approximatively 1.5 m and during a storm the setup due to storm surge can be up to 2.5 m. The minimum water depth at Horns Rev is 3-4 m. Hence, to get accurate prediction of the wave conditions during a storm, it is important to include the effect of tidal variation and storm surge. Therefore, the time-varying water depth is in the wave simulation. The time-varying water depths are calculated using a two-dimensional hydrodynamic model. For the parameter in the breaking formulation $\gamma = 0.8$ is applied and for the bed friction a Nikuradse roughness $k_N = 0.04$ m is applied.

The results from the numerical model are compared to observations at two locations: Fjaltring and Horns Rev S. The positions of the two observation stations are given in Table 1. At Horns Rev and Fjaltring, the measurements are made using a Datawell Waverider Buoy. At Horns Rev S, the buoy is located on the south side of the shallow submerged reef (see Fig. 4) and the wave condition is strongly influenced by wave breaking on the reef for waves coming westerly to northerly directions.

Station	Longitude (Degree E)	Latitude (Degree N)	Depth, MSL (m)
Fjaltring	8 058221	56.475075	17.5
Horns Rev S	7.836733	55.483617	10.0

Table 1. Positions of the two measurement stations.

Timeseries of calculated and measured integral wave parameters are compared in Figs. 5 and 6, respectively at Fjaltring and Horns Rev S . The integral wave parameters are the significant wave height, $H_{m0} = 4\sqrt{m_0}$, the mean period, $T_{02} = \sqrt{m_0 / m_2}$, and the peak period, T_p . Here m_0 and m_2 are the zero-th and second-order moments of the energy density spectrum. The agreement between the numerical results and the observations is generally very good. To test the effect of including the time-varying water depth due to tide and surge, a simulation was also performed without this effect. As expected, the effect was very small at Fjaltring because the water depth of 17.5 m is large compared to the variation in the water level. However, at Horns Rev S the effect was very significant. When the time-variation of the depth is excluded, the significant wave height is significantly underestimated at the peak of the storm.

The calculated spectra are compared to the observed spectra at Fjaltring and Horns Rev S in Figs. 7 and 8, respectively. Spectra at the peak of the storm (00 UTC January 29) and after the storm (18 UTC January 31) are shown. The agreement is satisfactory. At Horns Rev S, the measured energy density spectrum at the peak of the storm strongly indicates transfer of energy to higher and lower harmonics due to

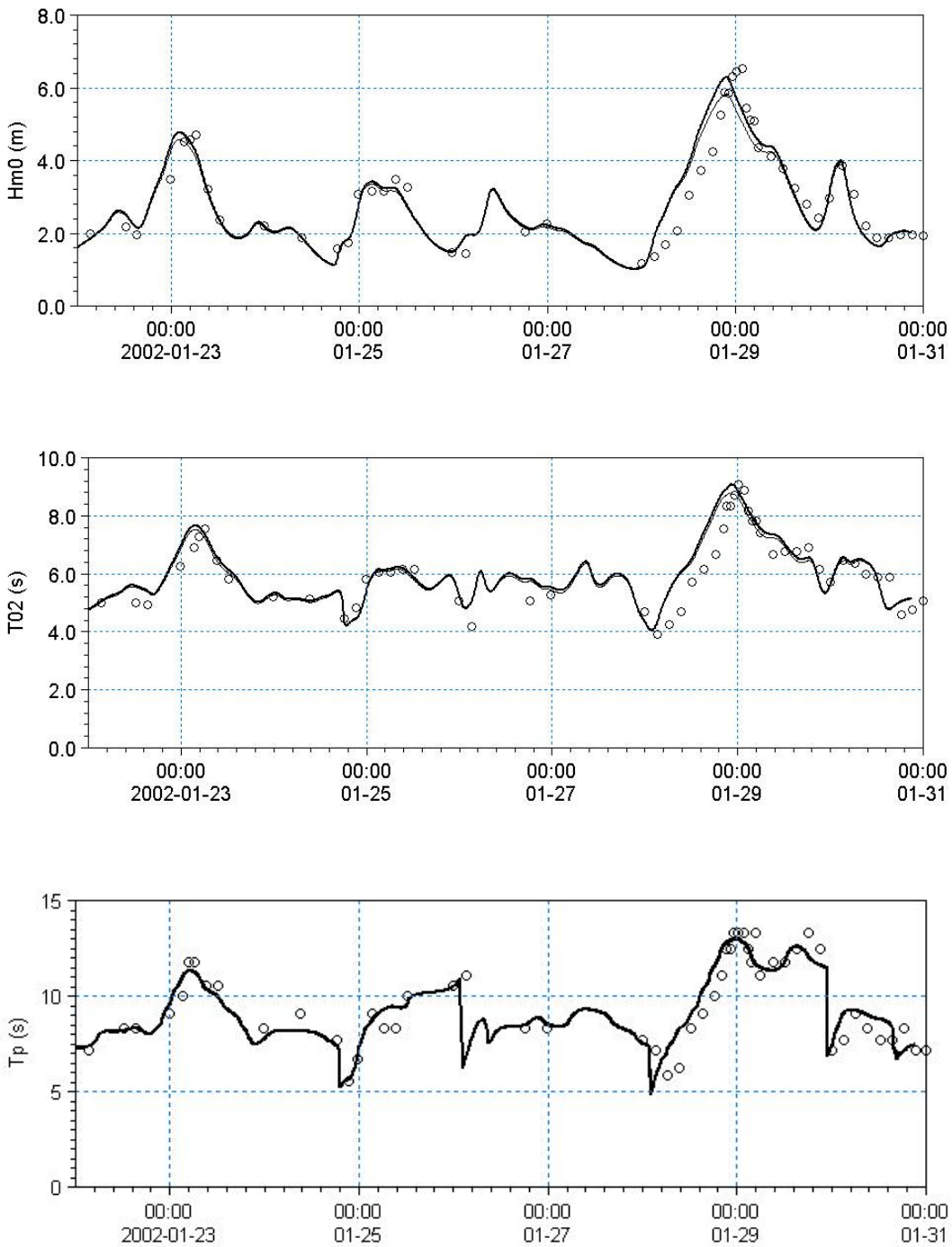


Fig. 5. Timeseries of significant wave height, H_{m0} , mean wave period, T_{02} , and peak wave period, T_p , at Fjaltring. — Calculations (including time-varying depth), — calculations (excluding time-varying depth) and o measurements.

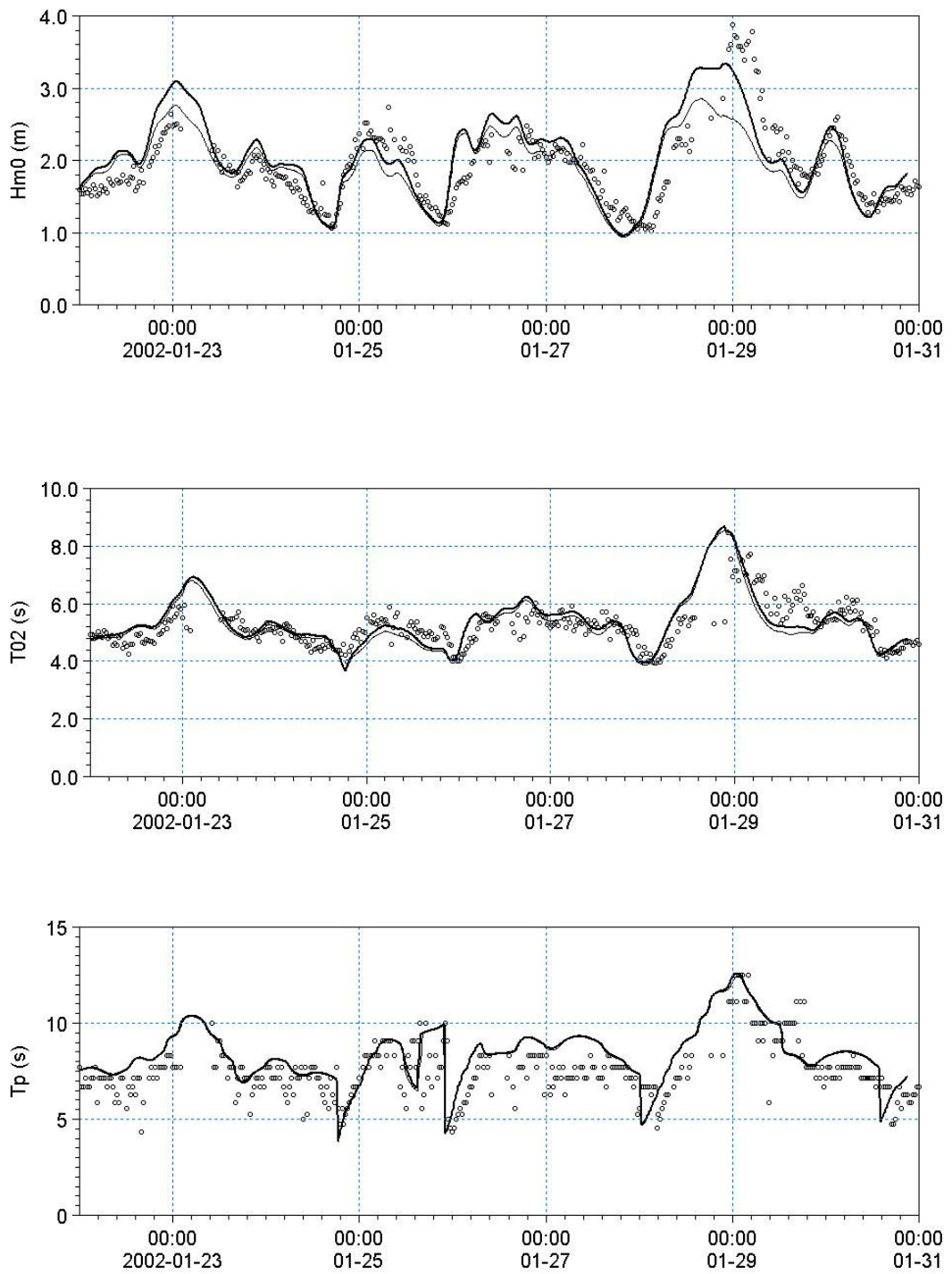


Fig. 6. Timeseries of significant wave height, H_{m0} , mean wave period, T_{02} , and peak wave period, T_p , at Horns Rev S. — Calculations (including time-varying depth), —calculations (excluding time-varying depth) and o measurements.

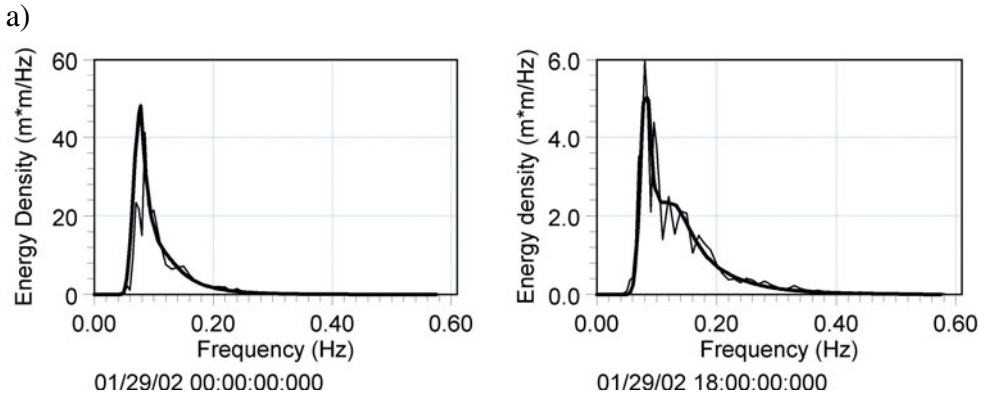


Fig. 7. Frequency spectrum at Fjaltring. — Calculations and — measurements. Note the difference in scales for the energy density.

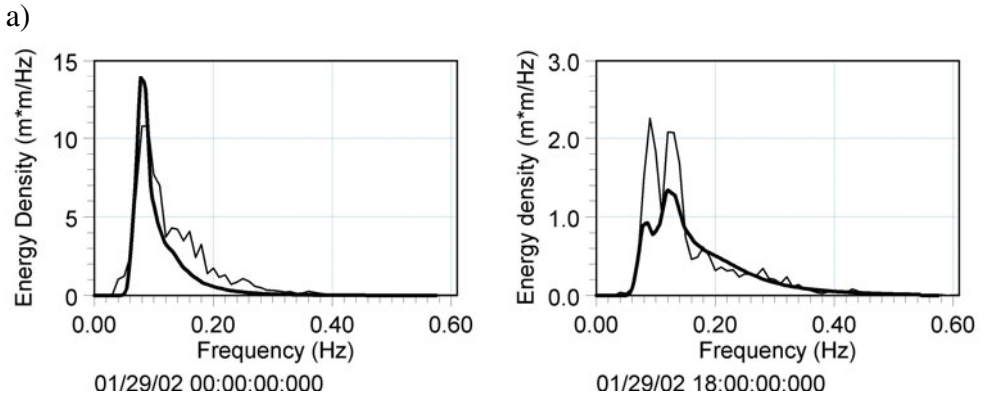
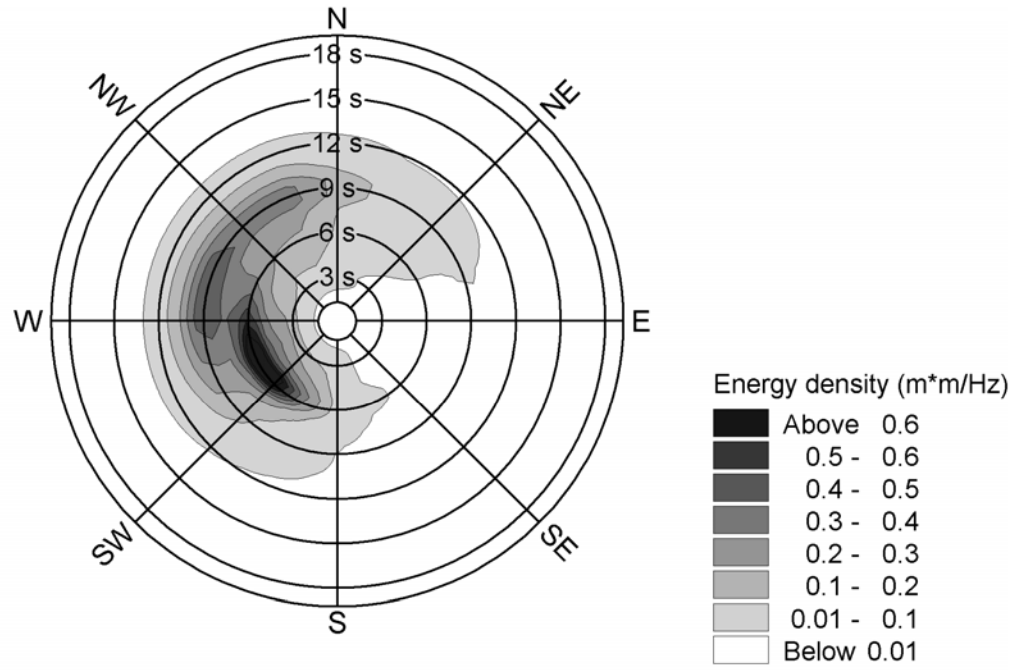


Fig. 8. Frequency spectrum at Horns Rev S. — Calculations and — measurements. Note the difference in scales for the energy density.

non-linear energy transfer. In shallow water, the non-linear energy transfer is dominated by triad wave-wave interactions. This effect is not included in the model, and therefore the energy at the peak frequency is overestimated and the energy at the secondary peak is underestimated. 18 hours after the peak of the storm, two peaks can be identified in the frequency spectrum with peak period of $T_p = 6$ s and 9 s. These two peaks are generated because the storm from W-NW is decreasing, while a new wind system from W-SW is reaching the area. In Fig. 9, the calculated directional-frequency spectrum at Horns Rev at 18 GMT January 31 is shown and two local peaks can clearly be identified.



01/29/02 18:00:00

Fig. 9. Directional-frequency spectrum at Horns Rev S.

5. Conclusion

A new third-generation spectral model is presented. The model is based on the finite volume method, where an unstructured mesh is applied in the geographical domain. The time integration is performed using an efficient multisequence explicit scheme. To verify the performance and accuracy of the new model, we have compared it against field observations in the North Sea for the 29 January 2002 storm. The agreement between the model results and measurements is found to be excellent.

The new numerical approach enables the accurate computations of the wave conditions in offshore and coastal areas including the effect of time-varying depths and currents. Due to the high degree of flexibility, unstructured meshes are very efficient to deal with problems of different characteristic scales. In coastal areas, a fine grid is needed to resolve the important physical phenomena and resolve complex bottom topographies, while in offshore areas coarser resolution is usually sufficient.

Acknowledgements

This research was partly funded by Eltra (the Electricity Transmission Company for Jylland and Fyn) as part of its "Public Service Obligation" (PSO), Project No 3187 - "Bølgeprognosemodeller". Their financial support is greatly appreciated. The observations at Horns Rev S were supplied by Elsam A/S and at Fjaltring by Kystdirektoratet.

References

- Battjes, J.A. and J.P.F.M. Janssen, (1978), Energy loss and set-up due to breaking of random waves, *Proc. 16th Int. Conf. Coastal Eng.*, ASCE, pp 569-587.
- Benoit, M., F. Marcos and F. Becq, (1996), Development of a third-generation shallow water wave model with unstructured spatial meshing, *Proc. 25th Int. Conf. Coastal Eng.*, ASCE, pp 465-478.
- Booij, N., R. C. Ris and L. H. Holthuijsen, (1999), A third-generation wave model for coastal regions. 1. Model description and validation. *J. Geophys. Res.*, **104**, 7649-7666.
- Eldeberky, Y. and J.A. Battjes. (1995), Parameterization of triad interactions in wave energy models, paper presented at Coastal Dynamics Conference, ASCE., Gdansk, Poland.
- Hasselmann K., (1974), On the spectral dissipation of ocean waves due to whitecapping, *Bound.Layer Meteor.*, **6**, 107-127.
- Hasselmann, S., K. Hasselmann, J.H. Allender and T.P. Barnett (1985), Computations and parameterizations of the non-linear energy transfer in gravity wave spectrum. Part II: Parameterisations of nonlinear energy transfer for applications in wave models, *J. Phys. Oceanogr.*, **15**, 1369-1377.
- Hersbach, H. and P. A. E. M. Janssen, (1999), Improvement of short-fetch behaviour in the wave ocean model, *J. Atmos. & Ocean Tech.*, **16**, 884-892.
- Komen, G.J., L. Cavalieri, M. Doneland, K. Hasselmann, S. Hasselmann and P.A.E.M. Janssen, (1994), *Dynamics and modelling of ocean waves*, Cambridge University Press, UK, 560 pp.
- Janssen, P.A.E.M., (1989), Wave induced stress and the drag of airflow over sea waves, *J. Phys. Oceanogr.*, **19**, 745-754.
- Janssen, P.A.E.M., (1991), Quasi-linear theory of wind wave generation applied to wave forecasting, *J. Phys. Oceanogr.*, **21**, 1631-1642.
- Janssen P.A.E.M. and Günther, (1992), Consequences of the effect of surface gravity waves on the mean air flow, *Int. Union of Theor. and Appl. Mech. (IUTAM)*, Sydney, Australia, 193-198.
- Johnson H.K., and H. Kofoed-Hansen, (1998), MIKE 21 OSW3G - Technical documentation, Internal Rep., Danish Hydraulic Institute.
- Johnson H.K., and H. Kofoed-Hansen, (2000), Influence of Bottom friction on sea

- roughness and its impact on shallow water wind wave modelling, *J. Phys. Oceanogr.*, **30**, 1743-1756 .
- Jonsson, I.G., (1966), Wave boundary layers and friction factors, *Proc. 10th Int. Conf. Coastal Eng.*, Tokyo, ASCE, pp 127-148.
- Jonsson I.G. and N.A. Carlsen, (1976), Experimental and theoretical investigations in an oscillatory turbulent boundary layer, *J. Hydraul. Res.*, **14**, 45-60.
- Ris, R.C., L.H. Holthuijsen and N. Booij, (1999), A third-generation wave model for coastal regions. 2. Verification, *J. Geophys. Res.*, **104C**, 7667-7681.
- Tolman, H.L., (1991), A third generation model for wind waves on slowly varying, unsteady and inhomogeneous depths and currents, *J. Phys. Oceanogr.*, **21**, 782-797.
- Tolmann, H.L. (1992), Effects of numerics on the physics in a third-generation wind_wave model, *J. Phys. Oceanogr*, **22**, 1095-1111.
- Tolman, H.L. and D. Chalikov, (1996), Source terms in a third-generation wind-wave model. *J. Phys. Oceanogr.*, **26**, 2497-2518.
- Van Vledder, G.P, J.G. de Ronde and M.J.F. Stive, (1994), Performance of a spectral wind-wave model in shallow water, *Proc. 24th Int. Conf. Coastal Eng.*, ASCE, pp 761-774.
- Vilsmeier R. and D. Hänel, (1995), Adaptive solutions for unsteady laminar flows on unstructured grids, *Int. J. Numer. Meth. Fluids.*, Vol. 22, 85-101.
- Young I.R., (1999), Wind generated ocean waves, In Elsevier Ocean Engineering Book Series, Volume 2. Eds. R. Bhattacharyya and M.E. McCormick, Elsevier.
- WAMDI Group, (1988), The WAM model – A third generation ocean wave prediction model, *J. Phys. Oceanogr.*, **18**, 1775-1810.
- Weber, S.L, (1991), Bottom friction for wind sea and swell in extreme depth-limited situations, *J. Phys. Oceanogr.*, **10**, 1712-1733.

Key Words

Third-generation spectral wave model

Coastal areas

Nearshore wave climate

Offshore wave climate

Wave action

Finite volume method

Unstructured mesh

Time integration scheme

B I L A G E

Time Series Analysis and Forecasting using Artificial Neural Networks (på engelsk)

TIME SERIES ANALYSIS AND FORECASTING USING ARTIFICIAL NEURAL NETWORKS

VLADAN BABOVIC

TIME SERIES ANALYSIS AND FORECASTING USING ARTIFICIAL NEURAL NETWORKS

ABSTRACT

Throughout scientific research, measured time series are regarded as the basis for the characterisation of the behaviour of an observed system and for predicting its future behaviour. Analysis of time series has clearly three goals: *forecasting*, *modelling* and *characterisation*. The purpose of forecasting is to provide a short-term evolution of the system under consideration. The purpose of modelling is to provide a description that accurately captures the long-term behaviour of the system. Characterisation attempts with little or no *a priori* knowledge to define properties of the system, such as the number of degrees of freedom or the amount of randomness.

Traditionally, forecasting and characterisation of time series is done using linear auto-regressive (AR) or moving average (MA) models, or even combinations of the two, thus giving ARMA and ARIMA models. Such linear time series models have two particularly desirable features: they can be understood in great detail and they are straight-forward to implement. The price to be paid for this convenience is that they may be entirely inappropriate for even moderately complicated (*i.e.* non-linear) systems.

Constructing models from time series with non-trivial dynamics is a perplexing problem. In this report few methods for building non-linear models from data are discussed and described. Also, in final chapter, novel means of time series characterisation through a process of embedding of time series in a state-space are presented.

The report is structured as follows:

Firstly, a technique for global fitting of data, namely Artificial Neural Networks (ANNs), is described. Emphasis is given to the description of a special kind of ANN - Time Delayed Neural Network (TDNN) - which is best suited for operation in a time domain.

Following brief description of neural networks, an approach to application of neural networks as a data assimilation routine is described.

In closing chapter, description of *direct characterisation* of time series via state-space (embedding of time series in a state-space) is given. This primarily involves utilisation of information-theoretic measures to find optimal embedding lags. Concepts and quantities such as *joint entropy* and *mutual information* are used to provide guidelines for choosing the optimal time-lagged values in reconstructing the state-space for a given time series. The information generated in this process is used to induce a family of local models, which are then used to forecast short term evolution of a physical system under consideration.

1. INTRODUCTION	1
2. WEAK MODELLING	1
3. FORECASTING	1
3.1 LINEAR MODELS	1
3.1.1 MOVING AVERAGE (MA) MODELS	1
3.1.2 AUTO REGRESSIVE (AR) MODELS	2
3.1.3 AUTOREGRESSIVE MOVING-AVERAGE (ARMA) MODELS	3
3.1.4 THE BREAKDOWN OF THE LINEAR PARADIGM	3
4. A VENTURE INTO NONLINEAR MODELS	3
5. SHORT DESCRIPTION OF ARTIFICIAL NEURAL NETWORKS (ANN)	5
5.1 FUNDAMENTAL IDEAS	5
5.2 PATTERN RECOGNITION	5
5.3 THE NEURON	6
5.4 MULTI-LAYER PERCEPTRON NETWORKS (MLPs)	7
5.4.1 SPECIAL CASE – LINEAR TRANSFER FUNCTION	9
5.5 TRAINING	11
5.6 DYNAMIC NETWORKS	12
5.7 TLRN THEORETICAL SUMMARY	15
5.7.1 FIR NETWORKS	15
5.8 ADVANTAGES OF TLRNs	18
6. ISSUES IN CONNECTIONIST LEARNING	20
6.1 TERMINATION OF TRAINING	20
6.2 DIRECT VERSUS ITERATED PREDICTIONS	21
7. NEURAL NETWORKS AS A DATA ASSIMILATION ROUTINE	22
7.1 HOW CAN WE MAKE MORE ACCURATE MODELS?	23
APPENDIX A — STATE-SPACE RECONSTRUCTION	26
SOME INFORMATION THEORETIC BACKGROUND	26
MUTUAL INFORMATION	26
REFERENCES	28

1. INTRODUCTION

The desire to predict the future and understand the past drives the search for laws that explain the behaviour of observed phenomena. If there are known underlying deterministic equations, in principle they can be solved to forecast the outcome of an experiment based on knowledge of the initial conditions. To make a forecast if the equations are not known, one must find both the rules and the state of the system. Here we focus on phenomena for which underlying equations are not given: the rules that govern the evolution of a system must be inferred from regularities occurring in the past.

2. WEAK MODELLING

Strong models have strong assumptions. They are usually expressed in a few equations with a few parameters and can often explain a plethora of phenomena. In weak models, on the other hand, there are only a few domain-specific assumptions. To compensate for the lack of explicit knowledge, weak models usually contain many more parameters (which can make a clear interpretation difficult!). It can be helpful to conceptualise models in the two-dimensional space spanned by the axes data poor \leftrightarrow data rich and theory poor \leftrightarrow theory rich. Because of the dramatic expansion of the capability for automatic data acquisition and processing, it is increasingly feasible to venture into theory-poor and data-rich domain.

3. FORECASTING

The goal of time series prediction or forecasting is formulated as follows:

Given: $y(1), y(2), y(3), \dots, y(N)$
Find: $y(N+1), y(N+2), \dots$

Series is the sampling of continuous system and may be either stochastic or deterministic in origin.

3.1 LINEAR MODELS

3.1.1 MOVING AVERAGE (MA) MODELS

Assume that we are given an external input series $\{e_i\}$ and want to modify it to produce another (the observed) series $\{y_i\}$. Assuming the linearity of the system and causality (the present value of y is influenced by the present and N past values of input series e), the relationship between the input and the output is

$$y(k) = \sum_{n=1}^N b(n) e(k-n) \quad (1)$$

This equation describes a convolution filter: the new series y is generated by a linear filter with coefficients b_0, b_1, \dots, b_N . Statisticians and econometricians refer to such N -th order *moving average model* as MA(N) — Equation (1) —, whereas engineers call this *finite impulse response* (FIR) filter because its output is guaranteed to go to zero at N time steps after the input becomes zero. Properties of the output series y clearly depends on the input series e . The task is to describe the system independent of a specific input sequence. For a linear system, the response of the filter is independent of the input.

Sometimes it is more convenient to describe the filter behaviour in the frequency domain. If the input to a MA model is an impulse (which has a flat power spectrum), the discrete Fourier transform of the output is given by (see, for example, Box and Jenkins, 1976, p. 69)

$$\sum_{n=0}^N b_n \exp(-i2\pi nf) \quad (2)$$

The power spectrum is given by the squared magnitude of this:

$$f = \left| \sum_{n=0}^N b_n \exp(-i2\pi nf) \right|^2 \quad (3)$$

Autocorrelation coefficients of, defined in the terms of the mean $\mu = \langle y_t \rangle$, and the variance $\sigma^2 = \langle (y_t - \mu)^2 \rangle$ by:

$$\rho \equiv \frac{1}{\sigma^2} \langle (y_t - \mu)(y_{t-\tau} - \mu) \rangle \quad (4)$$

The angular brackets $\langle \bullet \rangle$ denote expectation values. The autocorrelation coefficients describe how much, on average, two values of a series that are τ time steps apart co-vary with each other.

3.1.2 AUTO REGRESSIVE (AR) MODELS

Yule (1927) proposed autoregressive¹ (AR) class of models defined as follows:

$$y(k) = \sum_{n=1}^M a(n) y(k-n) + e(k) = \hat{y}(k) + e(k) \quad (5)$$

This is an Mth order autoregressive model [AM(M)]. Depending on the application, $e(k)$ can represent either a controlled input to the system or noise. If e is white noise, the autocorrelation coefficients of the output series can be expressed in terms of model coefficients. Autocorrelation coefficients of an AR model are found by solving a set of, traditionally referred to as *Yule-Walker* equations, presented in the sequel:

$$\rho_\tau = \sum_{m=1}^M a_m \rho_{\tau-m}; \quad \tau > 0 \quad (6)$$

Unlike the MA case, the autocorrelation coefficients need not vanish after M steps.

The power spectrum of output is:

¹ An M-th order *autoregressive model* AR(M) — Equation (5) — is referred to as *infinite impulse response* (IIR) filter, because the output can continue after the input ceases.

$$f = \frac{1}{\left| 1 - \sum_{m=1}^M a_m e^{i2\pi mf} \right|^2} \quad (7)$$

The Yule-Walker set of linear equations (6) allowed us to express the autocorrelation coefficients of a time series in terms of the AR coefficients that generated it. They also allow us to estimate the coefficients of an AR(M) model from the observed correlational structure of an observed signal.

3.1.3 AUTOREGRESSIVE MOVING-AVERAGE (ARMA) MODELS

The next step in complexity is to allow both AR and MA parts in the model; this is called an ARMA(M, N) model:

$$y_t = \sum_{m=1}^M a_m y_{t-m} + \sum_{n=1}^N b_n e_{t-n} \quad (8)$$

The analysis of an ARMA process in terms of Fourier spectrum is presented in Weigend (1996) and it will not be repeated here.

ARMA models have dominated all areas of time series analysis and discrete-time signal processing for more than half a century. If the model is good, it transforms the signal into a small number of coefficients plus residual white noise (of one kind or another).

3.1.4 THE BREAKDOWN OF THE LINEAR PARADIGM

We have seen that AR, MA (and implicitly ARMA) coefficients, power spectra and autocorrelation coefficients contain the same information about a linear system driven by uncorrelated white noise. Thus, *if and only if* the power spectrum fully characterises the relevant features of a time series, a linear model (AR, MA or ARMA) will be the appropriate description. This appealing simplicity can fail entirely for even simple nonlinearities if they can lead to complicated power spectra — as they can. Two time series can have very similar broadband spectra but can be generated from systems with very different properties, such as a linear system that is driven stochastically by external noise, and a deterministic (noise-free) nonlinear system with a small number of degrees of freedom. One of the key problems addressed in this text is how these cases can be distinguished. Linear operators definitely will not be able to do the job.

4. A VENTURE INTO NONLINEAR MODELS

Yule's original idea for forecasting was that future predictions can be improved by using immediately preceding values. An ARMA model — equation (8) — can be rewritten as a dot product between vectors of the time-lagged variables and coefficients:

$$x_t = \mathbf{a} \mathbf{x}_{t-1} + \mathbf{b} \mathbf{e}_t \quad (9)$$

where $\mathbf{x}_t = (x_t, x_{t-1}, x_{t-2}, \dots, x_{t-(d-1)})$ and $\mathbf{a} = (a_1, a_2, a_3, \dots, a_d)$ ². Such lag vectors, also called tapped delay lines are used routinely in the context of signal processing and time series analysis, suggesting that they are more than just a typographical convenience.

² Note that a notation has been slightly altered here. What was M (the order of the AR model) is now called *d* (for dimension).

In fact, there is a deep connection between time-lagged vectors and underlying dynamics. This connection was first proposed by Packard *et al.* (1980) and Takens (1981; she published the first proof) and later strengthened by Sauer *et al.* (1991). Delay vectors of sufficient length are not just representation of the state of a linear system — it turns out that delay vectors can recover the full geometrical structure of a nonlinear system. These results address the general problem of inferring the behaviour of the intrinsic degrees of freedom when a function of the state of the system is measured. If the governing equations and the functional form of the observable are known in advance, then a Kalman filter is the optimal linear estimator of the state of the system (Catlin, 1989). In the present case, we focus on the case where there is little or no *a priori* information available about the origin of the time series.

Takens' Time-delay Embedding Theorem (1981), can be written as follows:

Given a dynamical system with a d-dimensional solution space and evolving solution $\mathbf{x}(t)$, let y be some observation $y(\mathbf{x}(t))$. Let us also define the lag vector (with dimension d and time delay τ) $\mathbf{y}_t \equiv (y_t, y_{t-\tau}, y_{t-2\tau}, y_{t-3\tau}, \dots, y_{t-(d-1)\tau})$. Then, under general conditions, the space of vectors \mathbf{y}_t generated by the dynamics contains all of the information of the space of solution vectors \mathbf{x}_t . The mapping between them is smooth and invertible (diffeomorphism) - and this is referred to as embedding. Thus, study of the time series y_t is also the study of the solutions of the underlying dynamical system $\mathbf{x}(t)$ via a particular coordinate system given by the observable y .

This can be interpreted into a plain English text as follows. Science is based on the principle of repeatability: each time a system experiences similar conditions — both internal to the system and forces exerted externally on the system — we expect the system to exhibit a similar response. Forecasting exploits this principle by using the observed behaviour of a system to predict behaviour when similar conditions recur — and clearly, tapped delay line represents a history (evolution) of a system under consideration. Even if the equations describing a system are unknown, we can nevertheless use forecasting to learn about the system. For some purposes — such as weather forecasting or noise reduction — predicting the future is the primary goal of the forecasting. For the purpose of characterising systems dynamics, in contrast, predictions are made in an exploratory manner to learn what kinds of models perform best.

Takens' theorem implies that there exist, in theory, a nonlinear autoregression of the form

$$y(k) = g[y(k-1), y(k-2), y(k-3), \dots, y(k-T) + e(k)] \quad (10)$$

which models the series exactly (assuming no noise).

The question we are addressing in this text is the one of finding this non-linear autoregression. Presently we focus on use of ANN Artificial Neural Networks — ANNs.

Motivation to use neural networks as a technique to extend linear paradigm is summarised in the sequel. The basic form:

$$y(k) = \hat{y}(k) + e(k) \quad (11)$$

is still retained.

Here, the estimate $\hat{y}(k)$ is taken as output of a neural network N , driven by past values of the sequence. This may be written as:

$$y(k) = \hat{y}(k) + e(k) = N[y(k-1), y(k-2), y(k-3), \dots, y(k-T) + e(k)] \quad (12)$$

Equation (12) may be trivially extended for multivariate case.

Question: Why use this particular form of non-linear regression? Why prefer Equation (12) over equation (11)? Answer: It has been demonstrated (Hornik *et al*, 1989; Irie and Miyake, 1988) that a feed-forward neural network N with an arbitrary number of neurons is **universal function approximator**. Thus, ANNs can approximate any function and from this perspective the motivation to use neural network N to form an approximation to the ideal function $g(\bullet)$ is rather clear.

5. SHORT DESCRIPTION OF ARTIFICIAL NEURAL NETWORKS (ANN)

A neural network is simply a set of interconnected individual units called neurons.

5.1 FUNDAMENTAL IDEAS

A numerical model is implemented to represent a process. In classical modelling, one usually decomposes this representation into detailed steps, each of which is a numerical description resulting from empirical knowledge or from mathematical equations. These steps are then integrated to produce desired model.

Once the model is translated into computer language, a numerical algorithm that performs a series of operations *sequentially* is said to be obtained. That is, given an input information, a series of calculations follows, where intermediate values are evaluated and fed into the next step, until the final result of computation is reached. All our knowledge about underlying processes is contained and orderly arranged in the executed set of steps. This corresponds to the process of generating strong models (as defined in Section 1).

In contrast, ANN models are computer algorithms based on the principle of *parallel distributed processing* (PDP). In ANNs, information is processed simultaneously at all processing units and the results transferred to other units through their mutual connections. No knowledge about underlying process is directly implemented. This corresponds to the process of building weak models (again, as defined in Section 1).

5.2 PATTERN RECOGNITION

In pattern recognition problems, one is interested in the correct association of cause and effect, or problem-solution association. A complete *pattern* is a combination of a set of input values (the input vector) and a set of output values (the output vector). If one deals with a system that describes a physical process, the input vector then consists of the mutually independent physical parameters that take part in the process, and the output vector of the resulting parameters caused by it (which denotes system's response). The ensemble of patterns should ideally contain as many patterns as needed to represent the whole range of parameter values one is interested in.

An ANN model is implemented to act as a memory, *i.e.* to recall the stored patterns. Ideally the ANN will perform a complex classification task in which input and output vectors are associated according to the features incorporated from the data set, in a multi-dimensional feature space. Thus, the quality of the resulting model depends largely on the quality of the data one uses.

In order to obtain the model, one must present the ANN with selected set of representative patterns and let it learn from them, *i.e.* adjust ANN's configuration values (weights on the

connections between processing units) until the error function (which related the difference between the produced network output values and desired output vector values) is minimised. This phase is referred to as a *training phase* of an ANN.

Once trained, the ANN model should be able to correctly recall the output vector values when presented with the input vector again. In addition to this, the model should be able to *generalise*. This implies that the trained network should reproduce patterns which were not explicitly included in the training set. This is in principle possible because the network has during the training phase established a complex relationship between input and output values for the domain presented by the features inherent in the training data. The performance may decrease considerably if testing input vectors lie considerably outside the range of the training set.

A considerable care must be paid while training an ANN. If the ANN is *over-trained* it will produce an overly detailed representation which tends to individualise more and correspondingly learn even the noise included in the training signal. The network loses its ability to generalise on the input domain.

The correct performance of the resulting model is evaluated with a set of testing patterns. Testing the network with new (unseen) patterns is the best way to make sure the induced model performs as well as it should. This phase is referred to as *validation of a model*. The data used during the testing phase should also be representative for the problem under the consideration.

5.3 THE NEURON

Simulations of interconnected networks of simple threshold-based processing units called *artificial neurons* have been an object of scientific investigation ever since the earliest days of the computer (McCulloch and Pitts, 1943; Hebb, 1949). These neurons are in fact a special form of general automaton (Hopcroft and Ullman, 1979) that in fact form a conceptual basis for any computer programming language. The McCulloch-Pitts neuron is depicted in **Figure 1**.

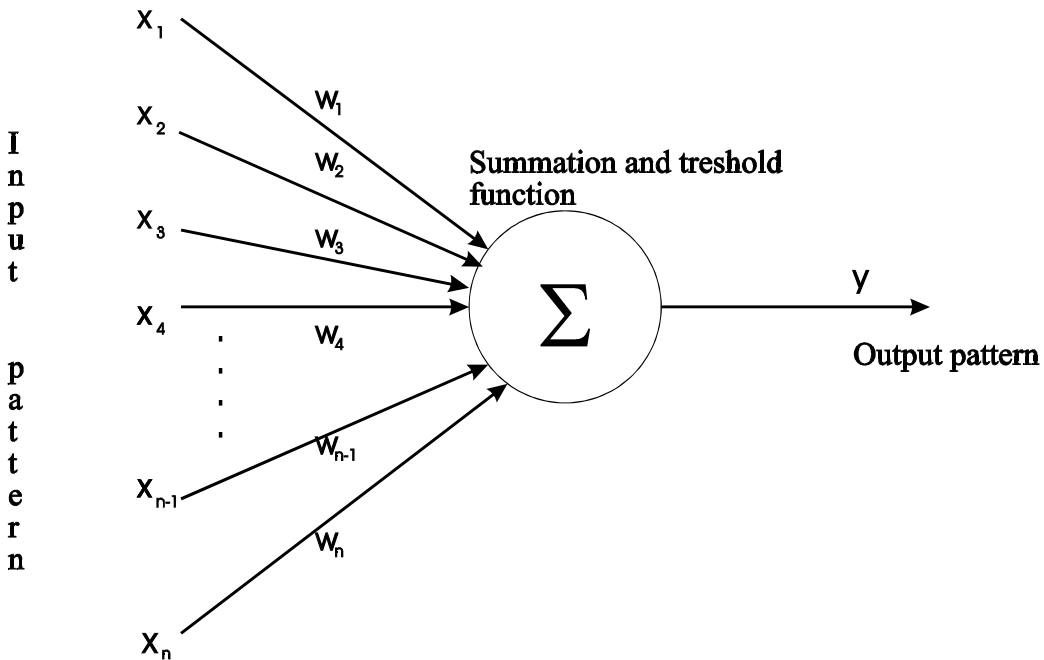


Figure 1 Schematisation of a McCulloch-Pitts neuron

An individual neuron has a finite number of scalar inputs $\{x_i, i=1, 2, \dots, n\}$ and one scalar output $\{y\}$. Associated with each input is a scalar weighting value $\{w_i, i=1, 2, \dots, n\}$. The input

signals are multiplied by these weighting values and added at the summation junction (*i.e.* $u = \sum_{i=1}^r w_i x_i$). The combined signal is then passed through an activation function $\gamma(u)$ producing the output signal. The activation function $\gamma(u)$ can take a variety of forms, one of the most common being a sigmoid function:

$$\gamma(u) = \frac{1 + e^{u+\theta}}{1 + e^{-u-\theta}} \quad (13)$$

with $u = \sum x_i w_i$ being the weighted sum of all input signals x_i that the neuron receives and θ is the threshold value associated with the neuron. Many other forms of activation function $\gamma(u)$ are possible and they range from linear form ($\gamma(u)=au+b$) to other non-linear bounded forms, such as $\gamma(u)=\tanh(u)$.

Individual neurons receive input signals in the form of numbers. These numbers propagate through network, where they are amplified using weights along the connections. As it has been mentioned earlier, every individual neuron receives as input the weighted signals from the neighbours with which it is connected. These input signals are then summed at every individual node and the individual output signals are calculated using $\gamma(u)$:

$$\gamma(u) = \frac{1 + e^{(\sum_i w_i x_i + \theta)}}{1 + e^{-(\sum_i w_i x_i + \theta)}} \quad (14)$$

where $u = \sum x_i w_i$ is the weighted sum of all input signals x_i that the neuron receives and θ is the threshold value associated with the neuron. During the training phase optimal weight values w_i are sought for the connections.

The activation function $\gamma(u)$ of the form (13) serves as a non-linear element in a neuron and also acts as a limiter that bounds the incoming signal. This activation function has a linear range about the origin, and is bounded between -1 and +1. If an output of a neuron is bounded between $-\alpha$ and $+\alpha$ a neuron can still approximate this function as long as taking $\bar{\gamma}(u)=\alpha \gamma(u)$ as its activation function. Therefore, the activation function can be taken to be between -1 and +1 provided that an additional factor is inserted after the neuron. In practise this implies that all the data that a neural networks operates upon has to be normalised (usually between -1 and +1). De-normalisation process can be performed at the output signal without any loss of generality.

Rosenblatt (1958, 1962) proposed, following Hebb (1949), an algorithm referred to as a *perceptron learning rule* that adapts weights in a neuron (or, in Rosenblatt's terminology *perceptron*) in order to perform a certain, pre-defined task. Minsky and Papert (1969) showed, however, that a single perceptron, although a promising technique, is not capable of solving linearly non-separable problems, like exclusive or (XOR) problems. Publication of this book has effectively inhibited a research work on neural networks for the next 15 years.

5.4 MULTI-LAYER PERCEPTRON NETWORKS (MLPS)

The breakthrough and re-formation of so-called *connectionism* occurred only through the research directions that utilised collections of these simple computational units with a set of weighted interconnections (Hopfield, 1982; Ackley *et. al.* 1985; Rummelhart and McClelland, 1986). The repeated and parallel execution of these simple numerical operations at each and every neuron emerges in a useful behaviour of a network as a whole. The performance on the network depends

strongly on its architecture, or topology of connectivity among individual neurons. As in the simple perceptron, the weights are adjusted during the training process.

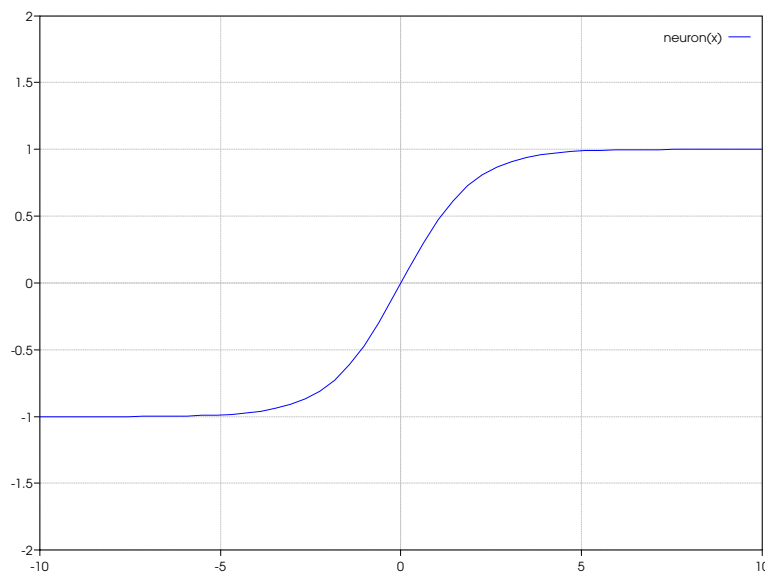


Figure 2 The sigmoid function

A neural network is simply a set of interconnected individual computational elements called neurons. In the case of the multi-layer neural networks, the neurons are arranged in a series of layers. A layer is usually a group of neurons, each of which is connected to all neurons in the adjacent layer (Figure 3).

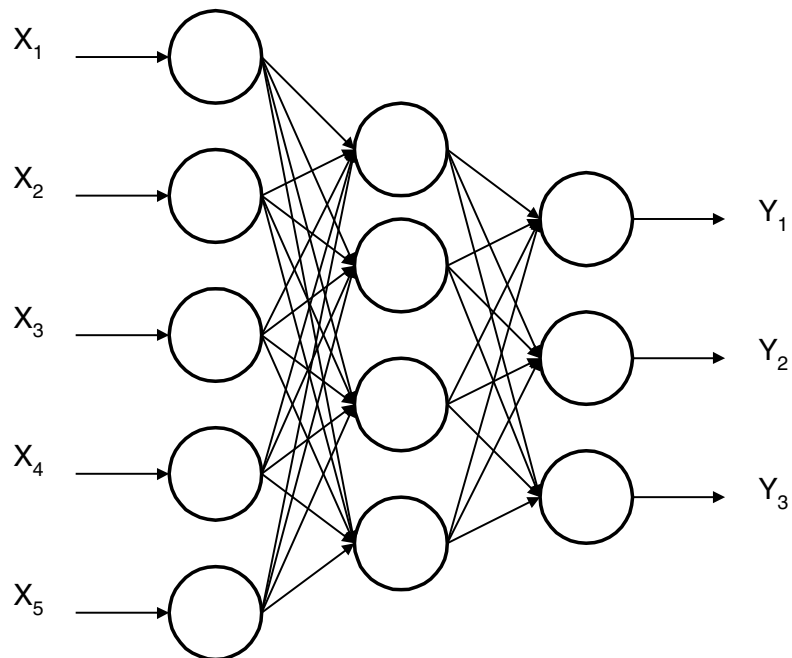


Figure 3 Schematisation of a multi-layer, feed-forward neural network with hidden layer of neurons. This neural network receives five inputs, produces three outputs and has one hidden layer of fours neurons

Figure 3 illustrates a three-layer neural network containing one hidden layer. The figure illustrates that neurons in the input layer are connected only to those in the hidden layer. The neurons in the hidden layer are connected to those of both the input and the output layer, while those of the output layer have no connections other to those of the hidden layer. There are no connections between the neurons within any one of the three layers.

A hidden layer of neurons may be defined as one without having direct connection paths to external inputs or outputs. Hidden layers add a degree of flexibility to the performance of the neural networks and to the internal representation of the problem under consideration. In most cases, presence of a hidden layer considerably enhances the capability of the network to approximate the data, as well as to robustly and efficiently deal with inherently complex non-linear relations existing in the data.

In practical applications, the design of the multi-layer neural network architecture requires specification of many factors, such as the number of neurons in the different layers, the number of hidden layers and the type of neuron transfer function $\gamma(u)$ to be used.

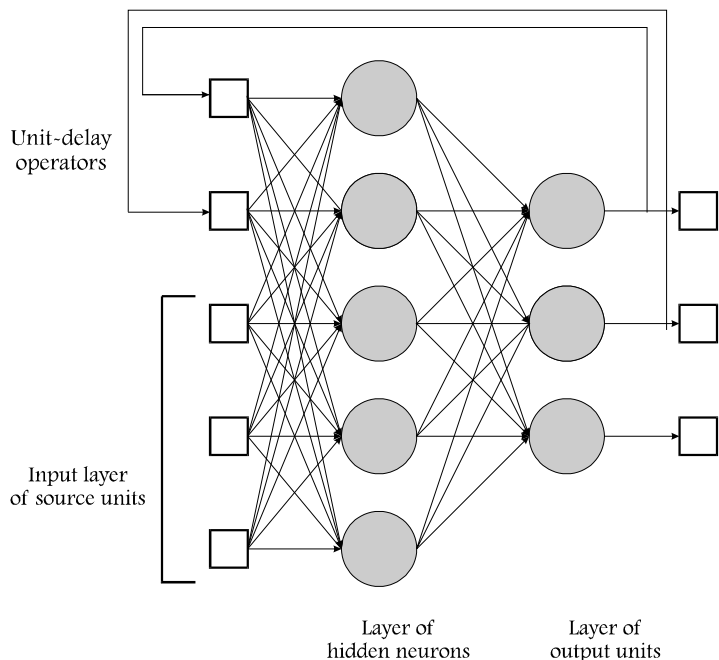


Figure 4 Schematisation of a recurrent neural network

Depending on the connection between the neurons there are two basic types of networks known as the multi-layer feedforward networks and the recurrent networks. The network without any loops or multiple connections between individual neurons is called a *feed-forward* (Figure 3); otherwise a feedforward network with time delay feedback elements it is said to be *recurrent* (**Figure 4**). The delay elements take the outputs of certain neurons in the network, delay them for the certain number of time steps, and feed back as inputs to other neurons. A special one layer network where the delayed outputs of the neurons are fed back as inputs to themselves is called a Hopfield network.

5.4.1 SPECIAL CASE – LINEAR TRANSFER FUNCTION

If the activation function is a linear function, for example $\gamma(u)=u$, the neuron is a linear neuron. The input output relationship of such a neuron is simply:

$$y = \sum_{i=1}^r w_i x_i \quad (15)$$

Equation above simply implies that the output signal is a weighted combination of the input signals with the weighting coefficients being the weights of the neuron.

Phan *et al* (1993) provide an illustrative example. Consider the feedforward network shown in **Figure 5** with the activation function being a linear function — Equation (15).

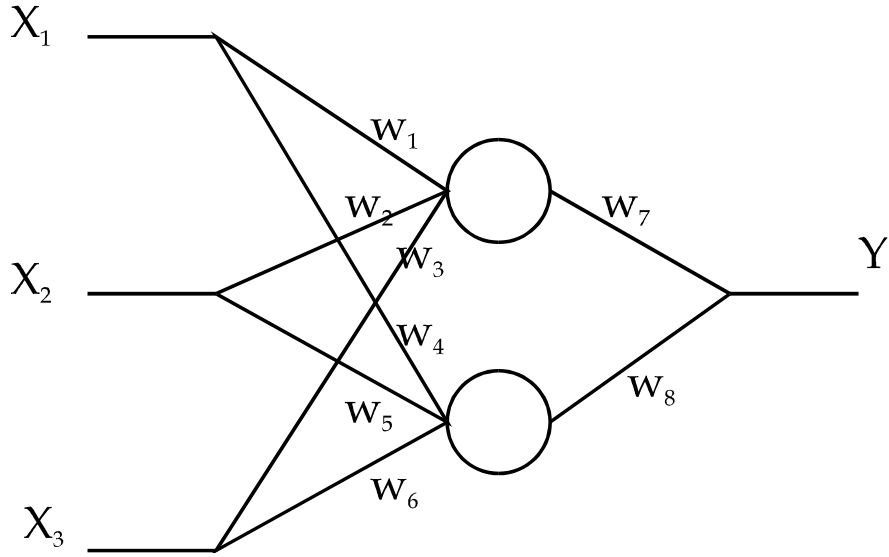


Figure 5 A two-layer three-input one-output feed forward neural network on linear neurons

The network weights between the individual corrections are shown in

Figure 5. Since the transfer functions in the neurons are linear, each neuron is represented by a summation junction. The output of the network from

Figure 5 is the simply:

$$\begin{aligned} y &= w_7(w_1x_1 + w_2x_2 + w_3x_3) + w_8(w_4x_1 + w_5x_2 + w_6x_3) \\ &= (w_7w_1 + w_8w_4)x_1 + (w_7w_2 + w_8w_5)x_2 + (w_7w_3 + w_8w_6)x_3 \\ &= \bar{w}_1x_1 + \bar{w}_2x_2 + \bar{w}_3x_3 \end{aligned} \quad (16)$$

which is equivalent to the output of a single neuron with the following weights:

$$\begin{aligned} \bar{w}_1 &= w_7w_1 + w_8w_4 \\ \bar{w}_2 &= w_7w_2 + w_8w_5 \\ \bar{w}_3 &= w_7w_3 + w_8w_6 \end{aligned} \quad (17)$$

The above example can be immediately generalised to show that a single-output, multi-layer ANN with linear activation functions is equivalent to a single linear neuron with appropriate weights. Thus, a multi-layer feedforward network of linear neurons is simply an over-parametrised set of linear equations where the over-parametrisation takes the form of the type shown in equations (17). This form is non-linear in the parameters. Thus the problem of

determining these parameters from known input-output data is non-linear parameters estimation problem even if the network is linear. Since any single-output feed forward network of linear neurons is equivalent to a particular single linear neuron, there is no benefit in using an over-parametrised multi-layer linear network for linear system identification. In fact, in such an over-parametrised model the network weights cannot be uniquely determined from input-output data. This is obvious from example above. The set of equations (17) consists of three equations and contains eight unknowns. Thus use of complicated multi-layer linear network for linear system identification is therefore neither advantageous nor necessary. The same is true for the case of using a non-linear network to identify a linear system.

Thus, in order to model linear system one is better off by using linear paradigms such as AR, MA or ARMA. For nonlinear cases, one has to seek the resort in networks of nonlinear neurons.

5.5 TRAINING

In order to induce the model which approximates the data, one must present the ANN with a selected set of representative patterns and let it learn from them. In practise, ANN's configuration values (weights on the connections between processing units) have to be adjusted until the error function measuring the difference between the ANN-produced output values and desired output values is minimised. This phase is referred to as a *training phase* of an ANN.

It is clear from the previous two sections, that a neural network is essentially an over-parametrised set of equations with a potentially very large number of free parameters w_i { $i=1, 2, \dots, n$ } and $\theta=w_{n+1}$. During the training phase the set of optimal weights w_i are sought on the basis of response to training data. The training process establishes a set of free parameters w_i that produces the most accurate input-output mapping.

The training data usually consist of inputs as well as desired responses to these stimuli. During training, the output calculated by the network y_j is compared with the actual (desired) output d_j and the difference between the two is calculated. These differences are then added over the entire training set containing Tr samples to form the error function, i.e. $E = \sum_{j=1}^{Tr} |d_j - y_j|$.

The value of the neural network output y_j is a function of the free parameters w_i . The aim of training is to find a set of weights that will produce the minimum of the error function $E=f(w_i)$.

Initially, the free parameters are assigned a small, randomly chosen values. As training progresses, the parameters are updated systematically using a learning rule. The generic rule for weight updating takes the following form:

$$w_i(t+1) = w_i(t) + \Delta w_i(t+1) + \mu \Delta w_i(t) \quad (18)$$

where μ denotes a so-called momentum value. There are several ways of establishing the weights increment Δw_i represented by an optimisation algorithm. There are many parametric training techniques, all of which are intended to search more effectively for the most appropriate collection of weights. They vary from a form of simulated annealing (Ackley *et al*, 1985) to a generalised learning rule, called a *delta learning rule* (Rummelhart and McClelland, 1986), which is basically the gradient descent method:

$$\Delta w_i = \eta \frac{\partial E}{\partial w} \quad (19)$$

Such gradient descent method results in weight being changed in the direction of steepest descent down the error surface. The size of the steps is determined by a so-called learning rate η .

It has been shown that an artificial neural network, given a sufficiently long training time and a sufficient rich topology, can act as *universal function approximator* (Hornik, 1989). Thus, given a sufficiently long training time, and sufficiently representative training data set, an artificial neural network can approximate any function to an arbitrary degree of accuracy.

5.6 DYNAMIC NETWORKS

Many applications of neural networks involve data $\mathbf{x} = \mathbf{x}(\tau)$ which varies as a function of time τ . The goal is to predict the value of \mathbf{x} at some time in the future. Techniques based on feed-forward networks, of the kind described in the previous sections, can be applied directly to such problems. Let us, for simplicity consider a single-channelled time dependent variable $x(\tau)$. One common approach is to sample $x(\tau)$ at regular time intervals to generate a series of discrete values $x_{\tau 1}, x_{\tau 2}, x_{\tau+1}$ and so on. A set of d such values $x_{\tau d+1}, x_{\tau d+2}, \dots, x_{\tau}$ can be used as inputs to a feed-forward network, and the value $x_{\tau+1}$ as the target output of the network as indicated in Figure 6.

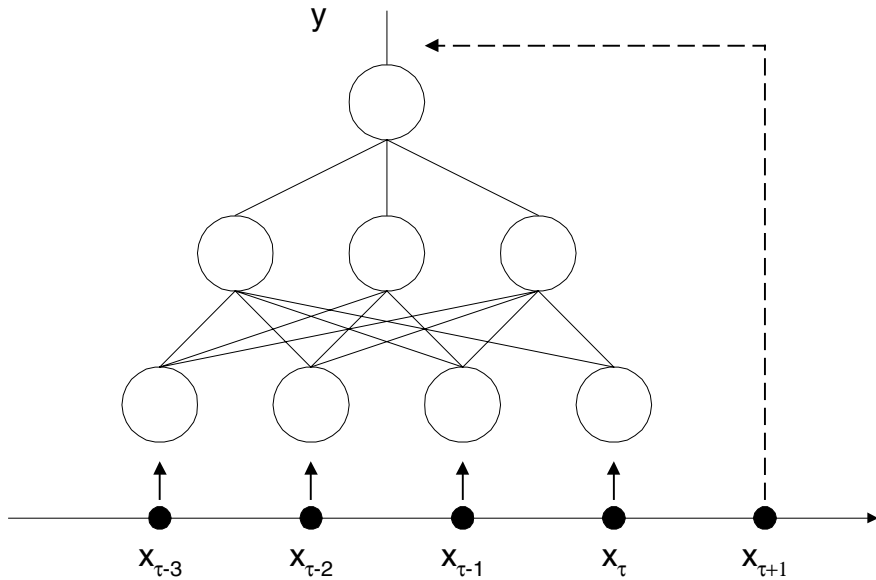


Figure 6 Sampling of a time series at discrete steps used to generate a set of training data for a feed-forward network. Successive values of the time-dependent variable $x(\tau)$, given by the $x_{\tau d+1}, x_{\tau d+2}, \dots, x_{\tau}$ form the inputs to a feed-forward network, and the corresponding target value is given by $x_{\tau+1}$

By stepping along time axis, a training data set can be created consisting of many instances of input values with corresponding target values. One of the main problems of applying ANNs in time domain is determining a length of the memory buffer d . Too large memory may lead to overfitting, whereas too small to an under-representation of the process and poor accuracy.

The simplest way of providing memory is creating a tap delay line operator — which functions as a local memory kernel. The tap delay line operator simply stores past values in a memory kernel, thus providing a history of input signal. A dynamic neural network can be best understood as a static neural network with an extended memory mechanism, which is able to store past values of the input signal. There are also other possibilities of storing past values, such as finite-impulse response filter (deVries and Principe, 1992), but discussion on these slightly more advanced topics is left outside the present presentation.

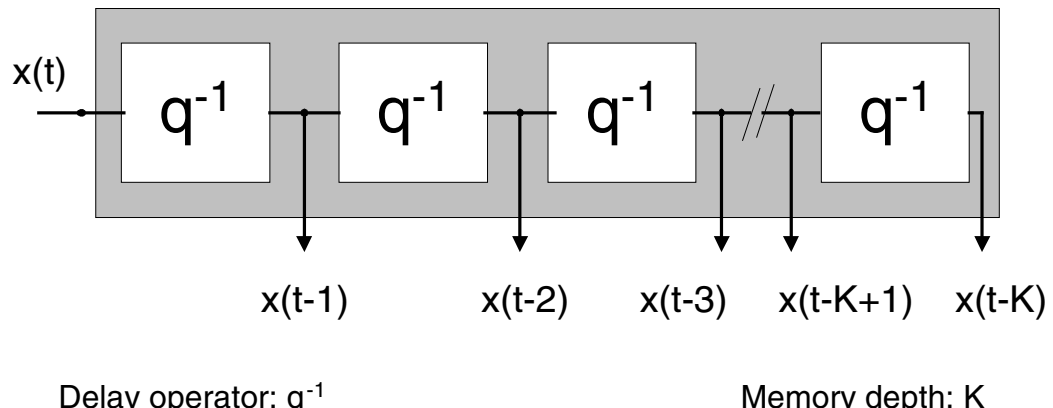


Figure 7 Tap delay line operator

Dynamic networks are a very important class of neural network topologies that are able to process time varying signals. They can be viewed as a non-linear extension of adaptive linear filters, or an extension of static neural networks to time varying inputs. As the basic ANN architecture for the present forecasting application a special dynamic network — a so-called Time-Delayed Neural Network (TDNN) structure has been selected. This is the same architecture as outlined before – essentially a multi-layer neural additionally equipped with short-term memory structures as depicted in Figure 7.

TDNNs with the memory confined to the input only can be thought of as input pre-processor. The information is represented across time instead of simply across the static input patterns. Memories can be applied to any layer in the network, producing very sophisticated neural topologies very useful for time series prediction and system identification and temporal pattern recognition.

Given a signal in time the network must process that signal to determine where in time the relevant information lies. A brute force approach would be to use a long time window. However, this method does not work in practice because it creates very large networks that are difficult to train (particularly if the data is noisy) and rather susceptible to overfit. In TDNN, establishment of an optimal memory depth K is an integral part of the training process, thus providing a very good alternative to the brute force approach.

The simplest way of doing this is creating a tap delay line operator - which functions as a local memory kernel - as indicated in Figure 7. The tap delay line operator simply stores past values in a memory kernel, thus providing a history of input signal. The other, more advantageous methods of achieving the same goals - locally recurrent time delay operators based on linear filters will be explained later in sub-section 5.7.1.

Tap delay line

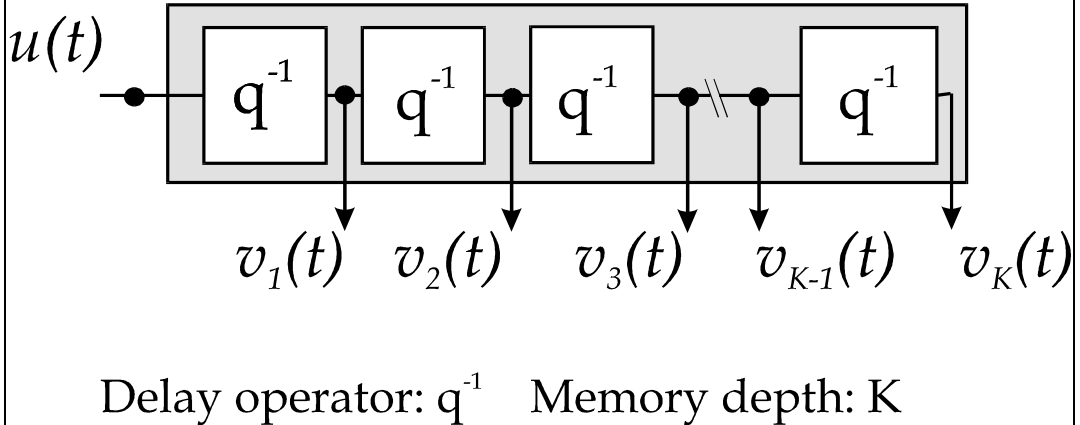


Figure 8 Tap delay line operator

Thus, a dynamic neural network can be understood as a static neural network with an extended memory mechanism which is able to store past values of the input signal. In many applications (system identification, classification of patterns in time, non-linear prediction) memory is important for allowing decisions based on input behaviour over a period of time. A static classifier makes decisions based on the present input only; it can therefore not perform functions which involve knowledge about the history of the input signal.

In dynamic neural networks, the most common memory structures are linear filters. In the so-called Time Delay Neural Network (TDNN) the memory is a tap delay line, i.e. a set of memory locations that store the past of the input. Self recurrent connections (feeding the output of a processing element - PE - to the input) have also been used as memory, and these units are called context units.

A modification of the basic neuron is accomplished by replacing each static synaptic weight by an FIR filter.

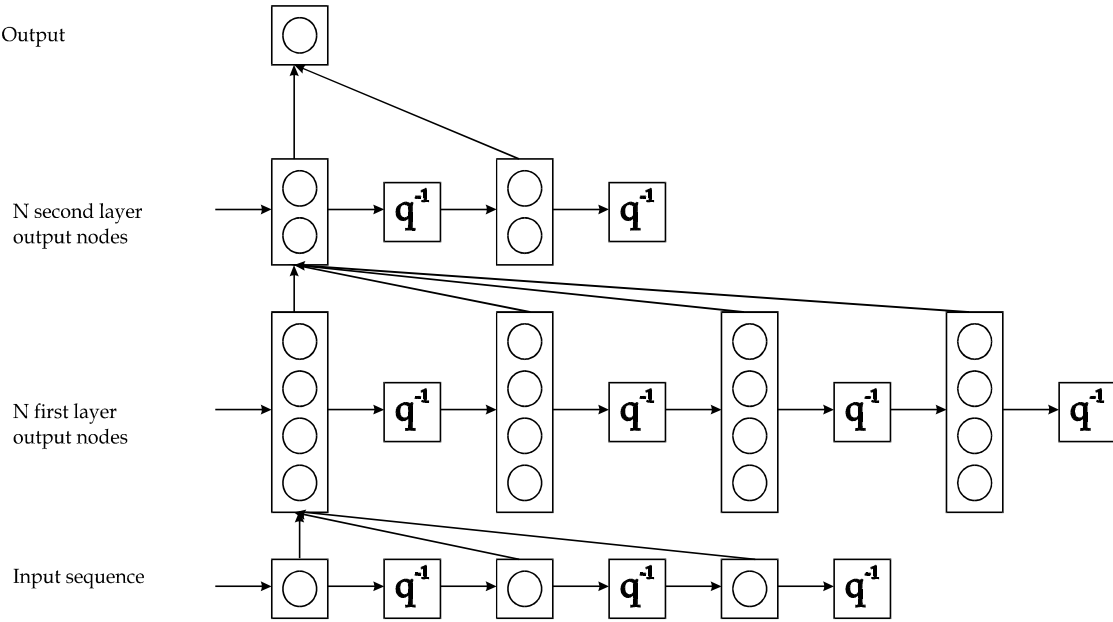


Figure 9 Time delay neural network. All node outputs in a given layer are buffered over several time steps. The outputs and the buffered states are then fed fully connected to the next layer. The structure is functionally equivalent to an FIR network.

Memories can be appended to any layer in the network, producing very sophisticated neural topologies very useful for time series prediction and system identification and temporal pattern recognition (see **Figure 14**).

5.7 TLRN THEORETICAL SUMMARY

As the basic architecture of the artificial neural network (ANN) for this application of forecasting, a dynamic network - a so called Time-Lagged Recurrent Network (TLRN) structure has been selected. This is fundamentally the same architecture as the standard multi-layer perceptron (MLP) neural network that is additionally equipped with short-term memory structures that have local recurrent connections — see **Figure 9**.

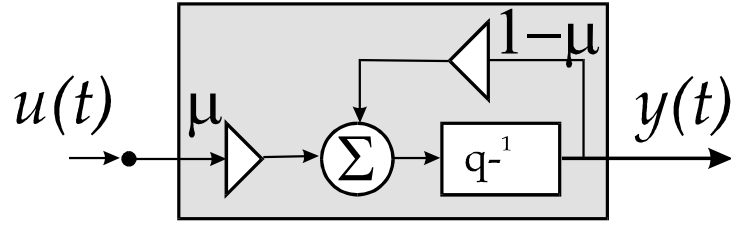
TLRNs with the memory layer confined to the input can be thought of as an input pre-processor. The information is represented across time instead of simply across the static input patterns. Given a signal in time the network must process that signal to determine where in time the relevant information lies. The term signal processing is used here in a general sense; it can be substituted for prediction, identification of dynamics, or classification.

A brute force approach is to use a long time window. This method does not work in practice because it creates very large networks that are difficult to train (particularly if the data is noisy). TLRNs are a very good alternative to this brute force approach.

5.7.1 FIR NETWORKS

The most studied TLRN network is the FIR Network (Wan, 1993) which is sometimes also referred to as a Gamma model (Principe *et al*, 1993) — these two terms will be in this text used interchangeably. The gamma model is characterised by a memory structure that is a cascade of FIRs.

Context Unit



$$\text{Delay operator: } \frac{\mu}{q - (1-\mu)} \quad \begin{matrix} \text{Memory depth: } 1/\mu \\ \text{Memory resolution: } \mu \end{matrix}$$

Figure 10 Schematisation of a context unit for FIR memory model

The FIR (see **Figure 13** and Equation (20)) is a structure that cascades self recurrent connections (de Vries and Principe, 1992). It is therefore a structure with local feedback, that extends the context unit with more versatile storage, and accepts the tap delay line (as exemplified in Figure 7 as a special case ($\mu=1$)).

μ is an adaptive parameter that controls the depth of the memory. This structure has a memory depth of k/μ , where k is the number of taps in the cascade. Its resolution is μ (de Vries and Principe, 1992). Since this topology is recurrent, a form of temporal learning must be used to adapt the gamma parameter μ (i.e. either real time recurrent learning or backpropagation through time — for explanation of these techniques see for example Haykin, 1994). The advantage of this structure in dynamic networks is that we can, with a pre-defined number of taps, provide a controllable memory. And since the network adapts the gamma μ parameter to minimise the output mean square error, the best compromise depth/resolution is achieved.

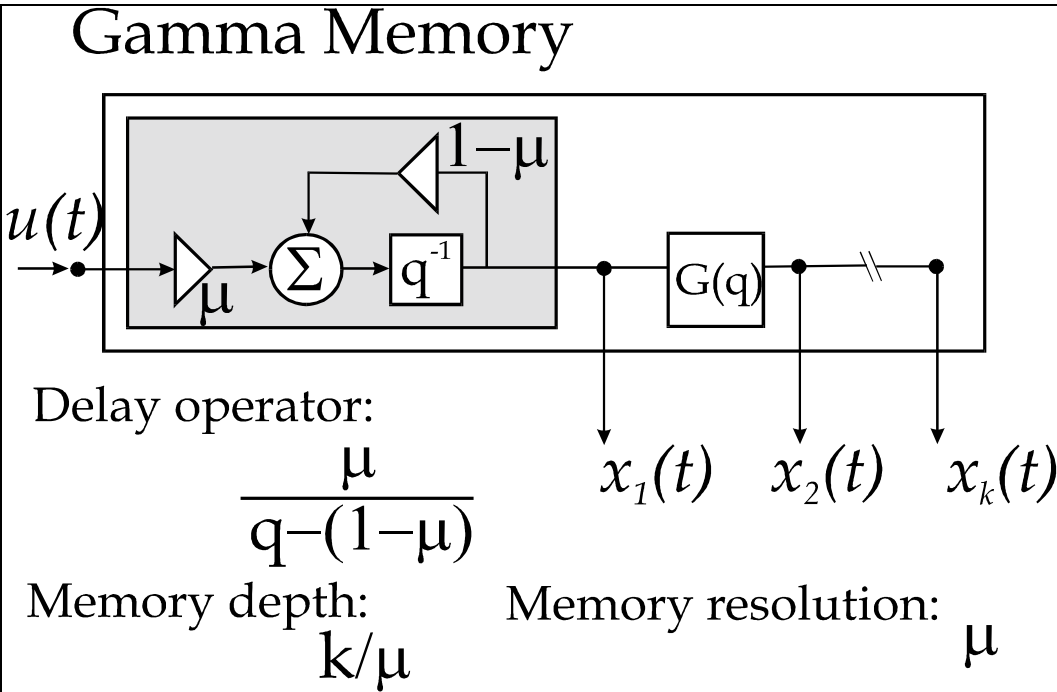


Figure 11 Block diagram of the FIR memory structure

Note that the point in time where the response has a peak is approximately given by k/μ , where μ is the feedback parameter (see **Figure 12**). This means that the neural network can control the depth of the memory by changing the value of the feedback parameter μ , instead of requiring a topological change in the number of input taps. The parameter μ can be adapted using gradient descent procedures, just like the other parameters in the network. Since this parameter is recursive, a more powerful learning rule needs to be applied. In the current study backpropagation through time (BPTT) for the adaptation process has been implemented.

The signal at the taps of the FIR can be represented by³:

$$x_0(n) = u(n) \quad (20)$$

$$x_k(n) = (1 - \mu)x_k(n - 1) + \mu x_{k-1}(n - 1) \quad \forall k = 1, 2, \dots, K$$

Note that the signal at tap k is a smoothed version of the input, that holds the ‘voltage’ of a past event, creating a memory. When an impulse is presented in the input at time zero, the response of the different taps is shown in the illustration of the impulse responses of gamma (**Figure 12**).

³ Compare equation (20) to equation (5).

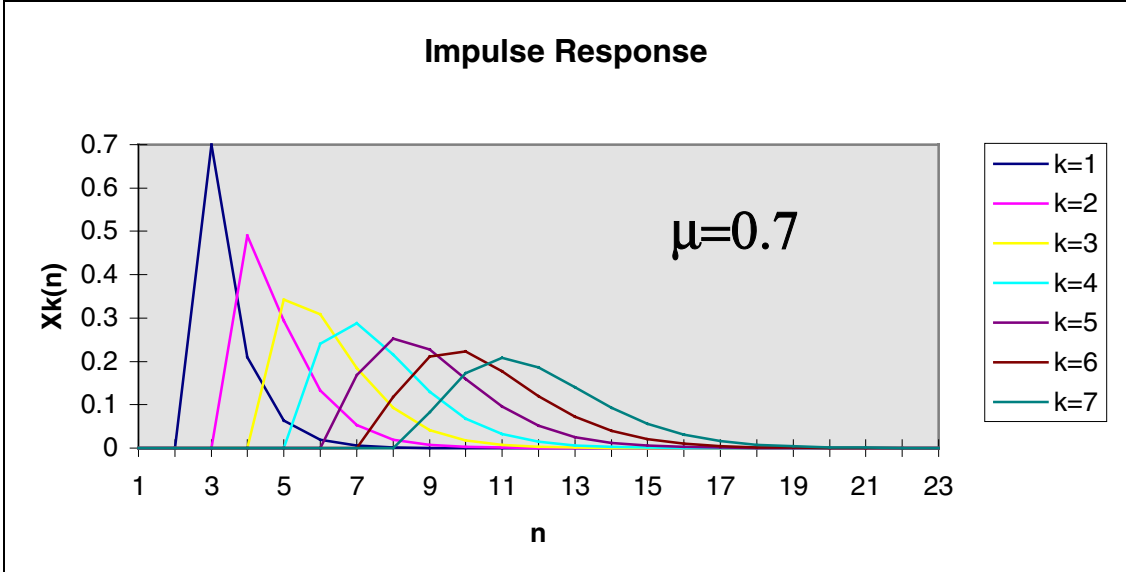


Figure 12 Impulse responses of each tap of a 7-tap FIR memory for $\mu=0.7$

The FIR memory can be applied to the input layer only (which is sometimes referred to as focused memory), to the hidden layer and to the output layer (see Figure 14). In each case FIR will store the activations of the respective layer and use their past values to compute the net output.

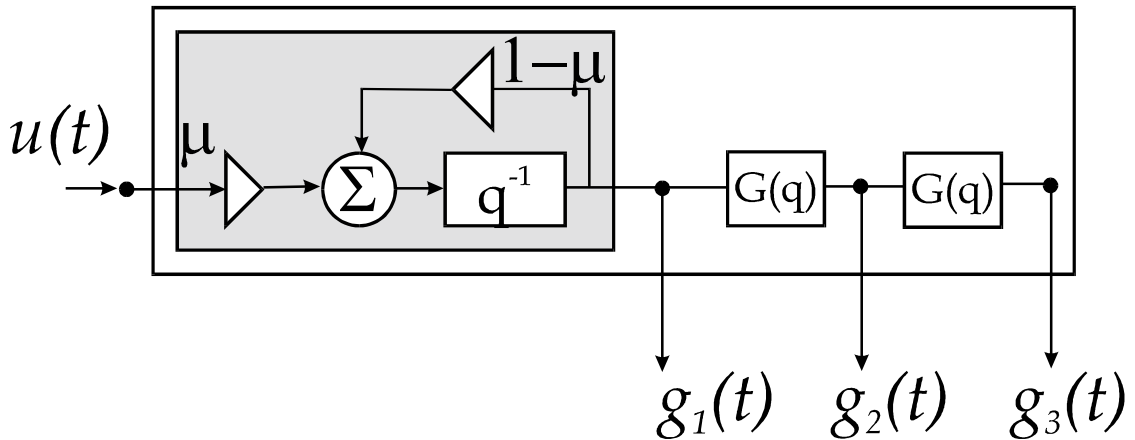


Figure 13 The FIR memory: $g_i(t)$ are inputs to the next layer processing elements

5.8 ADVANTAGES OF TLRNS

The main advantage of TLRNs is the smaller network size required to learn temporal problems when compared to MLPs that use extra inputs to represent the past samples (equivalent to the Time Delay Neural Networks — for evidence consult **Table 1**). An added advantage of TLRNs is their low sensitivity to noise. The recurrence of the TLRN provides the advantage of an adaptive memory depth (i.e., it finds the best duration of a history to represent the input signal's past).

From a system identification point of view, TLRNs implement non-linear moving average (NMA) models. With global feedback from the output to the hidden layer, they can be extended to non-linear ARMA (autoregressive moving average) models. These non-linear models can be used for optimal control applications, surpassing the performance of their linear counterparts.

An alternative representation of the FIR network (and TDNN) can be found by using a technique referred to as *unfolding in time*. The general strategy is to remove all time delays by expanding the network into a larger equivalent static structure.

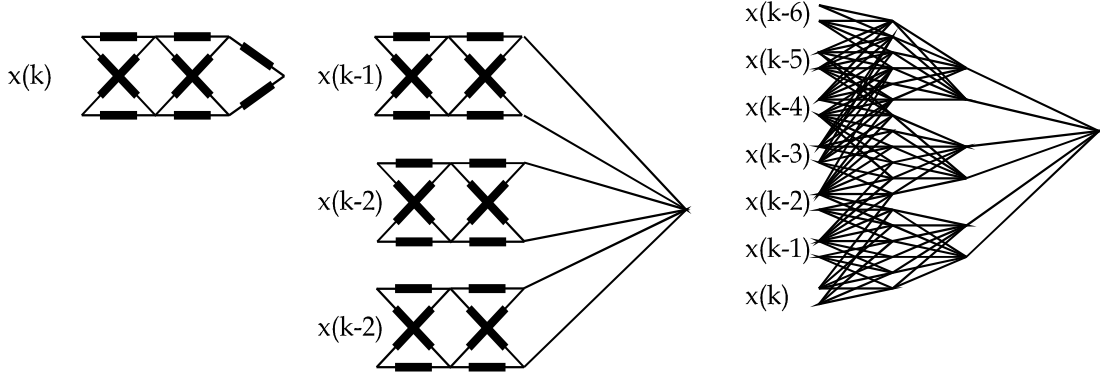


Figure 14 An FIR network with second-order taps for all connections is unfolded into a static network. The original structure has 30 variable filter coefficients while resulting network has 150 static synapses.

As an example, consider the very simple network shown in Figure 14 on the left hand side. The network consists of three layers with a single output neuron and two neurons at each hidden layer. All connections are made by second-order (two-tap) synapses. Thus, while there are only 10 synapses in the network, there are actually a total of 30 variable filter coefficients. Starting at the last layer, each tap is interpreted as a ‘virtual neuron’ whose input is delayed the appropriate number of time steps. A tap is then ‘removed’ by replicating the previous layers of networks and delaying the input to the network accordingly (illustration in the middle of Figure 14). The process is then continued backward through each layer until all delays have been removed. The final unfolded network is shown on the right hand side of Figure 14.

Table 1 FIR network versus Static Equivalent

Network Dimension		Variable Parameters	Static Equivalent
Nodes ¹	Order ²		
2×2×2×1	2:2:2	30	150
5×5×5×5	10:10:10	605	36355
3×3×3	9:9	180	990
3×3×3×3	9:9:9	270	9990
3 ⁿ	9 ⁿ⁻¹	(n-1)90	10 ⁿ⁻¹⁰

¹ Number of Inputs × Hidden Neurons × Outputs

² Order of FIR synapses in each layer

This method produces an equivalent of static structure where the time dependencies have been made external to the network itself. Notice that whereas there were initially 30 filter coefficients, the equivalent unfolded structure now has 150 static synapses. This can be seen as a result of redundancies in the static weights. In fact, the size of the equivalent static network grows *geometrically* with the number of layers and tap delays (see **Table 1**). In light of this one can view an FIR network as a compact representation of a larger static network.

6. ISSUES IN CONNECTIONIST LEARNING

6.1 TERMINATION OF TRAINING

One practical issue always appears while training neural networks. What is the criterion that is to be used as a termination of a training process? Quite obviously, one trains a neural network with one prime objective in mind and that is to create a truthful model of underlying process. The goal is not to blindly minimise the error created on the training set, but rather to maximise ANNs generalisation capabilities, *i.e.* to develop an ANN that is general enough and capable of truthfully reproducing any data set. The only way of doing so is cross-validation. This means that one should follow the errors produced by ANNs on both training and validation data sets and terminate the training process at the moment when the error on validation set start increasing⁴. When the error on validation set start increasing, it is said that the network is being *overtrained*, *i.e.* the network starts fitting even the noise inherent to the dynamics of the system contained in the training set.

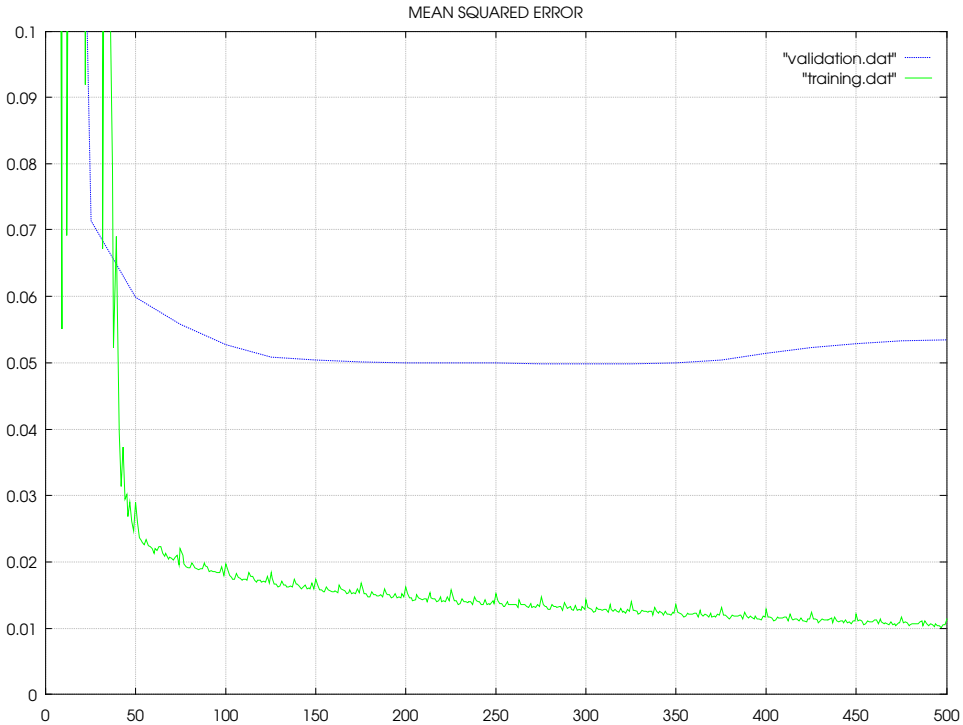


Figure 15 Evolution of errors for both, training and validation data sets during the training process

⁴ The underlying assumption here is that the data contained within both, training and validation data sets, truthfully represent underlying physical processes. More clearly, it is assumed that the minimum of error on validation set would correspond to the universally maximal generalisation properties, *i.e.* that validation on some other data set would result in exactly the same generalisation ANN's characteristics.

Upper line in **Figure 15** denotes evolution of error during the training process expressed as mean squared error (MSE) on validation the set, and the lower line on the training set. It is rather obvious that the error on validations set reaches its minimum somewhere around epoch 300, whereas the error on the training set continues to decrease.

6.2 DIRECT VERSUS ITERATED PREDICTIONS

Imagine the task where a requirement is to predict the value of a property at, say 10 steps ahead. A direct prediction model uses present and past information at the inputs and is trained with the values 10 steps ahead as targets. This network is strictly feedforward.

Iterated predictions are obtained by building a model that is trained to predict 1 step ahead. Its prediction is then entered into the input for another forward pass, yielding the prediction for the next step, etc. The question is ‘direct vs. iterated predictions?’

Table 2 Three neural networks for h-Step Ahead Predictions

Case	Architecture	Objective
Iterated	single step	minimise error after one iteration
Iterated	single step	minimise error after h iterations
Direct	h-step	minimise error for one h-step forecast

Physicist often view the time series as a sequence of measurements of some function of variables of a dynamical system. The key to the direct-vs.-iterated issue is to note that there are two time scales involved: the time scale of the dynamics of the system and the time scale of the measurements.

Consider the one extreme where the data are taken on a time scale much faster than the intrinsic dynamics of the system. An iterated predictor will try to capture variations that are primarily noise; the system does not change much from one time step to the next — only the noise does, because it typically has more high frequency components than the signal. In this case, a direct predictor will be more suited, because its longer prediction time will be closer to the dynamics of the system. In the other extreme where the system is severely undersampled, the time scale of the iterated predictor is closer to the intrinsic time scale, and an iterated predictor might be more appropriate. Table 2 classifies neural networks for h-step ahead predictions as the output of the network. Networks in the upper two rows have the same number of hidden units.

The first and second case both generate one-step ahead predictions as the output of the network. The output is used as an input in the next step; h such iterations yields the desired h -step ahead forecast. The difference between the two cases is how they are trained:

- In the first case, the parameters of the network are optimised to minimise the error on one-step ahead forecast. Subsequent iterating is an add on, done after training
- In the second case, the goal of network training is to minimise the error on iterated h-step ahead forecast. This can be viewed as putting h copies of identical networks ‘on the top of each other’, that is the second copy uses the output of the first one as one of its inputs, and so forth. The parameters are then adjusted to have the smallest error after h iterations, that is at the top of unfolded network.

- The third network has a different task: it projects directly from the present to the desired point b point steps in the future; it does not involve any intermediate predictions or feedback.

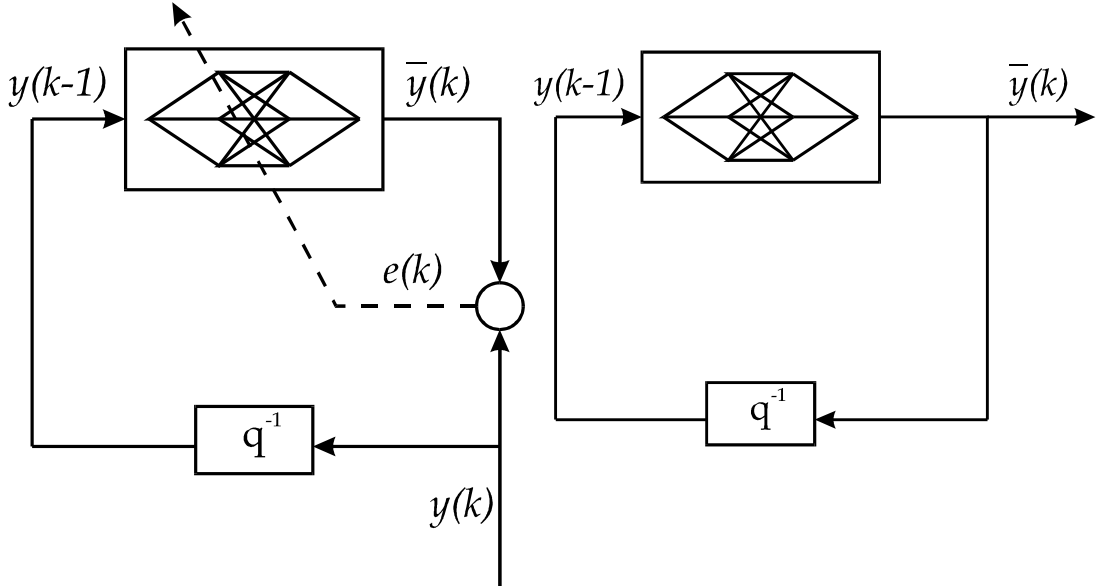


Figure 16 Network prediction configuration: The single step prediction $\hat{y}(k)$ is taken as the output driven by the previous sample of the sequence $y(k)$. During training (illustration on the left) the single step squared prediction error, $e^2(k) = [y(k) - \hat{y}(k)]^2$ is minimised. Feeding the estimate $\hat{y}(k)$ back forms a closed loop process used for long-term iterated predictions (illustration on the right-hand side).

7. NEURAL NETWORKS AS A DATA ASSIMILATION ROUTINE

The main purpose of the present project is to define a somewhat alternative approach of combining observations and numerical model results in order to produce a more accurate forecast routine. The approach utilises artificial neural networks (ANNs) to analyse and forecast the errors created by numerical model. The resulting, hybrid model should provide very good forecast skill that can be extended over a forecasting horizon of considerable length.

The desire to predict the future and understand the past governs the search for laws that explain the behaviour of observed phenomena. If the underlying deterministic equations are known, in principle they can be solved to forecast the outcome based on knowledge of the initial conditions and evolution of forcing terms. In hydraulic modelling, for example, governing laws are Navier-Stokes equations, whereas the forcing term is the evolution of the status of atmosphere (atmospheric pressures and resulting wind fields). Initial conditions describe the sea status (current speeds and directions, water levels) in entire computational domain at the beginning of computation. Once the initial and forcing terms are *precisely* specified, it should be possible to *precisely* calculate the evolution of the status of the sea, from its specified initial conditions and as a consequence of applied forcing.

However, even under these, almost ideal circumstances, the model results are not precise. Every model is indeed only a *model* of reality; it employs number of simplifying assumptions (for example depth averaging of velocities in vertically integrated 2D models) which inevitably produces inaccuracies. In a numerical modelling one discretises a domain, and therefore is not able to resolve numerous sub-grid phenomena. Also, the errors in the model parametrisation (mainly because most of model parameters cannot be directly measured) greatly contribute to errors of numerical models. Finally, it is impossible to *precisely* define initial conditions and

forcing terms in the *entire* computational domain. All these imprecisions and uncertainties can accumulate to produce fairly poor model results — despite our perfect knowledge of governing laws.

7.1 HOW CAN WE MAKE MORE ACCURATE MODELS?

It is accepted fact that numerical models are far from being perfect. In the present problem, the used numerical model is a hydraulic numerical model forced by dynamical open boundary conditions and the output of a regional atmospheric model. The degree of simplifications that are introduced in this model (model physics, numerical solution, grid discretisation, model parameters, etc.) together with the error associated with the forcing (open boundary conditions and atmospheric forcing) are the main sources of errors in the model solution. Various schemes may be utilised to make models more accurate. When observations of the modelled phenomena are available and some knowledge of the aforementioned errors exists, data assimilation methods can be used in order to improve the model solution. Data assimilation is a methodology which can optimise the extraction of reliable information from observations and combine it with, or assimilate it in, numerical models.

A number of different data assimilation procedures can be adopted. These are designed to either improve description of initial conditions at the time of forecast or provide correction of model predictions during a forecast period. The data assimilation procedures may be classified according to the variables modified during the updating process. In WMO (1992, see also Refsgård, 1997) four different methodologies have been defined (*Figure 17*). The four methodologies can be defined as follows:

- (1) *Updating of input parameters* — This is the classical method justified by the fact that input uncertainties may be the dominant error source in operational forecasting
- (2) *Updating of state variables* — Adjustment of the state variables can be done in different ways. The theoretically most comprehensive methodology is based on Kalman filtering (Gelb, 1974). Kalman filtering is the optimal updating procedure for linear systems, but can with some modifications also provide an approximate solution for non-linear hydrodynamic systems.
- (3) *Updating of model parameters* — continuous adaptation of model parameters is a matter of continuous debate. The prevailing view seems to be that for hydrodynamic models of non-trivial complexity recalibration of the model parameters at every time step has no real advantages, as the operation of any hydrodynamic system can not significantly change over the short interval of time.
- (4) *Updating of output variables (error prediction)* — The deviations between the simulation mode forecast and the observed variables such as current speed, are model errors. Possibility of forecasting these errors and superimposing them to the simulation mode forecasts, usually gives a more accurate performance. This method is most often referred to as error prediction and is the method employed in the present study.

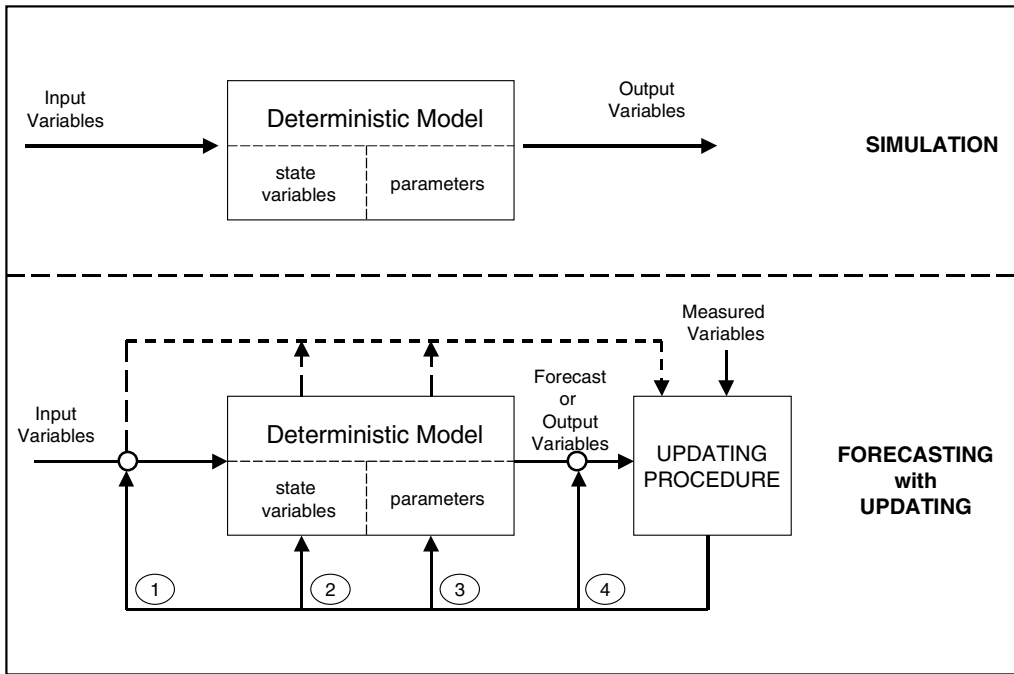


Figure 17 Schematic diagram of simulation and forecasting with emphasis on the four different updating methodologies (adapted from Refsgård, 1997)

If forecasting interest is limited to only a few variables at some specific locations with a high degree of accuracy and for a considerably long lead-time forecast, a data assimilation scheme based on updating of output variables (error prediction) may be the most suitable approach. In model error prediction other techniques such as artificial neural networks (Babovic, 1996; Van den Boogaard and Kruisbrink, 1996; Minns, 1998) or an approach based on chaos theory (Babovic and Keijzer, 1998) have demonstrated very good forecast skill. By using these techniques, one can combine the forecast of the numerical model (model output) at the point of interest with the latest observed data in order to obtain an improved forecast.

Another advantage of such an approach is that it allows the combination of different variables (for example, atmospheric data such as wind speed) to improve the accuracy. This cannot be done in conventional data assimilation methods where the data has to be introduced in the model state in order to be assimilated.

Means for data collection and distribution have never been so advanced as they are today. While advances in data storage and retrieval continue at a breakneck pace, the same cannot be asserted about advances in information and knowledge extraction from data. Without such developments, however, we risk missing most of what the data have to offer.

However, forecasting on the basis of the data *alone* is not the complete story. At least not in scientific and engineering domains. Although data-centric approach is at the focal point in many research areas, the current paper advocates a slightly different approach. Clearly, there is an enormous amount of knowledge and understanding of physical processes that should not just be thrown away. Forecast skill based on deterministic models should not be ignored! We strongly believe that the most appropriate way forward is to combine the best of the two approaches: theory-driven, understanding-rich with data-driven modelling process.

The presented an approach where a theory-driven deterministic model was coupled with a data-driven technique to produce a hybrid model with very good forecast skill. The resulting hybrid model performs much better than each of its constituents taken exclusively. The benefits

of coupling were expressed not only in the terms of accuracy, but also in the terms of extension of the forecast horizon.

APPENDIX A — STATE-SPACE RECONSTRUCTION

The embedding theorem (Takens, 1981 — see also page 3) is silent on the choice of time delay to use in constructing d-dimensional data vectors. Indeed, it allows *any* time delay (Sauer *et al*, 1991) — except certain multiples of the precise period of a periodic signal — as long as one has an infinite amount of infinitely accurate data. Since this is not realistic requirement for practical applications, we have to find a way of making choices that apply in practice.

Basically, one faces the problem of enriching the description of the representation of the process by taking into account some other source of information. In the present case one can use delayed co-ordinates $x'(t-t_1'), x'(t-t_2'), \dots, x'(t-t_n')$. The question, of course, arises how to select values t_1', t_2', \dots, t_n' . One may choose to take as many as possible, but bearing in mind possible chaotic dynamics and the complexity of the problem, it soon becomes clear that such a ‘brute force’ approach will not result in compact formulation containing only the most relevant information.

In order to address this issue we use the standard information theory originated by Khinchin (1957). A very brief discussion of the information theory is presented in the sequel. All the expressions presented apply to univariate cases but can easily be extended to multi-variate cases.

SOME INFORMATION THEORETIC BACKGROUND

The experimental process consists of performing measurements to obtain information. Consider an experiment a with possible outcomes $A_1, A_2, A_3, \dots, A_n$. If the respective probabilities are $p(A_1), p(A_2), p(A_3), \dots, p(A_n)$, the uncertainty of the outcome can be assessed. If, for example, all $p(A_i)$ are zero except one, there is no uncertainty in the outcome and there is no point in performing an experiment as no information can be gained in performing it. If on the other side, all $p(A_i)$ are equi-probable, the uncertainty of the outcome is at the maximum and the information gained by carrying out the experiment is also maximal.

Thus, if one carries out an experiment, the possible outcomes of which are described by a *given* scheme $\mathbf{A} = \{ [A_1, p(A_1)], [A_2, p(A_2)], [A_3, p(A_3)], \dots [A_n, p(A_n)] \}$, then in doing so one obtains *information* and the uncertainty of the outcome is eliminated. It can, therefore, be said that the information received by an observer is equal in magnitude to the uncertainty which existed before the experiment. The larger the uncertainty, the larger the amount of information obtained by removing it. Following this closely, the information obtained by a measurement of the outcome of a finite scheme \mathbf{A} can be expressed through the corresponding *entropy* $H(\mathbf{A})$ (see for example, Khinchin, A., 1957):

$$H(\mathbf{A}) = -\sum_{i=1}^n p(A_i) \log_2 p(A_i) \quad (21)$$

This describes the average information gained by performing the experiment and obtaining a measurement. The definition (21) can easily be generalised to continuous variables, *i.e.*

$$H(\mathbf{A}) = -\int_{-\infty}^{+\infty} p(x) \log_2 p(x) dx \quad (22)$$

MUTUAL INFORMATION

In order to determine higher order relationships, it is necessary to introduce higher order measures. If measurements are collected from two schemes $\mathbf{A} \equiv \{ [A_1, p(A_1)], [A_2, p(A_2)], [A_3, p(A_3)], \dots [A_n, p(A_n)] \}$ and $\mathbf{B} \equiv \{ [B_1, p(B_1)], [B_2, p(B_2)], [B_3, p(B_3)], \dots [B_m, p(B_m)] \}$, the mutual information $I(\mathbf{A}, \mathbf{B})$ is a measure of how much can be said about the one given the other.

$$I(A, B) = \sum_{j=1}^m \sum_{i=1}^n p(A_i B_j) \log_2 \frac{p(A_i B_j)}{p(A_i)p(B_j)} \quad (23)$$

$$I(A, B) = \sum_{j=1}^m \sum_{i=1}^n p(A_i B_j) \log_2 p_{ij} - \sum_{j=1}^m \sum_{i=1}^n p(A_i B_j) \log_2 p(A_i) - \sum_{j=1}^m \sum_{i=1}^n p(A_i B_j) \log_2 p(B_i) \quad (24)$$

The sum $p(A_i, B_j)$ over the A_i simply leaves $p(B_j)$ since $\sum p(A_i) = 1.0$. Therefore, the above equation (9) can be simplified into:

$$I(A, B) = \sum_{j=1}^m \sum_{i=1}^n p(A_i B_j) \log_2 p_{ij} - \sum_{i=1}^n p(A_i) \log_2 p(A_i) - \sum_{j=1}^n p(B_j) \log_2 p(B_j) \quad (25)$$

$$I(A, B) = H(A) + H(B) - H(AB) \quad (26)$$

where $H(A, B)$ is information obtained considering A and B together

$$H(A, B) = H_B(A) + H(B) \quad (27)$$

where $H_B(A)$ is *conditional entropy* — the entropy of A given B . If A and B are independent, the terms $H_B(A)$ and $H(A)$ become equal — $H_B(A) = H(A)$ — reducing $H(A, B)$ to $H(A) + H(B)$, resulting in $I(A, B) = 0$ — thus reducing the mutual information to zero.

Back to forecasting. If A is say $x(t)$ and B $x(t-t')$ one can try to maximise $I(A, B)$ by choosing t' . Moreover one can trivially generalise expression (26) to $I(A_1, A_2, \dots, A_n)$ and try to find the appropriate t'_1, t'_2, \dots, t'_n that would provide maximum information about $u(t)$ over the entire experimental sample. It should be noted that not even n should be kept constant, but should also be subjected to the search process.

In this way we would provide a state-space description that contains maximum information with respect to $x(t)$, i.e. $x(t-t'_1), x(t-t'_2), \dots, x(t-t'_n)$. The process of identification of appropriate time delays t'_1, t'_2, \dots, t'_n can be rather intensive.

REFERENCES

- Ackley, D.H., Hinton, D.E., and Sejnowski, T.J., 1985., A learning algorithm for Boltzman machines, *Cognitive Science*, Vol. **9**, pp. 147-169
- Babovic, V., 1996, *Emergence, Evolution, Intelligence; Hydroinformatics*, Balkema, Rotterdam
- Babovic, V., and Keijzer, M., 1999, Forecasting of river discharges in the presence of chaos and noise, in Marsalek, J., (ed), *Coping with Floods*, Kluwer, Dordrecht
- Box, G. E. P., and Jenkins, F. M., 1976., *Time Series Analysis: Forecasting and Control* (2nd edition), Holden-Day, Oakland
- Cañizares, R.T., 1999, *On the Application of Data Assimilation in Regional Coastal Models*, Ph.D. thesis, IHE-Delft, The Netherlands
- Cañizares, R.T., Heemink, A.W., and Vested, H.J., 1998, Application of advanced data assimilation methods for the initialisation of storm surge models, *Journal of Hydraulic Research*, Vol. 36, No.4, pp. 655-674
- Catlin, D.E., 1989., *Estimation, Control and the Discrete Kalman Filter*, Applied Mathematical Sciences, Vol. 71, Springer Verlag, New York
- DHI/LIC, 1997, *The Øresund Link: Transport and Installation Weather Windows*, Technical Note
- Friedman, J.H., 1997., On bias, variance 0/1-loss, and the curse of dimensionality, *Data Mining and Knowledge Discovery*, Vol. 1., No. 1., pp. 55-78
- Gelb, A., 1974, *Applied Optimal Estimation*, MIT Press, Cambridge
- German, S., Bienenstock, E., and Doursat, R., 1992., Neural networks and the bias/variance dilemma, *Neural Computation*, Vol. **5**, pp. 1-58
- Hebb, D. O., 1949., *Organisation of Behaviour*, John Wiley, New York
- Hopfield, J.J., 1982., Neural networks and physical systems with emergent collective computational abilities, *Proceedings of National Academy of Sciences USA*, Vol. **79** Biophysics, pp. 2254-2258
- Hopcroft, J.E., and Ullman, J.D., 1979., *Introduction to Automata Theory, Languages and Computation*, Addison-Wesley, Reading
- Hornik, K., Stinchcombe, M., and White H., 1989., Multilayer neural networks are universal approximators, *Neural Networks*, Vol. **2**, pp. 356-366
- Irie, B., and Miyake, S., 1988., Capabilities of three-layered perceptrons, in *Proceedings of IEEE International Conference of Neural Networks, San Diego, I*, pp. 641-648
- McCulloch, W.S., and Pitts, W., 1943., A logical calculus of the ideas immanent in nervous activity, *Bulletin of Mathematical Biophysics*, Vol. **5**, pp. 115-133
- Minns, A.W., 1998., *Artificial Neural Networks as Subsymbolic Model Descriptors*, Balkema Publishers, Rotterdam
- Minsky, M., and Papert, S., *Perceptrons*, The MIT Press, Cambridge, Mass.
- Packard, N.H., Crutchfeld, J.P., Farmer, J.D., and Shaw, R.S., 1980., Geometry from a time series, *Phys. Rev. Lett.*, Vol. **45**(9), pp. 712-716
- Phan, M., Juang, J.-N., and Hyland, D. C., 1993., *On Neural Networks in Identification and Control of Dynamic Systems*, NASA Technical Memorandum 107702
- deVries and Principe, J., 1992, The gamma model: A new neural network model for temporal processing, *Neural Networks*, Vol. 5, pp.565-576
- Refsgård, J.C., 1997., Validation and intercomparison of different updating procedures for real-time forecasting, *Nordic Hydrology*, Vol. 28, pp. 65-84
- Rosenblatt, F., 1958., The perceptron: A probabilistic model for information storage and organisation in the brain, *Psychological Review*, Vol. **65**, pp. 386-408
- Rosenblatt, F., 1962., *Principles of Neurodynamics: Perceptrons and the theory of Brain Mechanics*, Spartan Books, New York

- Rummelhart D., and McClelland, J., (eds.), 1986., *Parallel Distributed Processing: Explorations into the Microstructure of Cognition, Volume 1: Foundations*, The MIT Press, Cambridge, Mass.
- Sauer, T., Yorke, J., A., and Casdagli, M., 1991., Embedology, *J. Stat. Phys.*, Vol. **65** (3/4), pp. 579-616
- Takens, F., Detecting strange attractors in turbulence, in *Dynamical Systems and Turbulence*, Rand, D.A. and Young, L.-S. (eds), Lecture notes in mathematics, Vol. 898, pp. 336-381, Berlin: Springer-Verlag
- Verlaan, M., 1998., *Efficient Kalman filtering algorithms for hydrodynamic models*, Ph.D. Thesis, Technical University of Delft, the Netherlands
- Weigend, A.S., 1996., Time series analysis and prediction, in Smolensky, P, Mozer, M.C., and Rumelhart, D.E., (eds.), *Mathematical Perspectives on Neural Networks*, Lawrence Erlbaum, Mahwah
- WMO, 1992, Simulated real-time intercomparison of hydrological models, WMO operational hydrology report no 38, WMO no 779, World Meteorological Organisation, Geneva
- Yule, G., 1927., On a method of investigating periodicity in disturbed series with special reference to Wolfer's sunspot numbers, *Phil. Trans. Roy. Soc. London*, **A 226**: 267-298

B I L A G F

Internal Note - Improving Wave Forecast Data (på engelsk)

1 Improving wave forecast data – first version

The following is a step by step description of the parameters used to improve the raw OSW forecast of significant wave height. A forecast event is here defined as “a predicted timeseries of data starting at the last measurement known as good”.

The basis of the improved forecast is the OSW forecast at the desired time. An additional term is added to the OSW forecast of the form:

$$Hm0_{Forecast}(t_n + \Delta t) = r \left[\overline{Hm0_{OSW}}(t_n + \Delta t) + \frac{1}{1 + a\Delta t} (\overline{Hm0_{Measured}}(t_n) - Hm0_{OSW}(t_n + \Delta t)) \right]$$

where

a: Hyperbolic parameter [1/hour]

r: Reduction factor

n: Subscript, n, signifies the current time step, n-1 is the previous time-step etc. Each time-step is 0.5 hours

t_n: Current time from which the forecast is to be made

Δt: The forecast time [hours]

Averaged Hm0 measured at current time:

$$\overline{Hm0_{Measured}}(t_n) = \frac{1}{2} \sum_{i=n-1}^n Hm0_{Measured}(t_i)$$

Averaged Hm0 OSW at desired forecast time:

$$\overline{Hm0_{OSW}}(t_n + \Delta t) = \frac{1}{17} \sum_{i=n-8}^{n+8} Hm0_{OSW}(t_i + \Delta t)$$

It is evident from the above expression that the improved forecast is going to be equal to the averaged measured Hm0 at the time of forecast. Furthermore, the improved forecast is approaching the averaged OSW Hm0 for long forecasts controlled by the parameter, *a*, of the hyperbolic function (see Fig 1). The reduction factor is applied to handle systematically higher or lower waves calculated by OSW compared to measurements.

The number of time-steps to average Hm0 measured and OSW over has been found by optimisation.

The parameter, a , is constant for each forecast event generated and has been found by optimisation of the parameters of the following expressions:

$$a = a_{fac} \cdot \left(0.10 + 0.05 \cdot \frac{\overline{Hm0}_{Measured}(t_n)}{meter} \right) \cdot \left(1 + 0.28 \cdot \frac{\Delta t}{48 hours} \right)$$

where

$$a_{fac} = \begin{cases} 1.0/hour, & (Hm0_{Measured} - Hm0_{OSW}(t_n)) \cdot (Hm0_{Measured} - Hm0_{OSW}(t_n + \Delta t)) > 0 \\ 3.0/hour, & \text{else} \end{cases} .$$

Numerous other parameters have been tested for influence on the forecasted wave height without success. Amongst others:

Wind speed and direction, measured and OSW wave periods, shifting OSW wave heights along time-axis for best possible fit of hindcasted wave heights, etc.

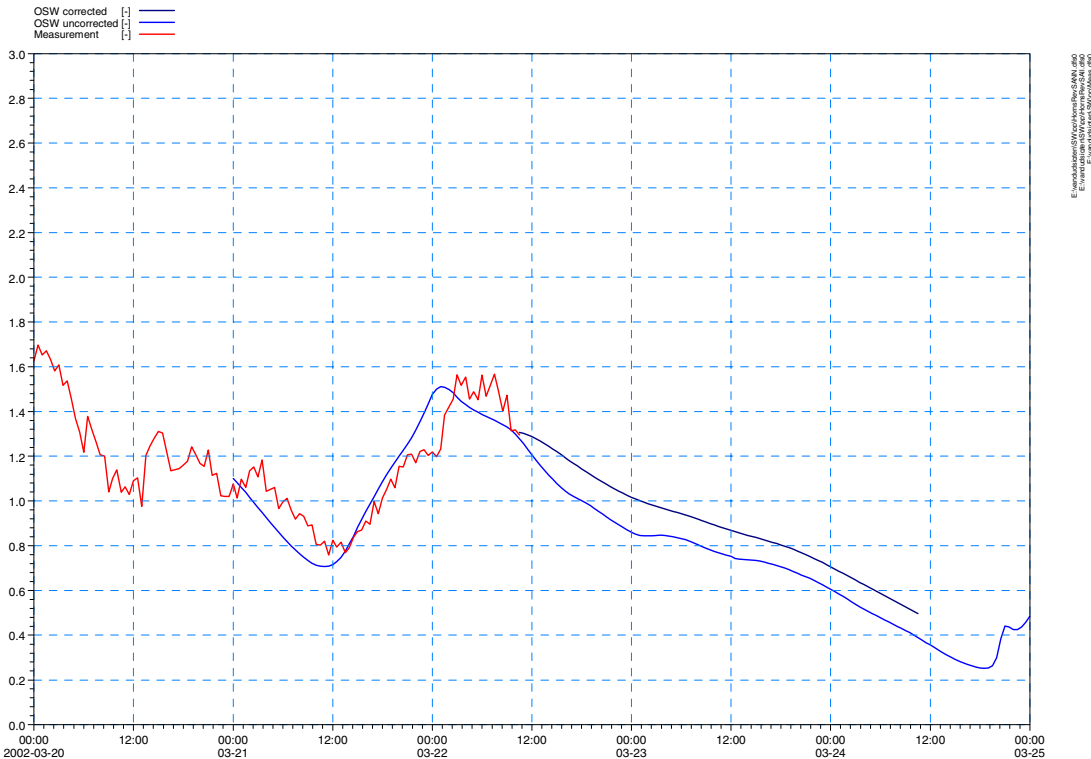


Fig 1 Wave heights obtained by measurement, simulation by OSW, and improvement of OSW forecast

Error finding in measured data

If there is something obviously wrong with the measured wave data, it is disregarded and OSW results are used as forecast.

If only the last couple of measured wave data are erroneous, the last wave data known as good is used for the improved forecast.

2 Improving wave forecast data – second version

The following is a step by step description of the parameters used to improve the raw OSW forecast of significant wave height. A forecast event is here defined as “a predicted timeseries of data starting at the last measurement known as good”.

The basis of the improved forecast is the OSW forecast at the desired time. An additional term is added to the OSW forecast of the form:

$$Hm0_{Forecast}(t_n + \Delta t) = \left[\overline{Hm0_{OSW}}(t_n + \Delta t) + \frac{1}{1+a\Delta t} (\overline{Hm0_{Measured}}(t_n) - Hm0_{OSW}(t_n + \Delta t)) \right]$$

where

a: Hyperbolic parameter [1/hour]

r: Reduction factor

n: Subscript, n, signifies the current time step, n-1 is the previous time-step etc. Each time-step is 0.5 hours

t_n: Current time from which the forecast is to be made

Δt: The forecast time [hours]

Averaged Hm0 measured at current time:

$$\overline{Hm0_{Measured}}(t_n) = Hm0_{Measured}(t_n)$$

Averaged Hm0 OSW at desired forecast time:

$$\overline{Hm0_{OSW}}(t_n + \Delta t) = r * Hm0_{OSW}(t_n + \Delta t)$$

It is evident from the above expression that the improved forecast is going to be equal to the averaged measured Hm0 at the time of forecast. Furthermore, the improved forecast is approaching the averaged OSW Hm0 for long forecasts controlled by the parameter, *a*, of the hyperbolic function. The reduction factor is applied to handle systematically higher or lower waves calculated by OSW compared to measurements.

The number of time-steps to average Hm0 measured and OSW over has been found by optimisation.

The parameter, a , is constant for each forecast event generated and has been found by optimisation of the parameters of the following expressions:

$$a = a_{fac} \cdot \left(0.12 + 0.00 \cdot \frac{\overline{Hm0}_{Measured}(t_n)}{meter} \right) \cdot \left(1 + 0.24 \cdot \frac{\Delta t}{48 hours} \right)$$

where

$$a_{fac} = \begin{cases} 1.0/hour, & (Hm0_{Measured} - Hm0_{OSW}(t_n)) \cdot (Hm0_{Measured} - Hm0_{OSW}(t_n + \Delta t)) > 0 \\ 7.0/hour, & \text{else} \end{cases} .$$

$$r = 1.09$$

Numerous other parameters have been tested for influence on the forecasted wave height without success. Amongst others:

Wind speed and direction, measured and OSW wave periods, shifting OSW wave heights along time-axis for best possible fit of hindcasted wave heights, etc.